Comparison of detrital and metamorphic zircon from metapelites in the Rayner Complex, east Antarctica: provenance and age of deposition investigated via U-Pb and Hf-analysis and interpretation of Th/U ratio, CL zonation and morphology.

K.R. Murray

ABSTRACT

In East Antarctica's Archaean-Proterozoic Rayner Complex, metasedimentary gneisses at Stillwell Hills in Kemp Land are interfolded with orthogneisses. At Cape Bruce and Forbes Glacier in MacRobertson Land, metasediments form more continuous exposures that are intruded by the Mawson Charnockite (c.980Ma) (Halpin et al 2005; Young & Black 1991). Detrital and metamorphic zircon grains from six metapelitic samples were analysed for U-Pb age, $T_{DM}{}^{c}$, εHf, Th-U ratio, length, CL zoning and morphology. This detailed analysis helped to determine their age of deposition as sediments, when they were metamorphosed and the provenance of the grains within each sample. Colbeck Gneiss from Cape Bruce (AC34) recorded a 207/206Pb maximum depositional age of 1258±23 Ma. A metapelitic lens within Painted Gneiss in Forbes Glacier (90024) recorded a maximum depositional age of 1251±27 Ma. These dates correlate with Young and Black (1991) whole rock analysis of these two Proterozoic gneisses. To better understand the regional history of Stillwell Hills, four metapelites were dated to determine their relative age compared with host Stillwell orthogneiss. This work indicates that even the oldest inherited zircons in these four metapelite samples are a minimum 340Ma younger than the youngest dated zircon from Archaean Stillwell orthogneiss (Halpin et al 2005). In order of deposition, Pink Gneiss (FS0214) maximum depositional age is 1317±51 Ma; followed by Green layered sequence (GS01) at 1316±33 Ma, Garnet-sillimanite metapelite (SW54) at 1260±47 Ma and Rusty gneiss (FS0223) the youngest at 1178±84 Ma. Petrogenesis of the majority of zircon grains in all six samples could be traced to felsic igneous events. Considering Antarctic basement rock is formed from igneous mafic granitoids (Veevers & Saeed 2011), this felsic trend indicates that most detritus originated not from Archaean basement protoliths, but younger, more crustally evolved, sources. All samples, to a greater or lesser extent, contained zircon grains whose U-Pb age, $T_{DM}{}^{c}$, εHf, Th-U ratio and CL patterns indicated shared provenance. Only two known rock types were identified as possible sources of provenance, which trended towards felsic igneous petrogenesis. Metamorphism shown by igneous zircon grains indicated regional peak metamorphism at Kemp or Macrobertson Land; after erosion, transportation and deposition from mostly unknown igneous protoliths.

1. Introduction

In Archaean-Proterozoic metasedimentary rare outcrops, such as those existing in Rayner Complex (and neighbouring Napier Complex) east Antarctica, detrital zircons often provide the most reliable data concerning the age, $T_{DM}{}^{c}$ and εHf of source rocks. Due to their resistance to weathering and erosion cycles, analysis of detrital zircon grains within exposed metapelites in ice-covered East Antarctica may suggest likely shared provenance with adjacent exposed terrains. Inherited cores of igneous zircon can often provide an identifiable geochemical portrait of their original source rock (Belousova et al 2002, p.620). However, this study does not suggest that the limited number of samples described is indicative of substantial subglacial lithologies of Kemp and MacRobertson Lands.

In order to conclusively prove provenance between a zircon's current place of deposition and its potential source region, evidence must be provided that the source region was exposed and undergoing erosion, and that a sediment transport system existed between both regions (Howard et al 2009, p.288). This is almost impossible to prove from sampling isolated outcrops in Antarctica; especially when high grade metamorphism has erased any record of sediment transport directions.

For sediment deposited today and in the most recent past, ice drainage basins in Antarctica often provided a pathway between the highest exposed topography and low-lying coastally-exposed outcrops (Figure 1). Relatively recent glacial ice can be dated and flow directions inferred. However, in the case of Archaean and Proterozoic sediment deposition, detrital zircon could be shed from highlands now residing on other continents that were once part of Gondwanaland; or from lithologies now completely eroded.

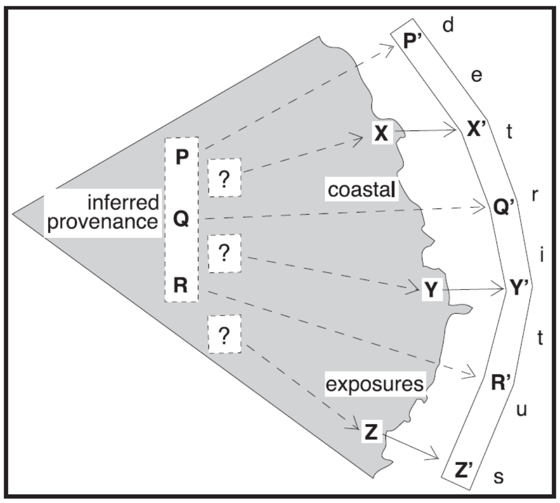

Figure 1. Veevers & Saeed (2011) model of an ice-drainage basin, illustrating the sedimentary transport of detrital zircon from a distal provenance upflow, to low-lying coastal exposures, before eventual outflow offshore (Veevers & Saeed 2011, p.3).

Provenance studies of detrital and metamorphic zircon at Stillwell Hills, Cape Bruce and Forbes Glacier.

Detrital and metamorphic zircon grains were sampled from Colbeck Gneiss at Cape Bruce (sample AC34), a garnet-cordierite-rich lens from Painted Gneiss at Forbes Glacier (sample 90024), metapelitic layers interfolded with Stillwell Orthogneiss in Stillwell Hills (samples FS0214 and GS01) and two proximal metapelites also from Stillwell Hills (SW54 and FS0223) (Figure 2).

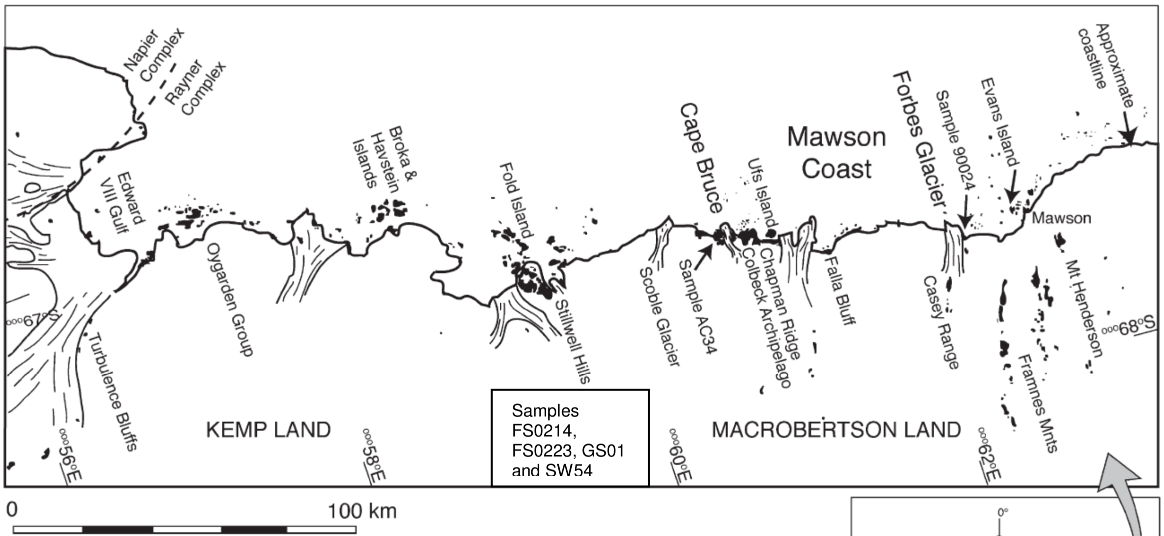

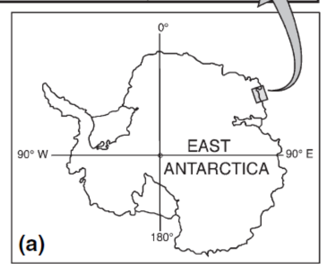

Figure 2. Location of Forbes Glacier (sample 90024) and Cape Bruce (sample AC34) in MacRobertson Land, East Antarctica (inset (a)). In Kemp Land, metapelitic gneissic samples FS0214, FS0223, GS01 and SW54 were taken from Stillwell Hills (Halpin et al 2005, p.684). The exact location of Stillwell Hills samples is detailed in Figure 12.

Information gathered from detrital zircon grains from these limited coastal exposures contained many concordant 207/206Pb-dated grains outside known age-clusters in proximal outcrops. Such age-gaps may provide information on the geochemistry of distal source rocks that exist within the subglacial ancient drainage basin servicing the Rayner Complex. Veevers & Saeed (2011) gathered data on detrital zircon to map known ages of rock outcrops in Antarctica and also predict ages of bedrock from subglacial sources upflow (Figure 3).

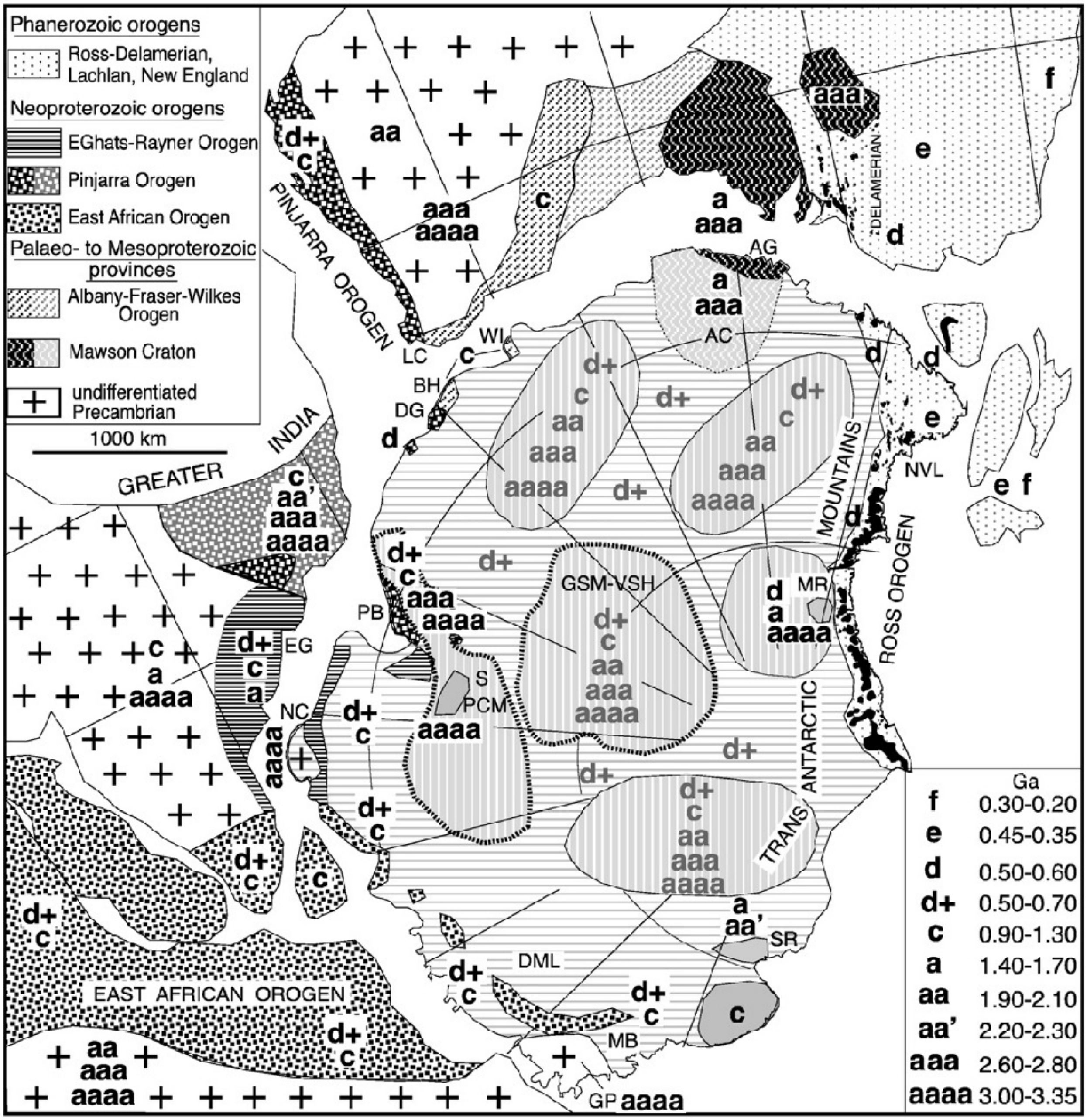

Figure 3. Ages of ice-covered Antarctic bedrock is shown in grey, from data collected from detrital zircon. Known age-clusters of currently exposed outcrops are shown in black, for both Antarctica and its Gondwanan neighbours. Antarctic ice-covered cratons contain rocks with age clusters aaaa to d+, set within orogenic fold belts of age cluster d+. Rayner Complex (striped horizontal lines behind Napier Complex (NC)) forms part of neoproterozoic Eastern Ghats-Rayner Orogen. Other abbreviations relevant to potential provences of detritus in the Rayner Complex include SPCM (southern Prince Charles Mountains) and GSM-VSH (Gamburtsev Subglacial Mountains – Vostok Subglacial Highlands) (Veevers & Saeed 2011, p.5).

2. Methods of analysis, presentation and interpretation of data.

Zircon grains were collected and prepared from crushed samples using standard techniques. Under binocular microscope zircons were mounted in epoxy blocks and polished for further analysis. Approximately 60-100 grains were analysed per sample. CL imagery was used to reveal zircon grains' internal structure (inherited cores, and igneous/metamorphic rims). Cathodoluminescence (CL) microscopy and Back-scattered electron (BSE) imaging was performed on a FEI Quanta 600 MLA environmental scanning electron microscope at the Central Science Laboratory, University of Tasmania.

U-Pb analysis

U-Pb zircon analyses were performed on a 193 nm excimer laser (Resolution M-50), equipped with a two-volume ablation cell and coupled with a quadrupole ICP-MS (Agilent 7700x), at the School of Earth Sciences, University of Tasmania.

Common-lead corrections, for small contributions of common Pb, were not applied to this data. Isoplot v.3 (Ludwig 2003) was used for U-Pb Concordia and Probability Density Plots. Age clusters were based on the 207Pb/206Pb ages for all grains. Data are presented in age probability plots (Ludwig 2003) which show the number of analyses within each 20 million-year interval.

Age data alone cannot distinguish between two zircon grains of similar age from dissimilar provenances. For the purpose of clarifying provenance, U-Pb ages and Hf-isotope measurements from single grains of zircon were analysed (Belousova et al 2002).

Hf-isotopes

Hf-isotope zircon analyses were performed on a New Wave UP-213 Nd:YAG laser ablation microprobe attached to a Nu Plasma multi-collector (MC)-ICPMS system, GEMOC, Macquarie University.

Spot size was between 60-40µm. The fluence, or laser's ablation energy, was 2J/cm^2.

Cores, overgrowths and rims were analysed in separate ablations. CL images were used to ensure that the same portion of the zircon grain was analysed.

During the period in which data was collected, repeated measurements of reference zircons demonstrated the accuracy and precision of the technique.

Analysis if Mud Tank zircon gave

176Hf/177Hf = 0.282516±16 (2sd, n=12)

which is within error of the long-term value obtained in the laboratory of 0.282522±42 (2sd, n = 2335) (Griffin et al 2007).

Analysis of Temora gave

176Hf/177Hf = 0.28687+23/-22 (2sd, n = 8)

which is within error of the long-term value obtained in the laboratory of 0.282684±14 (2sd, n = 24) (Xu et al 2004).

For the calculation of εHf values, which give the difference between the sample and a chondritic reservoir in parts/10^4, we have adopted the chondritic values of Blichert-Toft et al (1997).

The model of Blichert-Toft et al (1997) was also used to calculate model ages TDM and TDM^c. TDM model age gives a minimum age for magma formed from depleted-mantle at the time of the zircon grain's petrogenesis. It is calculated from the measured $^{176}Lu/^{177}Hf$ of each zircon grain. TDM^c is considered a more realistic crustal model age. It assumes that at the time of zircon petrogenesis, the grain's magmatic source was similar to an average continental crust (Veevers & Saeed 2011).

εHf values and model ages used in the figures were calculated using the value of the ^{176}Lu decay constant of 1.93×10^{-11} (Blichert-Toft et al 1997).

Tables of analytical data for metapelite samples 90024, AC34, FS0214, FS0224, SW54, GS01 are available in Appendix A.

Letter symbols of zircon age clusters from East Antarctica, relevant to my samples, were adopted from the comprehensive system used by Veevers & Saeed (2008). This age range was expanded to incorporate all concordant ages recorded in detrital zircon from the six samples used in this study (Table 1). Because of the large number of 207/206Pb-aged grains occurring at the 2500Ma border between Archaean and Proterozoic, age cluster **aa'** and **aaa** were expanded up to this boundary. Age cluster **a** was also expanded 100Ma.

Table 1. Cluster of zircon ages of bedrock in East Antarctica (modified from Veevers 2000; Veevers et al 2006, Veevers and Saeed 2008).

Code	Ga	Ma
d+	0.50 - 0.70	500 - 700
ddd	0.80 - 1.00	800 - 1000
c	0.90 - 1.30	900 - 1300
bb	1.30 - 1.40	1300 - 1400
a	1.40 - 1.80	1400 - 1800
aa	1.90 - 2.10	1900 - 2100
aa'	2.20 - 2.50	2200 - 2500
aaa	2.50 - 2.95	2500 - 2950
aaaa	3.0 - 3.35	3000 - 3350

Adopting Wang et al (2011) interpretation of Th/U ratios, every zircon grain was placed in one of three categories: felsic magmatic, mafic-intermediate magmatic and metamorphic grains either grown or recrystallised during metamorphic events. The Th/U ranges of the two igneous rock types overlap in Table 2, leading some scientists to disregard this method of Th/U ratio interpretation.

In many instances, a zircon grain retains its original magmatic Th/U ratio, even after undergoing metamorphism. According to Wang et al (2011), metamorphic zircon has Th/U < 0.1. A metamorphosed grain was either formed during a metamorphic event, or underwent intense metamorphism after petrogenesis. To help identify cases where a metamorphosed rock retained its original magmatic Th/U ratio, CL zoning and Th/U ratios were compared. This provided a more definitive answer to each grain's petrogenesis and subsequent magmatic and metamorphic history. Using this method enabled, for example, a clearer interpretation as to whether a homogenous rim was caused by a metamorphic or igneous event. For grains which displayed metamorphic CL zoning (ghost oscillatory zoning or sector zoning), but recorded a magmatic Th/U ratio, this led to a better understanding of their original host rock type.

Using Th/U ratios to further classify zircon grains according to their stage of magmatic zircon crystallization enabled clearer differentiation of the magmatic or metamorphic provenance of zircon populations, that could not be distinguished through analysis of εHf, morphology, CL zoning, 207/206 ages or T_{DM}^{c} (Wang et al 2011, p.170).

Table 2. Statistical data on U and Th contents providing the basis for my categorization of Th/U ratios from igneous zircon grains; sourced from felsic or mafic-intermediate magmatic host rocks (Wang et al 2011, p.168).

	Zircon in granitic rocks			Zircon in mafic to intermediate rocks		
	Data n=1684			Data n=667		
	U (ppm)	Th (ppm)	Th/U	U (ppm)	Th (ppm)	Th/U
Range	23–10799	3–9089	0.01–3.79	17–3948	5–9690	0.02–6.82
Mode	125	75	0.40	75	75	0.70
Median	350	140	0.52	270	170	0.81
Mean	600	310	0.59	450	450	0.93

Wang et al (2011) explained the causes of differing Th/U ratios as follows.

Early stage zircon (ESZ) has Th/U ≥ 0.1 – 0.2, forming during a low growth rate of zircon, with high and constant temperature within a deep magma chamber. It crystallized in near-equillibrium with magma.

This low Th/U ratio was caused by U and Th often being excluded from zircon lattice due to partition coefficients. U and Th were therefore unlikely to be enriched at the interface between zircon and melt because of their larger diffusion rate (Wang et al 2011, p.169).

Late stage zircon (LSZ) has Th/U peaking between 0.2 - 0.7. LSZ formed during a time of high zircon growth rate caused by Zr oversaturation with decreasing temperature; during the final emplacement of magma. This Zr oversaturation enabled U and Th to enter easily (Wang et al 2011, p.169).

Middle stage zircon (MSZ) has the highest Th/U ratio, beginning from 2.0 - 2.5. Similar to LSZ, MSZ formed during a time of high growth rate because of Zr oversaturation with decreasing temperature. But unlike LSZ, MSZ formed during the ascent of magma. Unlike ESZ, MSZ crystallised in disequilibrium with the melt, because U and Th content of the zircon were not controlled by zircon-melt partition coefficients. Extremely high Th/U magmatic ratios indicate extreme disequilibrium with the melt. There is also evidence that the zoning seen by CL imagery is indicative of crystallization under local disequilibrium conditions, where U and Th contents of zircon can vary significantly (Wang et al 2011, p.169).

For classification of zircon CL zoning, the methodology of Halpin et al 2005 was adopted (Table 3).

Table 3. Zircon core and rim classification as interpreted by CL imaging and morphology (modified from Halpin et al 2005, p.697).

Zircon type	Description	CL response	Interpretation	Samples
C1	Common oscillatory zoning, may get 'ghost' structures, mostly elongate, some stubby with rounded terminations	Mod to low	Magmatic, may be partially recrystallised or modified	90024, AC34, FS0214, FS0223
C2	Homogenous, may get faint/patchy zoning, commonly rounded/stubby	Low to mod	Metamorphic and highly modified magmatic grains	90024, AC34, FS0214, FS0223, SW54
C3	Most diverse internal zoning; radial and irregular sector zoning, planar growth banding	Low to mod	Crystallised from/grown in presence of anatectic melt at high temperatures	90024, AC34, FS0214, FS0223 SW54
C4	Broad concentric zoning, stubby to elongate	Mod to low	Metamorphic recrystallisation/ growth	FS0214
R1	'Bleached' appearance, broadly homogeneous, may preserve patchy concentric zoning	Mod to high	Recrystallisation/modification of pre-existing zircon during metamorphism	90024, SW54,
R2	Variable thickness and often discontinuous, homogeneous	Mod to low	Growth of new zircon during metamorphism	90024, AC34, FS0214, FS0223, SW54, GS01

Age of deposition

In this study, age of deposition has utilised Young and Black (1991) Rb-Sr whole rock ages of Colbeck Gneiss and Painted Gneiss to help pinpoint maximum age of deposition. Young and Black (1991) suggested initial deposition occurred before c.1250Ma. This has been interpreted to imply that all zircons younger than c.1250Ma must have formed during or been affected by metamorphism.

Therefore, grains greater than or equal to 1250Ma in 207/206Pb age, with minimal Pb-loss and a high percentage of concordance, formed the focus group. Oscillatory or concentric CL zoning and a Th/U ratio within Wang et al (2011) igneous range helped confirm the grain's igneous detrital origin. Only detrital igneous grain cores (not grown in situ) were considered. CL imagery also assisted in interpreting the degree of metamorphism. Zircons with recrystallisation features such as homogenous (potentially metamorphic), sector or chaotic CL zoning were avoided. Metamorphic episodes might have disturbed or reset original U-Pb age of detrital grains. However, most samples had undergone such widespread metamorphism, that some CL modification was unavoidable. Local igneous and metamorphic events were also taken into consideration.

3. Regional Geology

Mesoproterozoic Rayner Complex is formed partly from older reworked crust from neighbouring Archaean Napier complex, composed of rocks dated c.3800-2500Ma and anorthosites dated c.1450-1500Ma (Harley & Kelly 2007, p.156) (See later section: 'Comparison with properties of known rock types from Kemp and MacRobertson Lands'). A significant portion of the exposed outcrops in Rayner Complex are also composed of Proterozoic sediments and younger intrusives like c.960Ma charnockites. The known rock types reached granulite facies possibly during a combination of metamorphic events between c.1000-980Ma and c.930-920Ma, known as the Rayner Structural Episode (RSE) (Harley & Kelly 2007) (Figure 4).

Kemp Land (Stillwell Hills samples FS0214, FS0223, GS01 and SW54), underwent this metamorphic event c.930-920Ma. Metapelitic mineral assemblages occurring in Rusty Gneiss (FS0223) suggest peak metamorphic conditions of $T \approx 870 - 930°C$ at $P \approx 7.6 – 8.9$ kbar (Halpin et al 2007a, p.1323). Halpin et al (2007c) suggests Si-undersaturated metapelite hosted by pink gneiss (FS0214) indicated 'clockwise P-T-t evolution with post-peak decompression-cooling', whilst the addition of leucosome transgressing strong foliation suggests temperatures high enough to cause partial melting (Halpin 2007c, p.114). These factors suggest high-P and high-T metamorphic conditions were met (Ellis 1983; Kelly & Harley 2004).

In MacRobertson Land (Cape Bruce sample AC34 and Forbes Glacier sample 90024), this metamorphic event occurred c.1000-980Ma, and yet the P-T conditions were quite different, with the mineral assemblage of MacRobertson Land and northern Prince Charles Mountains suggesting lower-P conditions and a P-T path dominated by near-isobaric cooling (Halpin et al 2007b, p. 683).

Peak metamorphism is reported to have occurred at lower P-T conditions; with $P \approx 5\text{-}7$ Kbar and $T>700°C$ (Dunkley et al 2002).

Ice coverage between Kemp and MacRobertson Lands, and the intense deformation suffered by rocks in Kemp Land, makes confirmation of the structural relationship between these two regions difficult. It is possible that RSE metamorphic age discrepancy reflects a two-stage collision between the Ruker Terrane and the Mawson Continent (which included eastern India) and a microcontinent that included Archaean Napier complex (Harley & Kelly 2007, p.156) (See Eastern Ghats-Rayner Orogen in Figure 3).

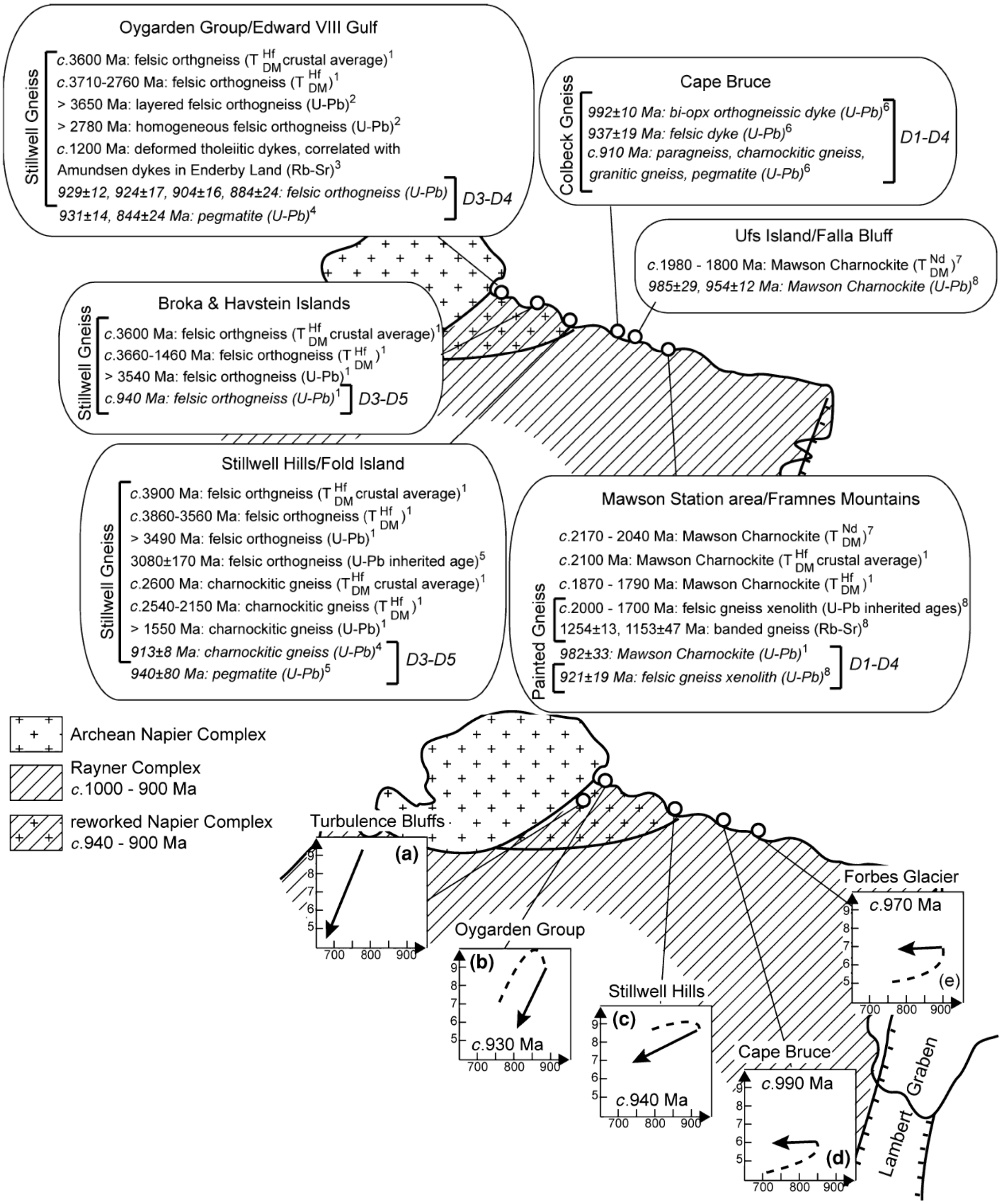

Figure 4. Geological history of Kemp and MacRobertson Lands, including deformational events and differing P-T-t conditions of peak metamorphism during RSE. Known rock types of Trail (1970) are shown, though various layers incorporated within these rock types (including metapelitic layers from Stillwell Hills) are conspicuously absent. Also shown is Archaean cratonic material from Napier complex, reworked during the Rayner Orogeny (Halpin et al 2005, p.686).

4. Results

4.1 Initial Hf ratio vs. age

In the plot of Initial Hf vs age, with the Chondritic Unfractionated Reservoir (CHUR) reference line at zero, zircons that plot above the line had host magmas derived in part from juvenile mantle (fertile) sources and those below the line from older reworked (recycled) crustal material (Figure 5). Zircon populations that contain clusters of grains plotting above and below the line, had a mix of host magmas generated by a combination of juvenile depleted mantle and older reworked crustal sources (Veevers & Saeed 2011). The higher the zircon plots towards the reference line of the Depleted Mantle (DM), the more likelihood of composition from a single pure depleted mantle source. Sample 90024 from Forbes Glacier and sample FS0214 from Stillwell Hills both contain zircon grains of near-identical composition to the Depleted Mantle that existed during their petrogenesis (TDM).

Samples 90024, AC34 from MacRobertson Land and GS01 from Stillwell Hills, Kemp Land, contain a significant number of grains with magmatic composition comparable to CHUR. Whereas the majority of grains from samples FS0214, FS0223 and SW54 are mostly composed of recycled crustal material.

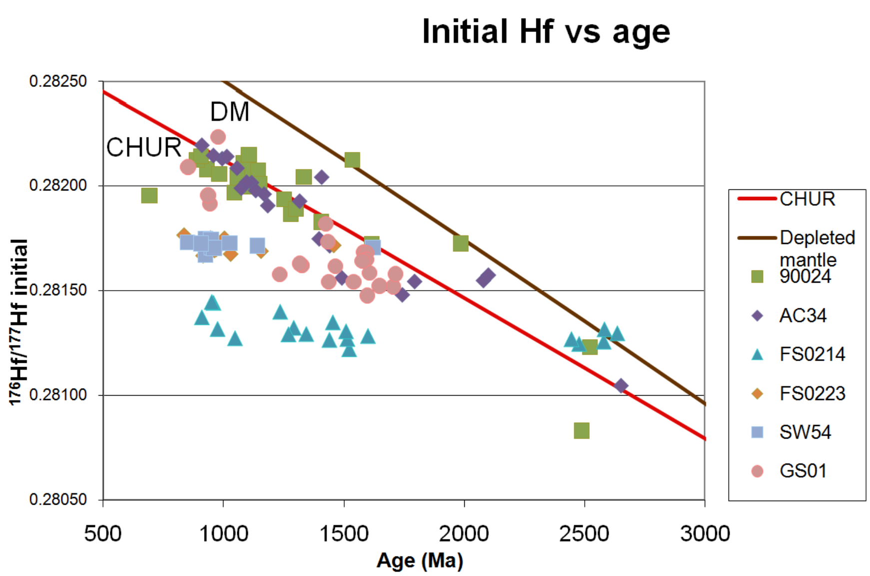

Figure 5. Initial Hf vs age of detrital and metamorphic zircon populations from metapelitic samples 90024, AC34, FS0214, FS0223, SW54 and GS01.

4.4 MacRobertson Land samples

Sample AC34: Colbeck Gneiss (metapelitic gneiss), Cape Bruce

Metasedimentary and granitic gneiss, known as Colbeck Gneiss (sample AC34), is suspected of being part of a conformable sequence with Forbes Glacier's Painted Gneiss (90024). It was intruded (as was Painted Gneiss) by Mawson charnockite at Cape Bruce (Halpin et al 2007b, p.684). In Figure 6, brown biotite with its perfect cleavage is intergrown with sillimanite, the highest temperature form of Al_2SiO_5. In this thin section, sillimanite occurs both as prismatic crystals, diamond-shaped in cross-section, and as needle-like crystals within other minerals. This rock has been metamorphosed in the lower pressure part of the granulite facies. Cordierite has low birefringence and low relief, common in alumina-rich rocks that have been thermally metamorphosed (MacKenzie & Adams 2009)

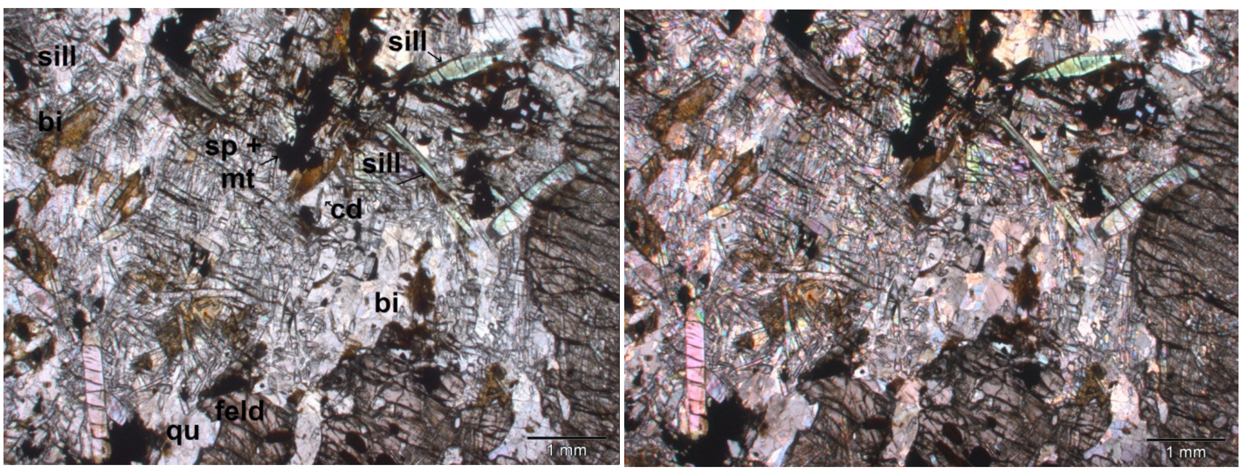

Figure 6. Textural relationships in metapelitic sample AC34 from Cape Bruce, MacRobertson Land. Mineral assemblage: sillimanite – biotite – spinel – magnetite – cordierite – quartz – feldspar. (Sample AC34, thin section in plane and crossed polar light).

Maximum age of deposition

Nd model ages of detrital zircon from Mawson charnockite of between c.2200-1600Ma indicates sample AC34 was deposited before sample 90024. Both Colbeck Gneiss and Painted Gneiss were underlain by Palaeoproterozoic basement (Young & Black 1991). In this study, after a single inherited grain from age cluster **aaa**, a steady stream of regular zircon ages begins with age cluster **aa**, **a** and onwards. With minimal Pb-loss, igneous oscillatory (C1) core grain 6A from age cluster **c** is dated 1258±23Ma. Th/U ratio of 0.47 is well within Wang et al (2011) felsic igneous range and concordance is 104%. However, patchy CL zonation in the R1 rim indicates possible modification of pre-existing zircon during metamorphism at a later date (Figure 7).

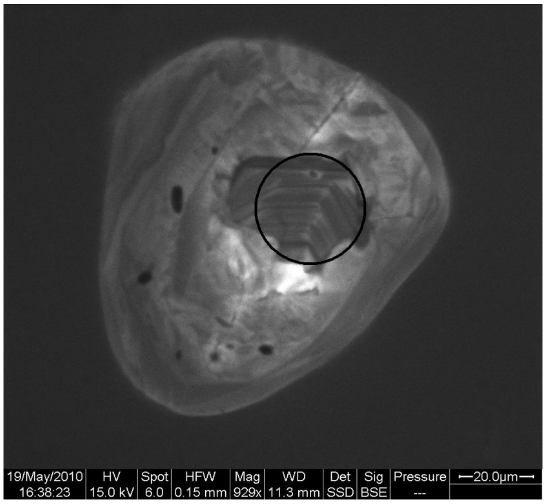

Figure 7. CL image of grain 6A, sample AC34, Cape Bruce. (Black circle shows location of U-Pb analysis).

Concordia diagram

Because of the multiple populations of zircon grains from different provenances in this study, and also because of Pb-loss suffered during c.945Ma RSE, the lower intercept on the Concordia diagrams in all six metapelite samples are poorly constrained. The upper intercept age of the chord represents a minimum crystallization age for the igneous population of grains in each sample.

In sample AC34, 88 analyses from cores and rims of detrital and metamorphic zircon grains yield an upper intercept age of 2050±110Ma (1se) and poorly-constrained lower intercept age of 1003±27Ma. (MSWD = 13). (Figure 8a).

Probability Density Plot

In AC34, the single peak occurs slightly earlier than sample 90024 at c.900Ma (age cluster **c**), but the overall population density curve between both MacRobertson Land samples is very similar (Figure 8b).

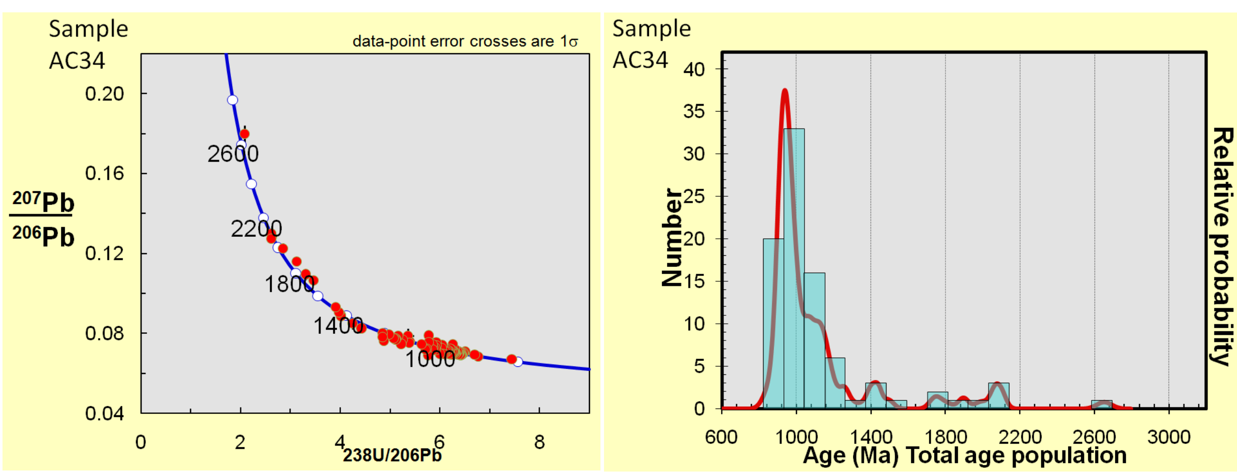

Figure 8. a) Concordia diagram and b) Probability Density Plot of total age population for sample AC34, Cape Bruce.

U-Pb and Hf-analysis of sample AC34

In sample AC34, 87 zircon grains were analysed (See Appendix A). 19 grains underwent Hf-analysis (Table 4). Grains were 207Pb/206Pb aged between 2650±40Ma (age cluster **aaa**) and 838±30Ma (age cluster **ddd**).

T_{DM} peaks occurred between 2.03-1.40Ga and 2.89-2.05Ga. Th/U ratios between 1.04 – 0.01 indicate a wide range of igneous and metamorphic formation; from mafic-felsic middle-to-late stage and ESZ magmatic crystallization to highly metamorphic ratios.

Igneous grains with Th/U ratio ≥0.1 – 0.2 are interpreted as ESZ, forming deep in a magma chamber during low growth rate and high and constant temperature; crystallizing in near-equillibrium with magma (Wang et al 2011, p.169). Grains with Th/U ratio peaking between 0.2 – 0.7 are interpreted as LSZ; forming during final magma emplacement and a high crystal growth rate due to Zr oversaturation with decreasing temperature and final emplacement of magma. Grains with Th/U ratio beginning 2.0 - 2.5 are interpreted as MSZ, forming during the ascent of magma; with high growth rate and in disequilibrium with the melt (Wang et al 2011, p.169). The higher the Th/U ratio, the greater the disequilibrium.

In this sample, there was only one distinctly inherited granitic grain (4) in its own age cluster; with Archaean age of 2650±40Ma and the oldest $T_{DM}{}^{c}$ of 3.07Ga. εHf of 0.60 (fertile) indicated a depleted mantle source close to CHUR standard, which already contained a mix of juvenile and recycled crustal material. This grain also had lowest initial Hf and third-lowest 176Lu/177Hf and 176Yb/177Hf ratios.

Metamorphic Th/U ratios <0.1 are shown in bold in Table 4. This does not mean that only the grains with metamorphic Th/U ratios underwent metamorphism or were of metamorphic origin. It is likely that many igneous grains in this sample underwent partial recrystallisation or modification; but retained a Th/U ratio within the igneous range of Wang et al (2011). But when Th/U ratio interpretation is used in conjunction with the zircon's CL image, a clearer understanding of the grain's geohistory can emerge.

Table 4. Sample AC34: Hf-analysis and Th/U ratios of selected grains from Colbeck Gneiss, Cape Bruce.

Zircon Age Clusters	Age (Ma)	Sample	Zircon Type	T(DM) crustal (Ga)	εHf	Th/U ratio
aaa (n=1)	**2650**	**AC34-4**	C1	3.07	0.60	0.46
aa	**2099**	**AC34-70**	C1	2.29	6.24	0.80
(n = 2)	**2078**	**AC34-27**	C3	2.37	4.81	0.51
a	**1792**	**AC34-5**	C1	2.57	-2.10	0.86
(n = 6)	**1741**	**AC34-68A**	C3	2.75	-5.57	0.23
	1490	**AC34-34**	C1	2.74	-8.58	0.59
	1440	**AC34-78**	C1	2.44	-4.31	0.55
	1406	**AC34-2A**	C1	1.74	6.53	0.60
	1396	**AC34-44**	C1	2.39	-4.17	0.53
bb (n=1)	**1315**	**AC34-85**	C1	2.05	0.33	0.39
c	**1182**	**AC34-36**	C1	2.19	-3.50	0.88
(n = 11)	**1167**	**AC34-87**	C1	2.08	-1.91	0.70
	1132	**AC34-3**	C1	2.06	-2.11	0.72
	1115	**AC34-14**	C2	1.99	-1.18	0.84
	1094	**AC34-23**	C1	2.00	-1.57	0.78
	1072	**AC34-18**	C1	2.08	-3.11	0.30
	1054	**AC34-48**	C1	1.88	-0.12	0.69
	1012	**AC34-2B**	R2	1.79	0.86	**0.01**
	993	**AC34-26**	C1	1.82	0.06	1.04
	956	**AC34-68B**	R2	1.81	-0.25	**0.01**
	908	**AC34-55**	C3	1.74	0.38	**0.06**

The first age cluster (**aa**) contains 5 grains, dated between 2099±25Ma and 1895±26 Ma. Th/U ratios indicate mixed petrogenesis between mafic-to-felsic igneous events. CL zoning includes igneous oscillatory patterns (C1), but also metamorphic indicators of ghost oscillatory (C1) and sector zoning (C3). Crystal morphology was mostly equant.

Age cluster **bb**, dated 1396±28Ma to 1315±62Ma, contains felsic-granitic grains 85 and 44 with εHf of 0.33 to -4.17, revealing a mix of both fertile and recycled sources. Older grain 44 had more enriched recycled εHf, whilst younger grain 85 had higher εHf fertile source; indicating a higher percentage of depleted mantle magma in the mix.

The most significant age cluster (**c)** contains 66 zircon grains. 19 grains underwent Hf-analysis. εHf ranged between 0.86 (close to CHUR) to -3.50 revealing a mix of both fertile and recycled magma content. The highest εHf in this sample, belonging to grain 2B, might indicate petrogeneisis during a felsic igneous event. Strongly metamorphosed Th/U ratio of 0.01 and chaotic (C2) zoning has erased previous history of this ovoid grain's formation.

The youngest age cluster (**ddd)** contained 2 grains aged 883±39Ma and 838±30MA. Although Hf-analysis was not undertaken, ghost oscillatory (C1) CL zoning reveals a history of igneous petrogenesis and partial metamorphism after deposition at Cape Bruce; with metamorphic Th/U of 0.07. Younger grain 84 reveals sector (C3) CL zoning; which combined with a Th/U ratio of 0.09 indicates possible metamorphic petrogenesis.

45 grains have a metamorphic Th/U ratio <0.1. Metamorphic ages range from c.1057Ma (age cluster **c**) to c.838Ma (age cluster **ddd**), with Th/U ratios 0.09 - 0.01. The majority are in age cluster **c**, metamorphosed during the Rayner Structural Episode (RSE).

The CL zoning of cores with a metamorphic Th/U ratio are mostly sector (C3) or homogenous/patchy/chaotic (C2). A minority retain ghost oscillatory zoning (C1) from igneous formation before subsequent metamorphism.

CL response ranged from low to high.

Grain morphology range from mostly ovoid (sub-round to sub-angular) to characteristically metamorphic equant (sub-round) crystal shapes. In this sample, only a few metamorphic grains are elongate; with the majority of elongated grains having magmatic Th/U ratios.

Sample 90024: Garnet-cordierite-rich lens from Painted Gneiss

Sample 90024 comes from a garnet-cordierite-rich lens, from within a layer of felsic gneiss referred to as Painted Gneiss. Painted Gneiss forms inclusions in the c.985-955Ma Mawson Charnockite, Mawson Coast (Halpin et al 2007b). (See sample 90030 in section: 'Comparison of properties of known rock types in Kemp and MacRobertson Lands).

In Figure 9, spinel and magnetite inclusions are enclosed within high relief garnet (<2mm across) and low relief cordierite (<1mm across). Cordierite is common in alumina-rich rocks which have been thermally metamorphosed. Cordierite and garnet are replaced by high relief colourless sillimanite and brown biotite at grain edges. Sillimanite is the highest temperature form of Al2SiO5 and in this rock it forms within garnet. Note spinel and ilmenite surrounded by a double corona of (inner) sillimanite and (outer) garnet.

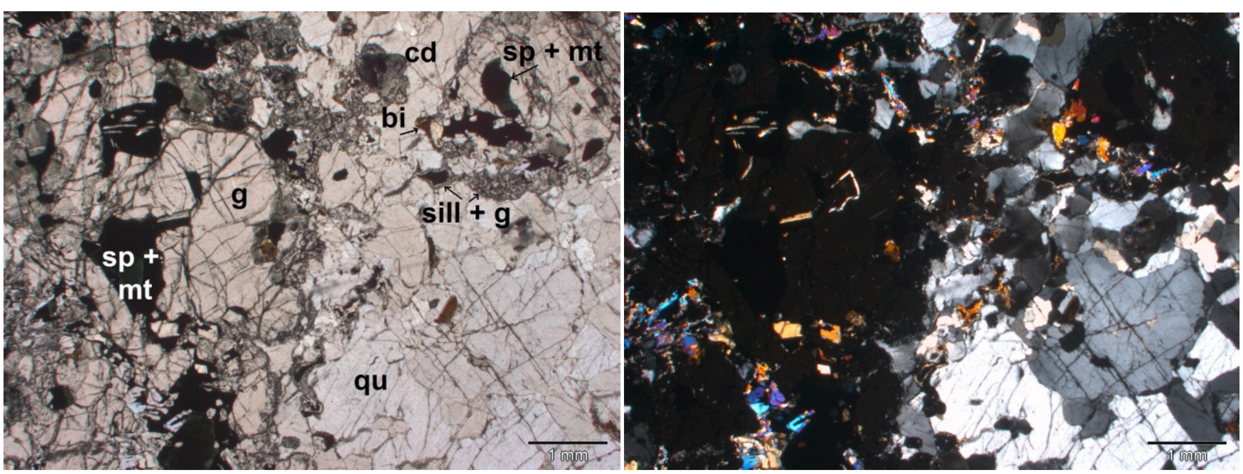

Figure 9. Textural relationships in metapelitic sample 90024 from Forbes Glacier. Mineral assemblage: Garnet – biotite – cordierite – sillimanite – spinel – magnetite – quartz (Sample 90024, thin section in plane and crossed polar light).

Maximum age of deposition

Rb-Sr whole rock ages of c.1250 – 1150Ma in Painted Gneiss (90024) suggested initial deposition occurred before c.1250Ma (Young & Black 1991). To ascertain maximum age of deposition, igneous oscillatory-zoned (C1) core of grain 3A was chosen from age cluster **c.** With felsic igneous Th/U ratio of 0.57, its core is 207/206Pb dated 1251±27 Ma. The core of grain 3A retains 98% concordance. The bleached CL zonation of this grain's (R1) outer rim suggests the existing grain underwent some modification during metamorphism at a later date (Figure 10).

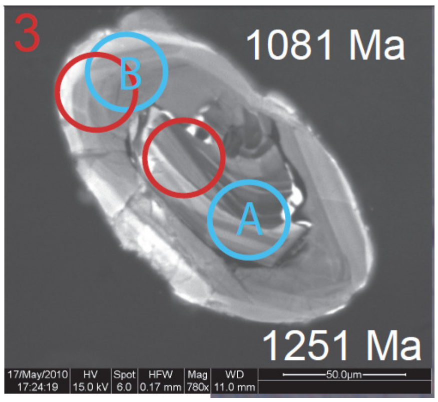

Figure 10. Grain 3A from sample 90024, Forbes Glacier, MacRobertson Land. (Blue circle A indicates location of U-Pb analysis in the core).

Concordia diagram

In sample 90024, 86 analyses from cores and rims of detrital and metamorphic zircon grains yielded an upper intercept age of 2156±120 Ma (1se) and poorly constrained lower intercept age of 964±21Ma. (MSWD = 10.5) (Figure 11a).

Probability Density Plot

In sample 90024, a single peak occurs c.950Ma (age cluster **c**) (Figure 11 b).

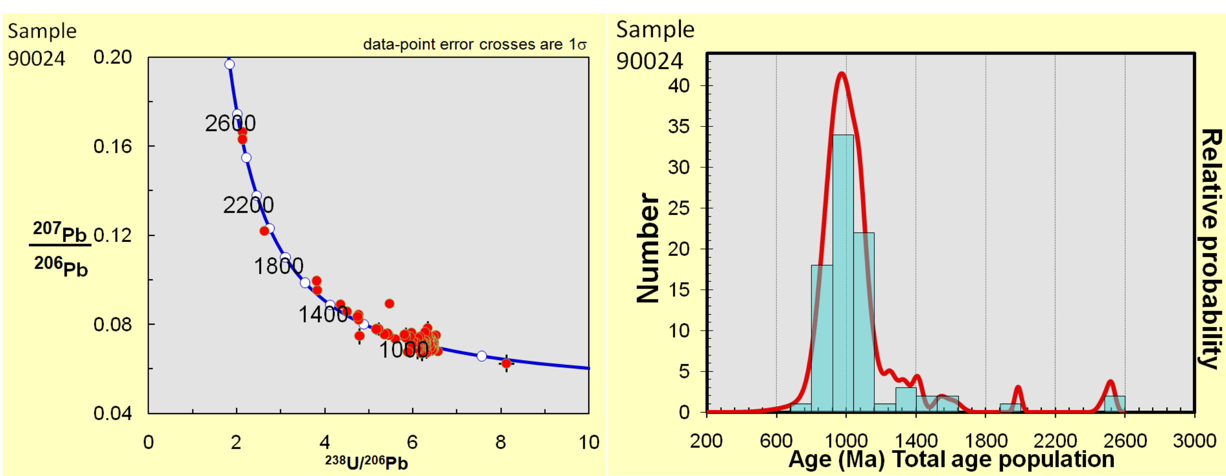

Figure 11. a) Concordia diagram and b) Probability Density Plot of total age population for sample 90024, Forbes Glacier.

U-Pb and Hf-analysis of sample 90024

76 zircon grains were U-Pb analysed from sample 90024 (See Appendix A). 20 of these grains also underwent Hf-analysis (Table 4).

Grain 207Pb/206Pb ages ranged between 2522±22Ma (age cluster **aaa**) and 692±131Ma (age cluster **d+**). T_{DM} peaks occured at 2.03-1.47Ga and 3.17-2.66Ga. (There is a T_{DM} gap between 2.03-2.66Ga). Th/U ratios between 1.06 – 0.08 incorporate mafic-to-felsic igneous Early stage zircon (ESZ), Middle stage zircon (MSZ) and Late stage zircon (LSZ) crystallization, as well as one grain that fell within Wang et al (2011) range for metamorphic zircon. (Metamorphic Th/U ratios <0.1 are shown in bold in Table 5).

Table 5. Sample 90024: Hf-analysis and Th/U ratios of selected grains from Painted gneiss (garnet-cordierite-rich lens), Forbes Glacier, MacRobertson land

Zircon Age Clusters	Age (Ma)	Sample	Zircon Type	T(DM) crustal (Ga)	εHf	Th/U ratio
aaa (n=1)	**2522**	**90024-15**	C1	2.75	4.10	0.41
aa	**2488**	**90024-42**	C2	3.65	-10.96	0.39
(n = 2)	**1986**	**90024-60**	C1	2.04	8.91	0.59
a	**1615**	**90024-83**	C3	2.30	0.06	0.46
(n = 3)	**1536**	**90024-51**	C1	1.48	12.42	0.82
	1406	**90024-81**	C1	2.21	-1.08	0.59
bb (n=1)	**1333**	**90024-37**	C2	1.79	4.84	0.20
c	**1300**	**90024-77**	C1-bk	2.15	-1.35	0.26
(n = 15)	**1280**	**90024-14**	C1	2.21	-2.72	0.25
	1251	**90024-3A**	C1	2.08	-0.89	0.57
	1150	**90024-75**	C1	1.98	-0.54	0.58
	1144	**90024-36**	C1	1.85	1.55	0.85
	1105	**90024-63A**	C1	1.71	3.28	1.06
	1084	**90024-41**	C1-bk	2.05	-2.59	0.50
	1084	**90024-22**	C1-bk	1.81	1.37	0.42
	1081	**90024-3B**	R2	1.88	0.13	0.10
	1057	**90024-50A**	C1	1.98	-1.67	0.53
	1046	**90024-71**	C1	2.14	-4.53	0.43
	982	**90024-63B**	R1	1.99	-2.87	0.70
	931	**90024-23**	R2	1.97	-3.21	**0.08**
	907	**90024-73**	R1	1.85	-1.58	0.21
	889	**90024-50B**	R1	1.90	-2.58	0.43
d+ (n=1)	**692**	**90024-20**	C1	2.39	-13.17	0.32

Properties of the total zircon grain population, divided into age clusters, in sample 90024

The oldest three grains, being single representatives of older age clusters (**aaa, aa', aa**), were possibly eroded contemporaneously with the younger grains of age cluster **a**. Howard et al (2009) documented such a case in the Gawler Craton, where erosion occurring between 1870-1850Ma produced detrital zircon age populations of c.2520, 2450 and 2000Ma (Howard et al 2009, p.284).

Age cluster **a** contains four grains 207/206Pb-aged between 1615±44 and 1406±31 Ma. εHf ranges from 12.42 to -1.08 (fertile – recycled) and $T_{DM}{}^{c}$ between 2.30-1.48 Ga.

In age group **bb**, grains 37 and 77 are dated 1333±29 and 1300±48 Ma respectively. εHf ranges from 4.82 to -1.35 (fertile – recycled) and $T_{DM}{}^{c}$ between 2.15-1.79 Ga.

The most significant age cluster **c** contains 67 grains ranging in age from 1280±67 to 901±141 Ma. Their εHf of 3.28 to -3.21 (fertile-recycled) is fairly constrained; revealing a juvenile-crustal signature. $T_{DM}{}^{c}$ lies between 2.21 – 1.71 Ga.

Age cluster **ddd** contains 7 grains, aged between 891±46Ma and 838±107 Ma. Hf-analysis of one grain recorded εHf of -2.58 (recycled) and $T_{DM}{}^{c}$ of 1.90Ga.

Age cluster **d+**, the youngest grain recorded in any of the metapelitic samples, has εHf of -13.17; indicative of substantial recycled crustal content and $T_{DM}{}^{c}$ of 2.39Ga. All grains in sample 90024 have retained a magmatic Th/U ratio signature, except for one grain in age cluster **c**.

4.5 Kemp Land samples: Stillwell Hills

The four metapelitic gneissic layers from Stillwell Hills discussed in this study (FS0214, SW54, GS01, FS0223) are tightly-to-isoclinally folded, deformed and dismembered within Archaean Stillwell Hills felsic-mafic orthogneiss (See sample SW268 in later section: 'Comparison of properties of known rock types from Kemp and MacRobertson Lands). Extreme deformation, probably during RSE, has made confirmation of depositional age of these four metapelitic layers problematic (Figure 12). This study was in part undertaken to use detrital and magmatic zircon grains from these metapelitic samples, to shed some light on their ages of deposition within the Stillwell Hills region of Kemp Land.

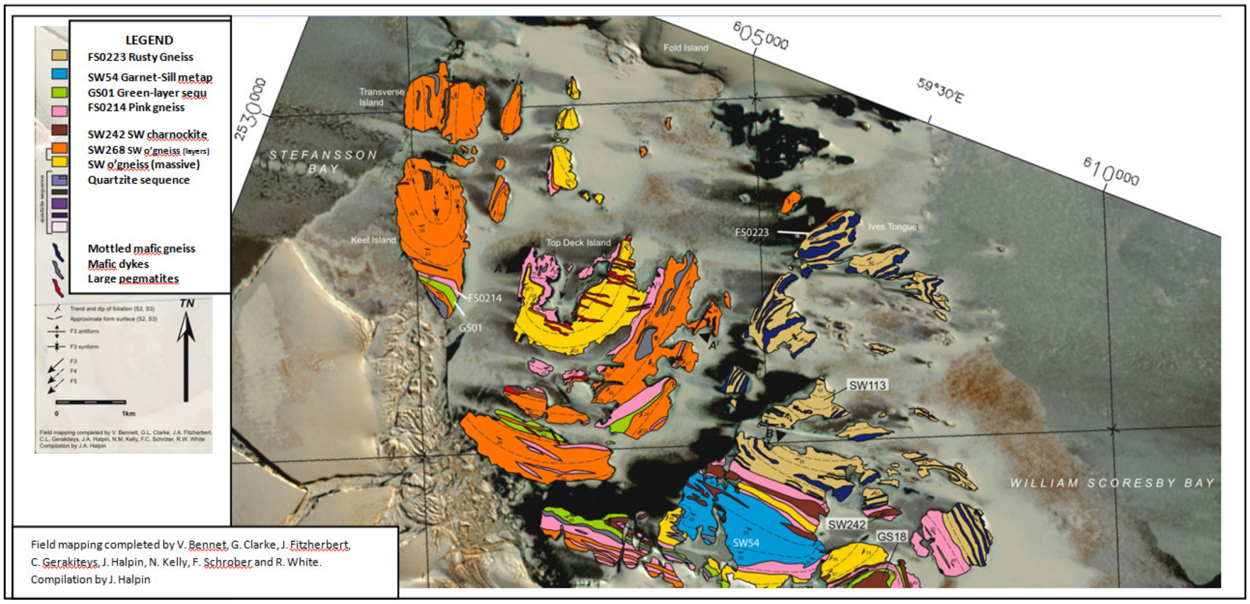

Figure 12. Field mapping of Stillwell Hills rock units, with locations of all four metapelite samples from Stillwell Hills used in this study (FS0223, SW54, GS01, FS0214). Included are proximal known rock types Stillwell Orthogneiss (well-layered) (SW268) and Stillwell Charnockite (SW242A).

Sample FS0214: Pink Gneiss, Keel Island, Stillwell Hills

Pink Gneiss is a massive-to-migmatic felsic gneiss with minor foliation evident, dominated by 'perthitic alkali feldspar, quartz and plagioclase with minor garnet and biotite' (Halpin et al 2007c, p.102).

In figure 13, very minor patches of garnet are clearly visible only under crossed polars. Minor magnetite grows between the crystal boundaries of polygonal alkali feldspar and quartz. Abundant alkali feldspar (65%) envelop smaller quartz crystals. Plagioclase is not evident in this thin section.

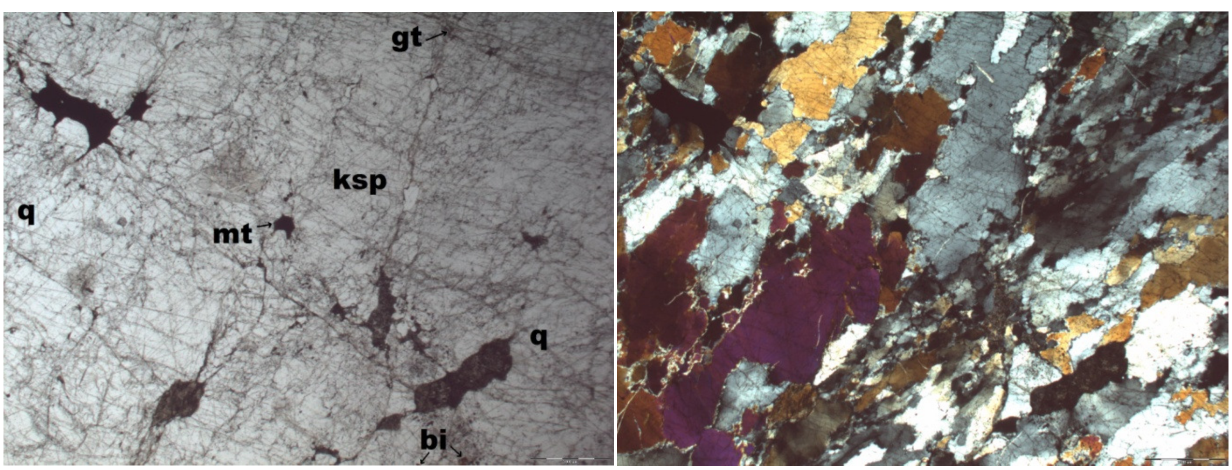

Figure 13. Textural relationships in Pink Gneiss FS0214. Mineral assemblage: quartz – magnetite – K-feldspar – garnet – biotite (just at bottom of photo). (Sample FS0214, thin section shown in plane and crossed polar light).

Maximum age of deposition

A steady stream of grains flowed in regular intervals consistently from the very first age cluster **aaa**, through age cluster **aa** and onwards. The igneous C1 core of subrounded elongate grain 30, in age cluster **bb,** has ghost oscillatory CL zoning and felsic igneous Th/U ratio of 0.23 (Figure 14). Dated 1317±51Ma, concordance is 93%.

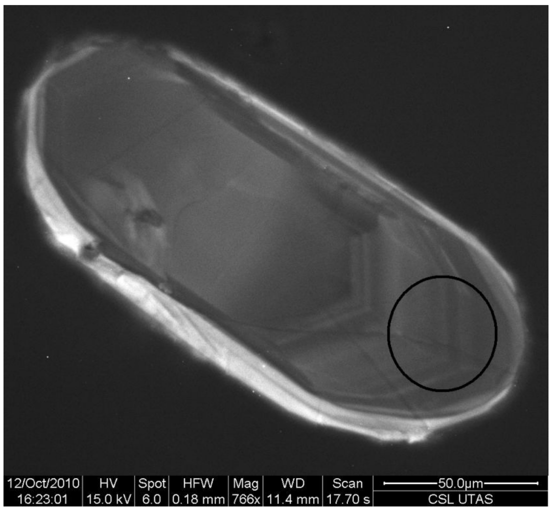

Figure 14. Grain 30 from sample FS0214, Stillwell Hills. (Black circle shows location of U-Pb analysis.)

Concordia Diagram

In sample FS0214, 78 analyses from cores and rims of detrital and metamorphic zircon grains yield an upper intercept age of 2398±95Ma (1se) and poorly constrained lower intercept age of 971±36Ma. (MSWD = 12) (Figure 15a).

Probability Density Plot

In sample FS0214, peaks occur at c.1500Ma and 1000Ma (Figure 15b).

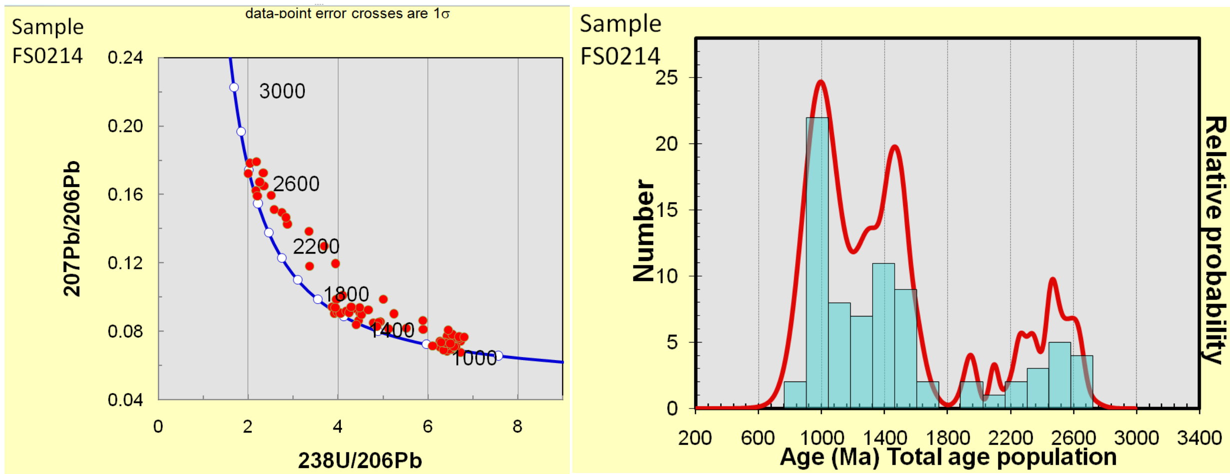

Figure 15. a) Concordia diagram and b) Probability Density Plot of total age population for sample FS0214, Stillwell Hills.

U-Pb and Hf-analysis of sample FS0214

Dated between 2646±83Ma (age cluster **aaa**) and 858±82Ma (age cluster **ddd**), a T_{DM} peak occurs 2.70-2.38Ga. Th/U ratios ranging 0.69 – 0.01 indicate mafic-felsic LSZ and ESZ crystallisation, as well as metamorphic grains.

67 grains were sampled within 1se concordance. 10 grains were rejected. Grains 49A, 78, 86, 93A, 12A and 101 were rejected due to common Pb and Pb loss. Grains 43A and 104 were rejected due to Pb loss throughout. Grain 3 was rejected due to the mix of old core and rim, with Pb loss and some common Pb loss. Grain 27 was rejected due to Common Pb loss and the U-Pb analysis hole drilling into a monazite inclusion (See Appendix A). 20 grains underwent Hf-analysis (Table 6).

Table 6. FS0214: Hf-analysis and Th/U ratios of selected grains from Pink gneiss (massive-migmatic), Keel Is, Stillwell Hills, Kemp Land

Zircon Age Clusters	Age (Ma)	Sample	Zircon Type	T(DM) crustal (Ga)	εHf	Th/U ratio
aaa	**2637**	**FS0214-37A**	C1	2.52	9.24	0.42
(n = 3)	**2583**	**FS0214-58A**	C1	2.52	8.61	0.69
	2580	**FS0214-24**	C1	2.65	6.46	0.34
aa	**2478**	**FS0214-10**	C1	2.75	3.65	0.50
(n = 2)	**2446**	**FS0214-23B**	R2	2.72	3.67	0.30
a	**1600**	**FS0214-36A**	C2	3.26	-15.82	**0.06**
(n = 6)	**1522**	**FS0214-14**	C2	3.44	-19.89	**0.05**
	1514	**FS0214-16B**	R2	3.34	-18.32	**0.03**
	1509	**FS0214-95**	C1-C3	3.27	-17.14	0.17
	1454	**FS0214-46**	C1	3.21	-16.92	**0.08**
	1440	**FS0214-69**	C3	3.40	-20.21	**0.08**
bb (n=1)	**1343**	**FS0214-61**	C2	3.40	-21.45	**0.01**
c	**1291**	**FS0214-102**	C1-bk	3.37	-21.63	**0.04**
(n = 8)	**1269**	**FS0214-97**	C3	3.45	-23.24	0.12
	1235	**FS0214-44**	C1	3.24	-20.23	**0.05**
	1047	**FS0214-79B**	C4	3.62	-29.05	**0.04**
	975	**FS0214-82**	C2	3.57	-29.16	0.34
	957	**FS0214-37B**	C3	3.32	-25.14	0.60
	950	**FS0214-42**	C2	3.32	-25.17	0.43
	909	**FS0214-06**	C1	3.49	-28.70	0.50

Archaean age cluster **aaa** contains 6 grains, dated 2646±83Ma to 2508±43Ma. Hf-analysis records εHf 9.24 to 6.46 fertile/depleted mantle content and T_{DM}^{c} from 2.65-2.52Ga.

Proterozoic age cluster **aa'** contains 8 grains, dated 2478±32Ma to 2207±50Ma. Hf-analysis records an intermediate igneous signature of εHf 3.67 to -18.32 fertile-recycled content and T_{DM}^{c} from 3.34-2.72Ga.

Age cluster **aa** contains 3 grains, dated 2096±28Ma to 1929±53Ma, with Th/U ratio indicating felsic igneous petrogenesis.

Age cluster **a** contains 18 grains, many of which have undergone metamorphism. Dated 1643±74Ma to 1422±50Ma, Hf-analysis records εHf -15.82 to -20.21 strongly recycled content and T_{DM}^{c} from 3.44-3.21Ga.

Age cluster **bb** contains 5 grains, dated 1348±62Ma to 1317±51Ma. Hf-analysis on one grain records an enriched metamorphic signature of εHf -21.45 recycled and T_{DM}^{c} of 3.40Ga.

Age cluster **c** contains 35 grains, dated 1291±57Ma to 904±93Ma. Hf-analysis records an enriched metamorphic signature of εHf -20.23 to -29.16 recycled crustal source and T_{DM}^{c} from 3.62-3.24Ga.

Age cluster **ddd** contains 2 grains, dated 887±93Ma to 858±82Ma. Th/U ratio indicates granitic-felsic provenance, chaotic CL zonation and equant morphology.

21 grains have a metamorphic Th/U ratio <0.1. Metamorphic ages range from c.1643Ma (age cluster a) to 1047Ma (age cluster c), with Th/U ratios 0.08 - 0.01. The majority are in age cluster c, metamorphosed during the Rayner Structural Episode (RSE). The predominant CL zoning is homogenous/patchy/chaotic (C2) with only a few grains showing sector zoning (C3) or ghost oscillatory (C1).

CL response ranges from mod-low to mod-high.

Grain morphology ranges from ovoid, elongate, to the characteristically metamorphic equant (sub-round to sub-angular) crystal shapes. In this sample, there is no characteristic difference between metamorphic and magmatic grain-shapes.

GSO1: Green layered sequence, Keel Island, Stillwell Hills

The Green layered sequence is made up of various layers of differing provenances. It is green where diopside-bearing assemblages predominate (Halpin et al 2007c, p.104). The gneissic layers can include assemblages of garnet, sillimanite, biotite and orthopyroxene, plus optional of cordierite, garnet, sapphire, spinel and corundum. The protolith of the metapelitic gneiss layer is sedimentary in origin.

In Figure 16, a metapelitic layer of GS01 contains an assemblage of garnet-orthopyroxene-biotite gneiss. Porphyroblastic garnet incorporates brown poorly-orientated lathes of biotite and inclusions of dark brown ilmenite. Porphyroblastic orthopyroxene shows irregular cracks and faint cleavages. Low relief plagioclase grows in light patches bordering garnet porphyroblasts. A peak metamorphic assemblage is indicated by the inclusion of all these minerals, although biotite can also indicate retrograde metamorphism.

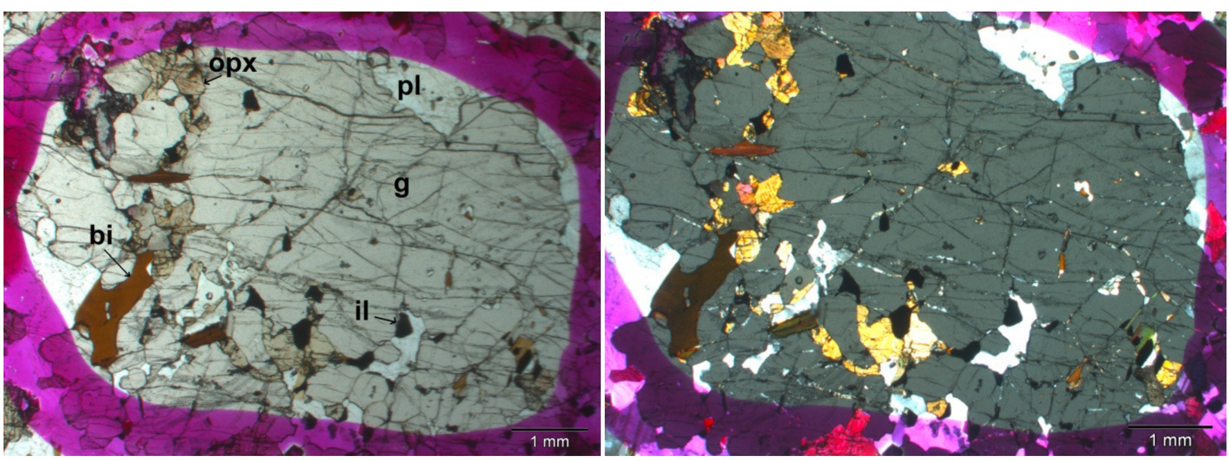

Figure 16.Textural relationships in metapelite GSO1 from Kemp Land. Mineral assemblage: biotite - orthopyroxene – ilmenite - plagioclase – garnet. (Purple colour is marker-pen on the thin section.) (Sample GS01, thin section in plane and crossed polar light).

Maximum age of deposition

The grains in sample GS01 have undergone such extensive metamorphism, the youngest igneous grain with minimal Pb-loss and 97% concordance, is an outer core from grain 96 in age cluster **bb** (Figure 17)**.** Dated 1316±33 Ma, with felsic igneous Th/U ratio of 0.15, the C1 outer core contains ghost structures with moderate CL response.

Younger grain 103 was discarded not only because of a lower concordance, but because its CL image showed metamorphic sector zonation within the dark core.

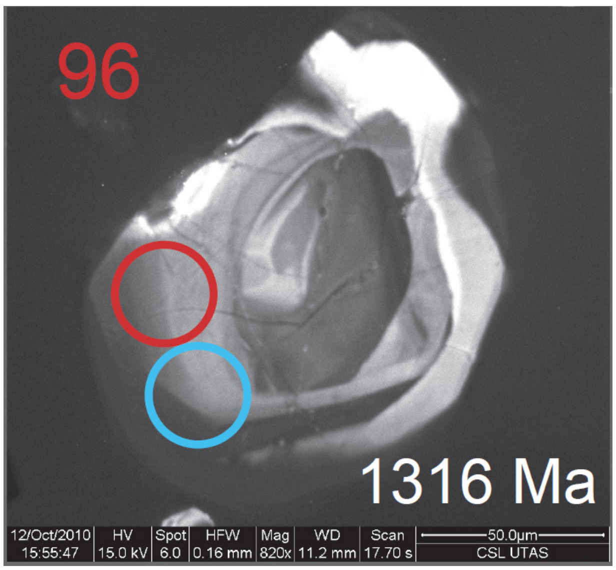

Figure 17. Grain 96 from sample GS01. (Blue circle shows location of U-Pb analysis).

Concordia Diagram

In sample GS01, 81 analyses from cores and rims of detrital and metamorphic zircon grains yield an upper intercept age of 1619±35Ma (1se) and poorly constrained lower intercept age of 967±22Ma. (MSWD = 1.5). (Figure 18a).

Probability Density Plot

The four samples from Stillwell Hills, Kemp Land have more individualistic age population clusters, but share similar aged peaks.

In GS01, peaks occur at c.1525Ma and c.925Ma (Figure 18b).

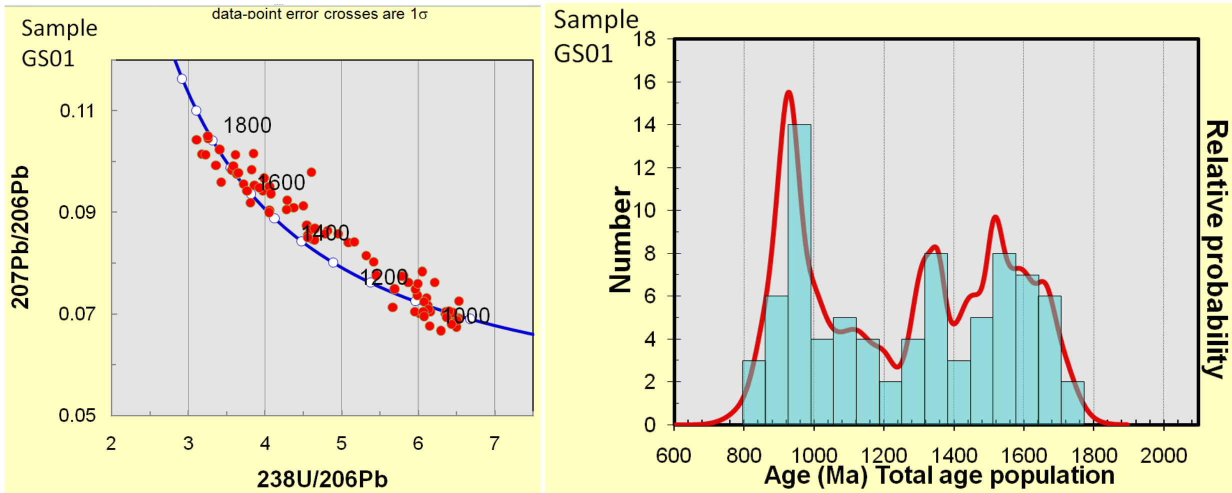

Figure 18. a) Concordia diagram and b) Probability Density Plot of total age population for sample GS01, Stillwell Hills.

U-Pb and Hf-analysis of sample GS01

In sample GS01, 70 grains were U-Pb dated within 1se concordance. Grain 100 was rejected due to common Pb and Pb loss and grain 94 from reverse discordance and Pb loss (Appendix A). 19 grains underwent Hf-analysis (Table 7).

207/207Pb dated between 1715±44Ma (age cluster **a**) and 829±56Ma (age cluster **ddd**), T_{DM} peaks occurred between 2.03-1.60Ga, 2.41-2.00Ga and 2.86-2.41Ga. Th/U ratios range between 0.92 – 0.06 (mafic-to-felsic and metamorphosed) indicating MSZ, LSZ and ESZ magmatic crystallization, as well as some metamorphic grains.

Age cluster **a** is dated between 1715±44Ma and 1425±54Ma. 14 grains were also Hf-analysed, with εHf -0.97 (close to CHUR) to -10.51 (recycled/enriched content). $T_{DM}{}^{c}$ is dated between 2.85-2.22Ga.

Age cluster **bb** is U-Pb dated between 1370±33Ma and 1306±29Ma. Despite 5 grains recording an igneous Th/U ratio >0.1, all bar one have metamorphic CL zoning patterns. Crystal shapes range between ovoid and equant; with low – high CL response.

Age cluster **c** is U-Pb dated between 1297±30Ma and 905±28Ma. Four grains were Hf-analysed with εHf 3.37 to -13.99 fertile-recycled content. $T_{DM}{}^{c}$ is dated between 2.86-1.60Ga.

Age cluster **ddd**, dated between 897±43Ma and 829±56Ma, have felsic-granitic Th/U ratios and ovoid – equant morphology. CL zoning ranges from patchy-chaotic, homogenous (C2) and sector (C3).

15 grains have a metamorphic Th/U ratio <0.1 (shown in bold in Table). Metamorphic ages range from 1668Ma (age cluster a) to 905Ma (age cluster c), with Th/U ratios 0.09 - 0.01. The majority are in age cluster **a**, when both Kemp and MacRobertson Lands were undergoing multiple metamorphic events (Halpin et al 2005).

Overall, CL zoning is mostly metamorphic sector (C3), with two homogenous (C2) and one oscillatory (C1) grain. CL response ranged from low to high.

Grain morphology is equant (sub-round), apart from four ovoid-shaped grains. In this sample, grains with equant morphology trend towards those with a metamorphic Th/U ratio.

Table 7. GS01: Hf-analysis and Th/U ratios of selected grains from Green-layered metapelitic gneiss, Keel Is, Stillwell Hills, Kemp Land

Zircon Age Clusters	Age (Ma)	Sample	Zircon Type	T(DM) crustal (Ga)	εHf	Th/U ratio
a	**1715**	**GS01-42**	C1	2.55	-2.67	0.23
(n = 14)	**1706**	**GS01-20A**	C1	2.68	-5.00	0.19
	1648	**GS01-22**	C1	2.71	-6.23	0.23
	1607	**GS01-68/70**	C2	2.61	-4.99	0.34
	1598	**GS01-86**	C2	2.85	-9.05	0.23
	1593	**GS01-105**	C3	2.41	-1.94	0.39
	1592	**GS01-14A**	C1-bk	2.48	-3.05	**0.08**
	1582	**GS01-102**	C2	2.41	-2.10	**0.06**
	1578	**GS01-97A**	C1	2.50	-3.70	**0.09**
	1540	**GS01-87**	C3	2.74	-8.07	0.28
	1465	**GS01-10**	C1-bk/C2	2.63	-7.22	**0.07**
	1437	**GS01-101A**	C1-bk	2.81	-10.51	0.14
	1433	**GS01-17**	C1	2.40	-3.81	**0.06**
	1425	**GS01-85A**	C1	2.22	-0.97	0.34
bb	**1326**	**GS01-9**	C2	2.72	-10.35	0.19
(n = 2)	**1316**	**GS01-96**	C2	2.70	-10.24	0.15
c	**1233**	**GS01-101B**	C3	2.86	-13.99	0.45
(n = 4)	**978**	**GS01-52**	C3	1.60	3.37	0.92
	942	**GS01-31**	C3	2.32	-8.75	0.52
	936	**GS01-85B**	R2	2.24	-7.49	0.23
ddd (n=1)	**852**	**GS01-11B**	R2	2.00	-4.64	0.21

Sample SW54: Garnet-Sillimanite Metapelite, south of Ives Tongue, Stillwell Hills

Halpin et al (2007c) describes Garnet-Sillimanite Metapelite as laterally expansive and outcropping in a basin-structure towards the north of the field area. Mostly consisting of garnet, sillimanite and alkali feldspar with or without biotite and magnetite, the sillimanite mode is variable (mostly 30-50%); defining a strong lineation.

In Figure 19, random decussate lathes of biotite and anhedral quartz grew between the boundaries of multi-twinned plagioclase and polygonal garnet. Tartan-twinned microcline is apparent in the bottom left corner. Dark inclusions of magnetite grow within and on the rim of poikiloblastic garnet.

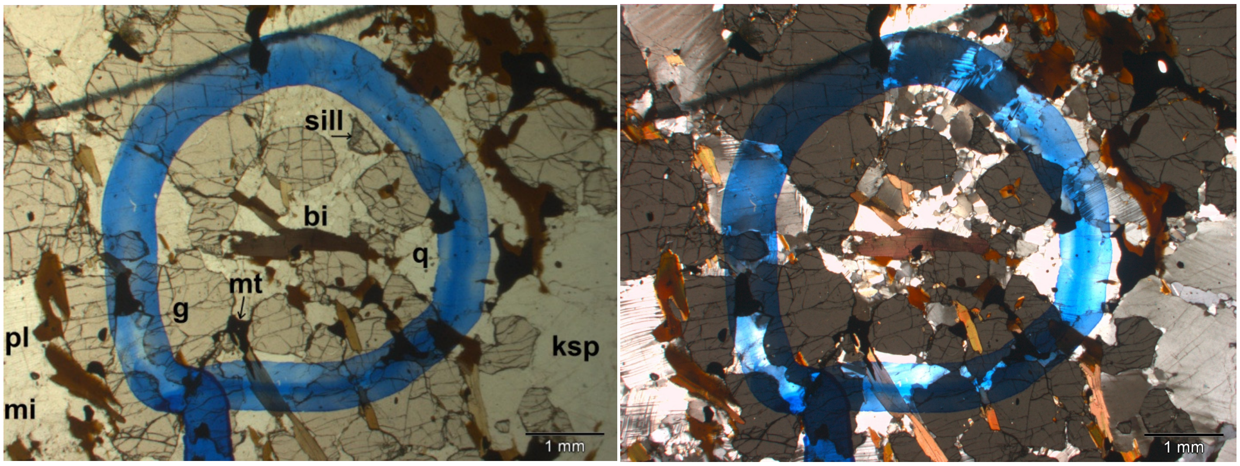

Figure 19. Textural relationships in Garnet-sillimanite metapelite SW54. Mineral assemblage: microcline – plagioclase – garnet – magnetite – K-feldspar – quartz – sillimanite (Blue colour is marker pen on the thin section). (Sample SW54, thin section under plane and crossed polar light).

Maximum age of deposition

The core of grain 48A in age cluster **c** has one of the highest concordance of 93% in the sample and minimal Pb loss**.** Dated 1260±47Ma (Figure 20), this igneous rounded grain records a felsic igneous Th/U ratio of 0.11. Its C1 ghost oscillatory core belongs to a grain which reveals metamorphic sector zoning in its outer rims. Most grains in this sample showed definite signs of metamorphism in their CL image.

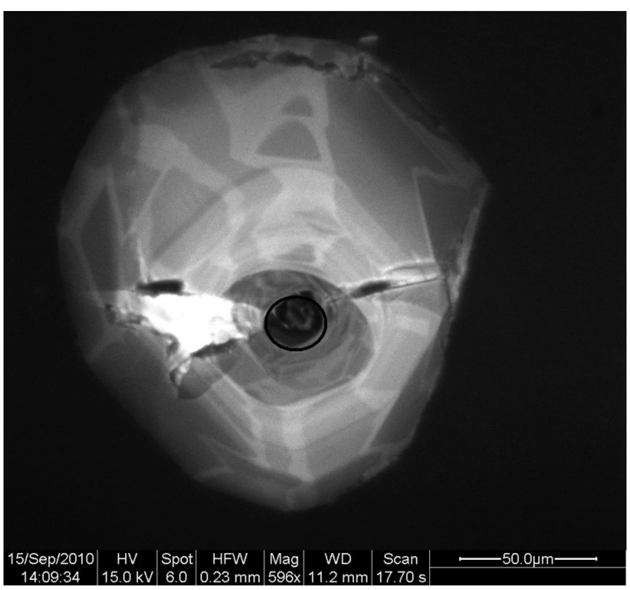

Figure 20. Grain 48A from sample SW54, Stillwell Hills. (Black circle indicates location of U-Pb analysis).

Concordia diagram

In sample SW54, 78 analyses from cores and rims of detrital and metamorphic zircon grains yield an upper intercept age of 2277±170Ma (1se) and poorly constrained lower intercept age of 906±12Ma. (MSWD = 3.6). (Figure 21a).

Probability Density Plot

In SW54, a single peak occurs at c.950Ma (Figure 21b).

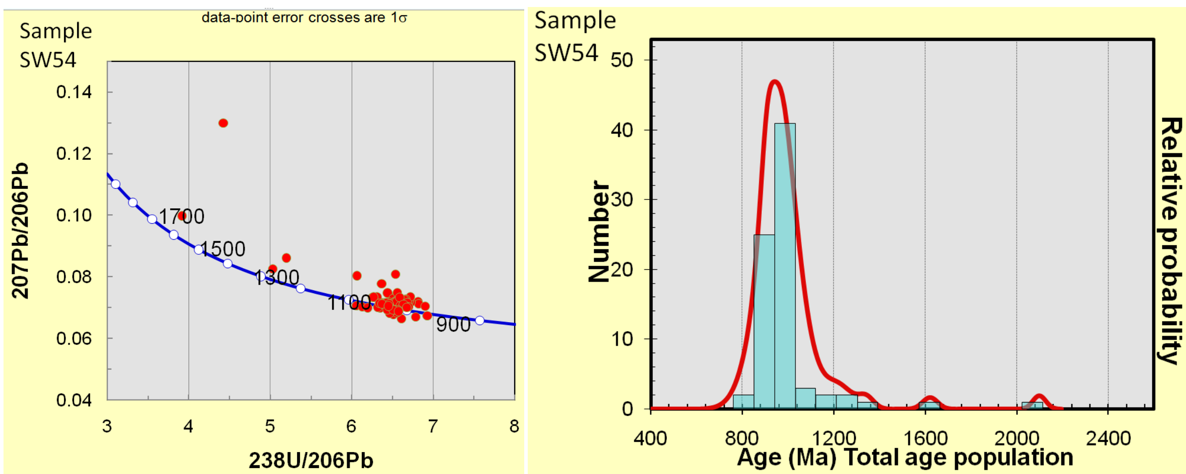

Figure 21. a) Concordia diagram and b) Probability Density Plot of total age population for sample SW54, Stillwell Hills.

U-Pb and Hf-analysis of sample SW54

Dated between 1620Ma (age cluster **a**) and 850Ma (age cluster **ddd**), a T_{DM} Peak occurs 2.09-1.99Ga. Th/U ratios range between 0.7 – 0.07 indicating mafic-felsic LSZ and ESZ magmatic crystallization and metamorphic grains.

61 grains were U-Pb dated, with two grains (41A and 100A) rejected due to being a mix of detrital seed and core and having common Pb and Pb loss (See Appendix A). 6 grains in total underwent Hf-analysis (Table 8).

Table 8. SW54: Hf-analysis and Th/U ratios of selected grains from Garnet-sillimanite metapelite, south of Ives Tongue, Stillwell Hills, Kemp Land

Zircon Age Clusters	Age (Ma)	Sample	Zircon Type	T(DM) crustal (Ga)	εHf	Th/U ratio
a (n=1)	**1620**	**SW54-98A**	C3	2.34	-0.42	0.48
c	**1141**	**SW54-41C**	R1	2.63	-11.28	0.67
(n = 9)	**1025**	**SW54-98B**	C3	2.67	-13.54	0.70
	960	**SW54-89B**	C3	2.76	-15.84	0.65
	948	**SW54-41D**	R2	2.77	-16.06	0.56
	948	**SW54-41B**	C1	2.69	-14.73	0.18
	940	**SW54-25A**	C3	2.72	-15.41	0.55
	925	**SW54-25B**	R2	2.69	-15.14	0.48
	924	**SW54-3**	C3	2.85	-17.83	0.60
	907	**SW54-89C**	R2	2.75	-16.32	**0.07**
ddd (n=1)	**850**	**SW54-62**	C2	2.77	-17.43	0.54

Age cluster **aa** has a single inherited grain 86, 207/206Pb dated 2097±28Ma. No Hf-analysis was undertaken, but chaotic CL zoning combined with equant morphology and Th/U ratio 0.08 indicates metamorphism.

Single grain 89A in age cluster **bb** is dated 1341±33Ma, with Th/U ratio of 0.18 indicating igneous petrogenesis; and yet sector (C3) CL zoning indicates at least partial metamorphism.

This first significant age cluster (**c**) is U-Pb dated between 1260±47 and 904±34Ma. Five grains were Hf-analysed, with εHf -11.28 to -17.83 strongly recycled content. $T_{DM}{}^{c}$ is dated between 2.85-2.63Ga.

The youngest age cluster (**ddd**) of 7 grains is U-Pb dated between 893±31 and 820±75Ma. They all have igneous Th/U ratios >0.1 and yet several show metamorphic sector zoning. Hf-analysis of one grain from this cluster recorded εHf -17.43 recycled crustal content, $T_{DM}{}^{c}$ of 2.77Ga and granitic Th/U ratio of 0.54.

Only 2 grains have a metamorphic Th/U ratio in this sample, despite the majority of grains in this sample displaying sector zoning characteristic of metamorphism.

FS0223: Rusty Gneiss, Ives Tongue, Stillwell Hills

Halpin et al (2007c) describes this metapelitic layer as an iron-stained, medium-to-coarse-grained metapelitic gneiss; consisting of garnet, sillimanite, quartz, perthitic alkali feldspar, biotite, rutile and ilmenite, with or without plagioclase, magnetite and iron sulphide.

A strong foliation (trending north-south in Figure 22) is defined by prismatic and fine-grained sillimanite, biotite, alkali feldspar, rutile inclusions and quartz. Rusty gneiss contains abundant leucosomes (not visible in the thin section), which mostly lie parallel to the main gneissosity (Halpin et al 2007c, pp.104-106). In this coarse-grained assemblage, poikiloblastic garnet is rimmed by fine-grained biotite lathes.

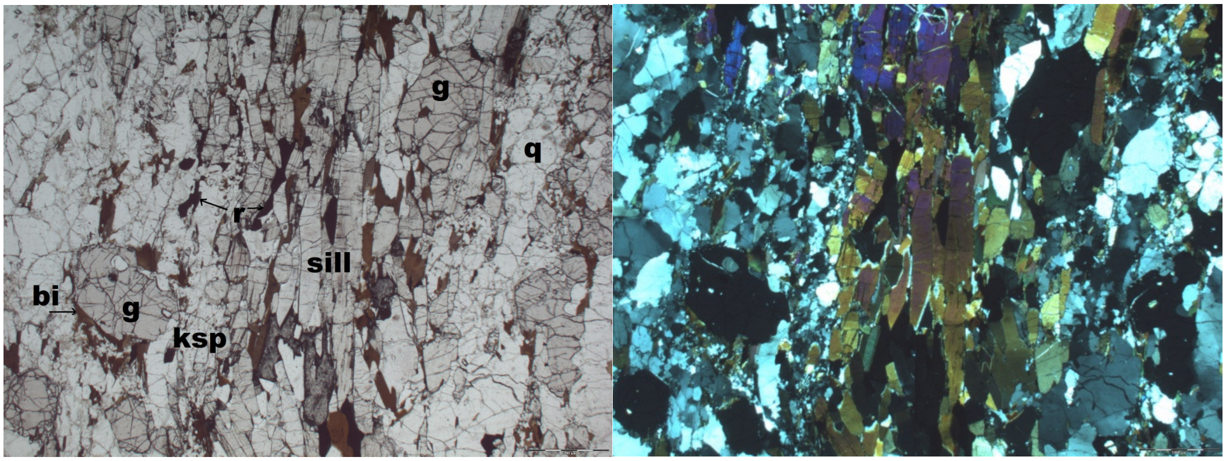

Figure 22. Textural relationships in Rusty Gneiss FS0223. Mineral assemblage: rutile – biotite – garnet – K-spar – sillimanite – quartz. (Sample FS223, thin section shown in plane and crossed polar light).

Maximum age of deposition

Age cluster **c** contains the second oldest felsic igneous grain 40, dated 1178±84Ma (Figure 23). The outer-core has a C2 patchy-homogenous CL image and only 79% concordance, indicating possible modification from later metamorphic events. Its Th/U ratio of 0.16 is within Wang et al (2011) felsic igneous range; but due to signs of metamorphism and this lower concordance, the maximum date recorded by this sample is poorly constrained.

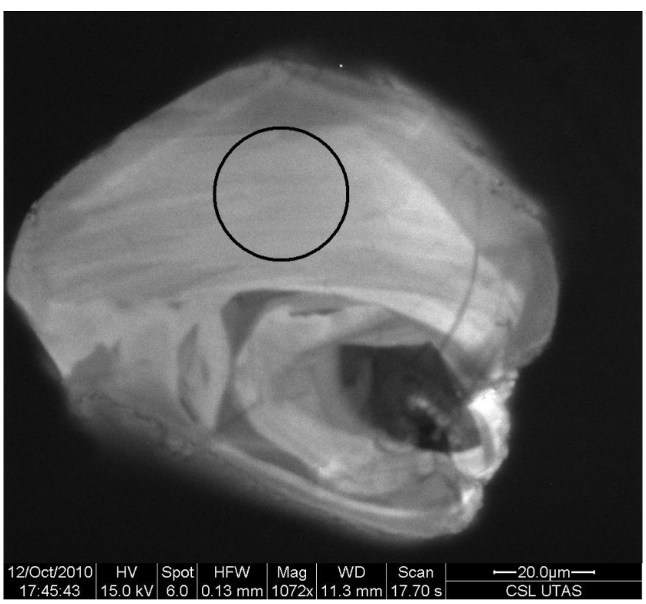

Figure 23. Grain 40 of sample FS0223, Stillwell Hills. (Black circle indicates location of U-Pb analysis).

Concordia diagram

In sample FS0223, 64 analyses from cores and rims of detrital and metamorphic zircon grains yield an upper intercept age of 1440±250Ma (1se) and poorly constrained lower intercept age of 911±29Ma. (MSWD = 0.76) (Figure 24a).

Probability Density Plot

In FS0223, a single peak occurs at c.950Ma, the same as sample SW54. (Figure 24b).

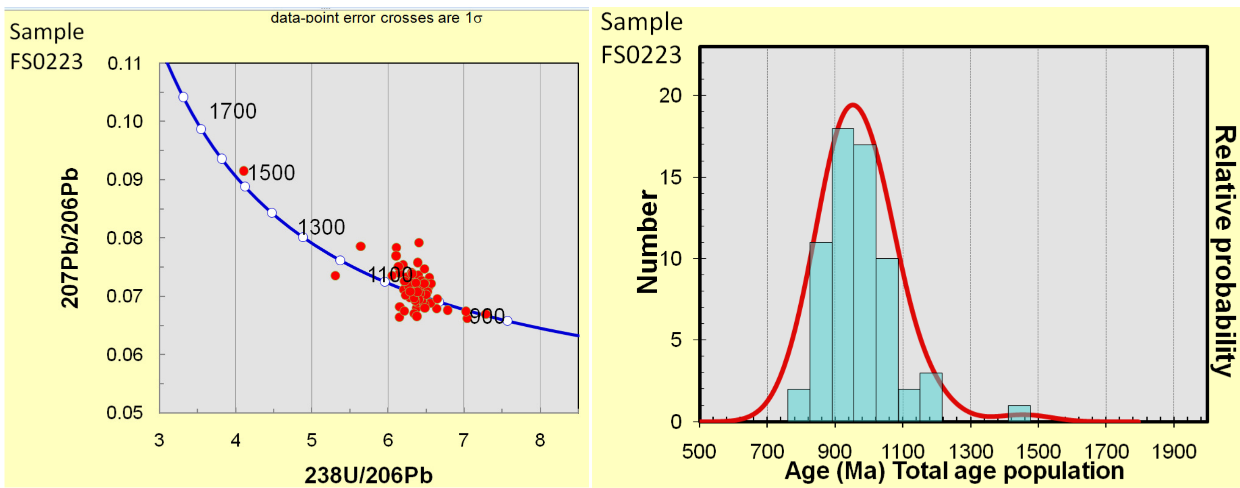

Figure 24. a) Concordia diagram and b) Population Density Plot for total age population of sample FS0223.

U-Pb and Hf-analysis of sample FS0223

Grains are dated between 1457±82Ma (age cluster **a**) and 814±87Ma (age cluster **ddd**), T_{DM} peaks occur between 1.90-1.35Ga and 2.09-1.90Ga. Th/U ratios between 0.2 – 0.01 indicate mafic-felsic LSZ and ESZ as well as metamorphic grains.

63 grains were sampled within 1se concordance of 207/206Pb age. Grain 5A was rejected due to common Pb and Pb loss (See Appendix A). 12 grains underwent Hf-analysis (Table 9).

Age cluster **a** contains single inherited grain 19, aged 1457±82Ma, with the highest εHf -3.80 recycled, and a strongly metamorphosed Th/U ratio of 0.01. Surprisingly, it has the youngest grain T_{DM}^{c} of 2.42Ga. It also has the highest 176Lu/177Hf and 176Yb/177Hf ratios. It was metamict at 1457Ma.

Age cluster **c** contains 47 grains, dated 1178±84Ma to 906±67Ma. Hf-analysis records a massive jump in the enriched metamorphic signature of εHf -11.80 to -18.14 recycled crustal source and T_{DM}^{c} from 2.87-2.63Ga.

Age cluster **ddd** contains 15 grains, dated 898±87Ma to 814±87Ma.

Table 9. FS0223: Hf-analysis and Th/U ratios of selected grains from Rusty gneiss (Iron-stained metapelitic), Ives Tongue, Stillwell Hills, Kemp Land

Zircon Age Clusters		Age (Ma)	Sample	Zircon Type	T(DM) crustal (Ga)	εHf	Th/U ratio
a	**(n=1)**	**1457**	**FS0223-19**	C2	2.42	-3.80	**0.01**
c		**1155**	**FS0223-36**	C2	2.67	-11.80	**0.07**
(n = 10)		**1029**	**FS0223-88**	C2	2.78	-15.22	**0.04**
		1003	**FS0223-89**	C2	2.63	-13.16	**0.09**
		979	**FS0223-76**	C2	2.71	-14.74	0.10
		970	**FS0223-10**	C2	2.77	-15.80	0.15
		962	**FS0223-56**	C2	2.78	-16.17	**0.09**
		953	**FS0223-92**	C3	2.74	-15.62	**0.08**
		945	**FS0223-5**	C2	2.67	-14.47	0.20
		938	**FS0223-59**	R2	2.78	-16.47	**0.07**
		915	**FS0223-35**	C1-bk/C2	2.87	-18.14	0.14
ddd	**(n=1)**	**836**	**FS0223-91**	C1-bk/C2	2.71	-16.49	**0.06**

39 grains have a metamorphic Th/U ratio <0.1. Metamorphic ages range from 1161Ma (age cluster **c**) to 814Ma (age cluster **ddd**), with Th/U ratios 0.08 - 0.01. The majority are in age cluster **c**, metamorphosed during the Rayner Structural Episode (RSE). CL zoning is divided evenly between homogenous/patchy/chaotic (C2) and sector zoning (C3). No sign of oscillatory zoning remains, indicative of either metamorphic petrogenesis or more likely, complete recrystallisation during high-temperature high-pressure metamorphism.

CL response ranges from mod-low to mod-high.

Grain morphology includes ovoid (sub-round to sub-angular), elongate (sub-round to sub-angular) and characteristically metamorphic equant (sub-round) crystal shapes. In this sample, there is no apparent trend between metamorphic and magmatic grain-shapes.

4.6 Th/U ratio vs age

As illustrated in figure 25, all six metapelite samples from Kemp and MacRobertson Land (FS0214, FS0223, GS01, SW54, 90024, AC34), contain a majority of grains with magmatic Th/U ratio >0.1. The highest ratios, signifying mafic-intermediate igneous petrogenesis (Wang et al 2011), are recorded in age cluster **c**. The exception to this is sample FS0214, which had the most mafic-intermediate igneous events occurring during earlier age clusters **a**, **aa'** and **aaa**.

Apart from SW54, there was a preference for lower felsic-granitic Th/U ratios in most age groups. This might indicate that the majority of igneous events forming zircon in Rayner Complex contained strong felsic crustal content. Otherwise, it is possible that the higher nucleation rate of zircon in felsic magma has biased the samples (Howard et al 2011).

The lowest Th/U ratios <0.1 in all samples belong to metamorphic grains, mostly from age cluster **c**; indicative of the widespread metamorphism throughout Kemp and MacRobertson Land during RSE.

Considering that both magmatic high and metamorphic low Th/U ratios co-existed during age cluster **c**, in all samples bar FS0214, it appears that RSE launched a major period of new zircon growth in both Kemp and MacRobertson Land coastlines.

4.7 Grain length vs age

In all metapelitic samples from Kemp and MacRobertson Land, both the longest and the shortest grain lengths were formed during age cluster **c**, during RSE. Earlier age clusters **aaa**, **aa**, **aa'** tended to fall within the mid-length range of zircon grains.

The vast majority of grains in sample 90024 came from age cluster **c**, with some of the longest and most elongate grains (up to 310µm). The middle-length range contained some grains from older age clusters **aaa**, **aa**, **aa'**, as well as a good representation from age cluster **c**. Some of the shortest length grains also came from age cluster **c**, intermixed with earlier and later age clusters **a**, **bb**, **ddd** and **d+**.

As per 90024, the majority of grains in sample AC34 came from age cluster **c**, making it difficult to pinpoint a definite trend. The longest grains (up to 220µm) came from age cluster **c**, as did the shortest grains. It is interesting to note that the minority of grains coming from earlier age clusters **aa** and **a**, fell in the middle-length range.

In sample FS0214, there was a definite trend in age versus length. Apart from the longest grain (250µm) coming from age cluster **a**, the remaining longest grains (185-210µm) all came from age cluster **c**.

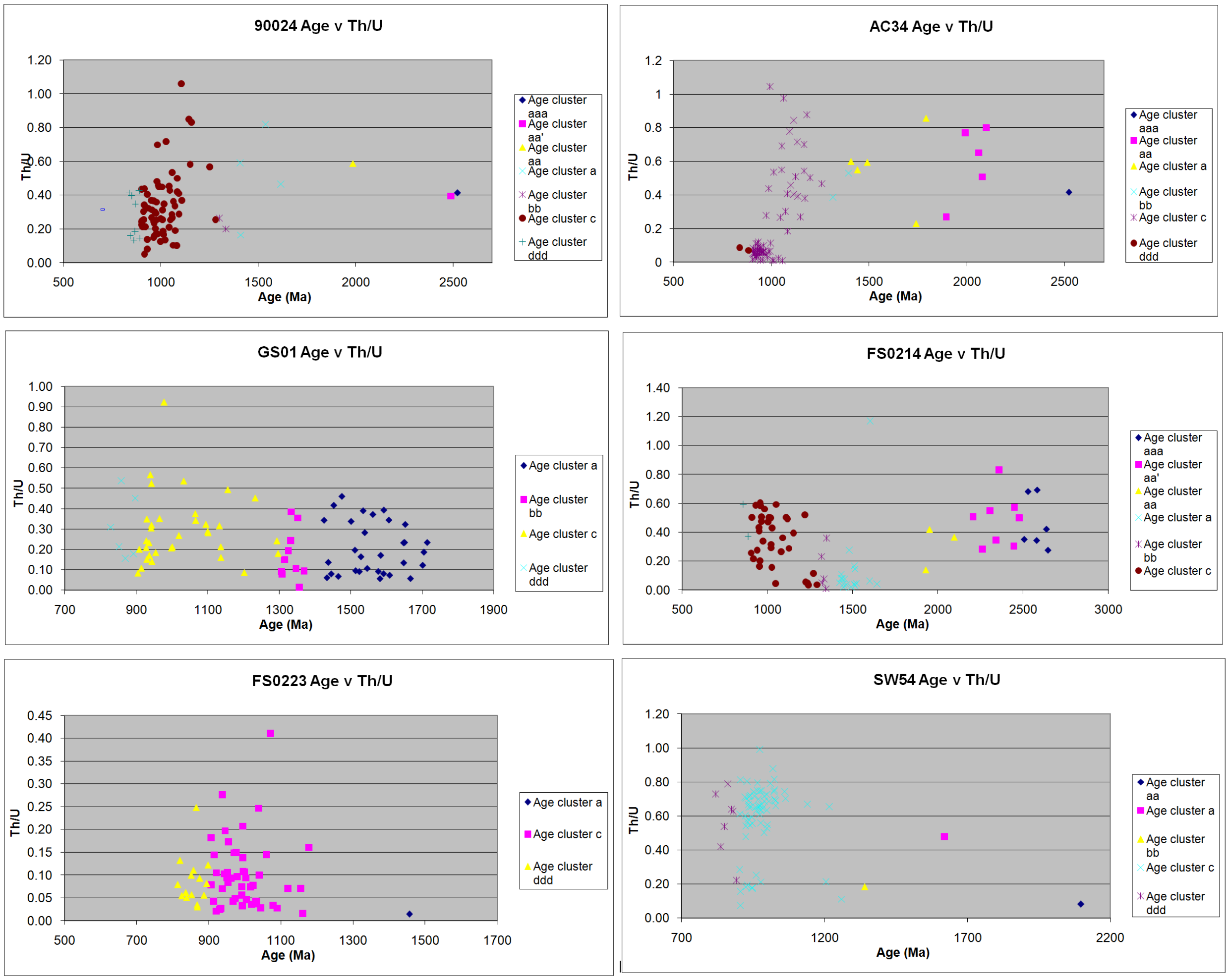

Figure 25. Age vs Th/U plots for metapelitic samples 90024, AC34, GS01, FS0214, FS0223 and SW54.

The middle-length range of grains was almost entirely composed of grains from earlier age clusters **aaa**, **aa'**, **aa** and **a**. The shortest length grains contained a mix of **aaa**, **aa**, **a**, **bb**, **c** and **ddd** age clusters.

In sample FS0223, the longest grains (220-150µm) all came from age cluster **c**, as did the majority of mid-length grains. The shortest grains came from an interwoven mix of age clusters **c** and **ddd**.

Sample GS01 bucked the trend of the longest grains coming predominantly from age cluster **c**. The longest grain (250µm) in this sample came from the earliest age cluster **ddd**; followed by grains from earlier age clusters **a**, **bb** and **c**.

The mid-length grains (120µm) were predominantly from age cluster **a**. Similar to previous samples, the shortest grains were predominantly from age cluster **c**.

In sample SW54, the longest grains (400-220µm) were from age cluster **c**, as were the mid-length and shortest grains; which included a tiny minority of earlier and later age clusters **a**, **aa**, **bb** and **ddd**.

4.8 Comparison to properties of six known rock types from Kemp Land and MacRobertson Land:

In order to prove or disprove provenance of zircon grains from samples 90024, AC34, FS0214, FS0223, SW54 and GS01, a summary of the properties of six known rock types, previously documented in Kemp and MacRobertson Lands (Halpin et al 2005) was undertaken. This was especially important to understand the order of deposition for the Stillwell Hills samples; where a series of deformation events had interwoven these metapelites inextricably with Stillwell Hills orthogneiss (SW268).

Sample 90030: Mawson Charnockitic Orthogneiss, Mawson Station, MacRobertson Land

Halpin et al (2005) U-Pb and Hf-analysed a total of 8 zircon grains, which were emplaced and in part metamorphosed during the Proterozoic (Table 10). A single T_{DM} Peak occurred between 1.87-1.79Ga. Th/U ratio was 2.16 – 0.15, all within range of mafic-felsic magmatic petrogenesis and indicating ESZ, LSZ and MSZ crystallisation.

Proterozoic age cluster **c** contained 6 grains, dated 1063±11Ma to 920±11Ma. εHf ranged from -6.20 to -10.71 recycled and $T_{DM}{}^{c}$ of 2.19-2.05Ga.

Age cluster (**ddd**) contained 2 grains, dated 853±15Ma to 846±14Ma. εHf ranged from -11.12 to -12.84 recycled and $T_{DM}{}^{c}$ of 2.21-2.13Ga.

Table 10. Sample 90030: K-feldspar megacrystic charnockite, Mawson Station, MacRobertson Land

Zircon Age Clusters	Age (Ma)	Sample	Zircon Type	T(DM) crustal (Ga)	εHf	Th/U ratio
c	**1063**	**90030-9**	C1	2.05	-6.2	0.98
(n = 6)	**1008**	**90030-7**	C3	2.09	-7.92	0.75
	996	**90030-11**	C1	2.19	-10.02	0.9
	987	**90030-6**	C3	2.14	-9.25	0.84
	961	**90030-18**	C1	2.09	-8.55	0.87
	920	**90030-10**	C1	2.16	-10.71	0.15
ddd	**853**	**90030-13**	C3	2.13	-11.12	2.16
(n = 2)	**846**	**90030-12**	C3	2.21	-12.84	0.81

Sample SW242: Stillwell Hills K-feldspar megacrystic charnockite (charnockitic gneiss), Kemp Land

Halpin et al (2005) published data on sample SW242A of Stillwell Hills K-feldspar megacrystic charnockite (Table 11). A total of 16 zircon grain were U-Pb and Hf-analysed, which were emplaced and underwent partial metamorphism during the Proterozoic. A single T_{DM} peak occurred 2.54-2.15Ga. Th/U ratio was 7.22 – 0.48, all within range of mafic-granitic LSZ and MSZ magmatic petrogenesis.

Proterozoic age cluster **a** contained 10 grains, dated 1574±11Ma to 1406±10Ma. εHf ranged from -6.37 to -16.07 recycled and $T_{DM}{}^{c}$ of 2.91-2.4Ga.

Age cluster **bb** contained 3 grains, dated 1397±11Ma to 1306±11Ma. εHf ranges from -13.42 to -17.24 recycled and $T_{DM}{}^{c}$ of 2.88-2.61Ga.

Age cluster **c** contained 3 grains, dated 1283±10Ma to 1034±10Ma. εHf ranges from -16.24 to -22.42 recycled and $T_{DM}{}^{c}$ of 2.89-2.63Ga.

Table 11. Sample SW242A: K-feldspar megacrystic charnockite, Stillwell Hills, Kemp Land

Zircon Age Clusters	Age (Ma)	Sample	Zircon Type	T(DM) crustal (Ga)	εHf	Th/U ratio
a	**1574**	**SW242A-7**	C1	2.68	-10.51	1.01
(n = 10)	**1562**	**SW242A-21**	C1	2.89	-14.85	2.36
	1535	**SW242A-22**	C1	2.48	-7.13	4.3
	1509	**SW242A-13**	C1	2.91	-16.07	0.87
	1499	**SW242A-20**	C1	2.68	-11.72	2.3
	1490	**SW242A-28**	C1	2.72	-12.67	3.41
	1480	**SW242A25**	C1	2.4	-6.37	7.22
	1479	**SW242A-16**	C1	2.53	-8.9	1.01
	1458	**SW242A-23**	C1-bk	2.46	-7.9	2.61
	1406	**SW242A-8**	C1	2.77	-14.98	0.53
bb	**1397**	**SW242A-3**	R1	2.88	-17.24	0.77
(n = 3)	**1380**	**SW242A-10**	C1	2.67	-13.44	0.48
	1306	**SW242A-27**	C1	2.61	-13.42	6.01
c	**1283**	**SW242A-18**	C3	2.89	-19.32	0.75
(n = 3)	**1151**	**SW242A-11**	C1	2.63	-16.24	0.61
	1034	**SW242A-5**	C1-bk	2.84	-22.42	0.74

Sample SW268: Stillwell Hills felsic-mafic orthogneiss, Kemp Land.

Halpin et al (2005) published data on a total of 11 zircon grains, which were U-Pb and Hf-analysed (Table 12). All were emplaced and metamorphosed during the Archaean. One T_{DM} peak occurred between 3.86-3.56Ga. Th/U ratio was 0.61 – 0.12, all within range of felsic-granitic magmatic petrogenesis and incorporating ESZ and LSZ.

Archaean age cluster **aaaa** contained 11 grains, dated 3467±29Ma to 2978±8Ma. εHf ranges from -1.9 to -16.36 recycled and $T_{DM}{}^{c}$ of 4.36-3.79Ga.

Table 12. Sample SW268: Stillwell Hills felsic-mafic orthogneiss (well-layered), southern Stillwell Hills, Kemp Land

Zircon Age Clusters	Age (Ma)	Sample	Zircon Type	T(DM) crustal (Ga)	εHf	Th/U ratio
aaaa	**3467**	**SW268-8**	C1-bk	3.98	-4.04	0.61
(n = 11)	**3400**	**SW268-12**	C1-bk	4.18	-8.15	0.15
	3390	**SW268-14**	C1-bk	3.79	-1.9	0.24
	3367	**SW268-2**	C1	3.97	-5.09	0.3
	3362	**SW268-16**	C1	3.86	-3.38	0.26
	3338	**SW268-3**	C1	4.02	-6.35	0.15
	3100	**SW268-5**	C1	4.24	-12.97	0.14
	3091	**SW268-22**	C1-bk	4.03	-11.45	0.12
	3084	**SW268-24**	C1-bk	4.21	-12.69	0.12
	3048	**SW268-9**	C1	3.92	-8.26	0.37
	2978	**SW268-4**	C1	4.36	-16.36	0.26

Sample BH290: Homogenous felsic orthogneiss, Broka and Havstein Islands, Kemp Land

Halpin et al (2005) U-Pb and Hf-analysed a total of 14 zircon grains; all but two were emplaced and metamorphosed during the Archaean (Table 13). T_{DM} peaks occurred between 2.43-1.46Ga and 2.87-2.43Ga. Th/U ratio was 0.43 – 0.05, with both felsic-granitic magmatic and metamorphic ranges recorded, with no clear trend in regard to age clusters. Th/U ratio ≥0.1-0.2 are interpreted as ESZ, whilst Th/U ratio between 0.2 and 0.7 are interpreted as LSZ. Th/U ratio <0.1 are interpreted has having either formed during metamorphism or undergone intense metamorphism after petrogenesis.

Age cluster **aaaa** contained 6 grains, dated 3538±7Ma to 3084±26Ma. εHf ranged from 34.69 to -1.97 fertile-recycled and T_{DM}^{c} of 3.59-1.59Ga. One grain had metamorphic Th/U ratio of 0.07.

Archaean age cluster **aaa** contained 6 grains, dated 2956±8Ma to 2520±9Ma. εHf ranged from 40.35 to -13.08 fertile-recycled and T_{DM}^{c} of 4.13-0.6Ga. Four grains had metamorphic Th/U ratios <0.1.

Proterozoic age cluster **aa'** contained 1 grain, dated 2393±8Ma. εHf was -17.89 recycled and T_{DM}^{c} was 4Ga. Th/U ratio 0.16 was within magmatic range.

Age cluster **c** contained 1 grain, dated 944±11Ma. εHf is -38.87 recycled and T_{DM}^{c} was 4.12Ga. Th/U metamorphic ratio was 0.06.

Table 13. Sample BH290: Homogenous felsic orthogneiss, Broka and Havstein Islands, Kemp Land

Zircon Age Clusters	Age (Ma)	Sample	Zircon Type	T(DM) crustal (Ga)	εHf	Th/U ratio
aaaa	**3538**	**BH290-22**	C3	1.59	34.69	0.21
(n = 6)	**3490**	**BH290-14**	C1	3.5	3.93	0.37
	3355	**BH290-13**	C3	3.59	0.9	0.43
	3292	**BH290-7**	C4	2.58	16.26	0.23
	3188	**BH290-19**	C4	3.29	3.6	0.16
	3084	**BH290-16**	C1	3.56	-1.97	**0.07**
aaa	**2956**	**BH290-17**	C2	4.13	-12.98	**0.05**
(n = 6)	**2706**	**BH290-8**	C2	0.6	40.35	0.18
	2582	**BH290-1**	C2	3.85	-13.08	**0.06**
	2580	**BH290-27**	C2	3.85	-13.01	0.14
	2545	**BH290-4**	C2	3.74	-11.65	**0.07**
	2520	**BH290-28**	C4	0.68	36.82	**0.05**
aa' (n=1)	**2393**	**BH290-6**	C3	4	-17.89	0.16
c (n=1)	**944**	**BH290-23**	C2	4.12	-38.87	**0.06**

OG614: Felsic layer of composite orthogneiss, Oygarden Group, Kemp Land

A total of 11 zircon grains were U-Pb and Hf-analysed; emplaced and partly metamorphosed during the Archaean (Halpin et al 2005) (Table 14). T_{DM} Peaks occurred between 3.22-2.76Ga and 3.71-3.22Ga. Th/U ratio was 0.56 – 0.25, within felsic-granitic magmatic range, crystallizing during LSZ.

Archaean age cluster **aaaa** contained 11 grains, dated 3594±8Ma to 3188±9Ma. εHf ranged from 17.41 to -9.36 fertile-recycled and $T_{DM}{}^{c}$ was 4.09-2.44Ga.

Table 14. Sample OG614: Felsic layer of composite orthogneiss, Oygarden Group, Kemp Land

Zircon Age Clusters	Age (Ma)	Sample	Zircon Type	T(DM) crustal (Ga)	εHf	Th/U ratio
aaaa	**3594**	**OG614-13**	C3	3.59	3.81	0.56
n = 11)	**3554**	**OG614-3**	C3	3.47	5.34	0.4
	3478	**OG614-19**	C3	3.56	2.96	0.42
	3443	**OG614-1**	C3	3.7	0.23	0.54
	3441	**OG614-4**	C3	3.06	10.43	0.25
	3434	**OG614-16**	C3	3.64	0.98	0.51
	3420	**OG614-7**	C3	3.58	1.78	0.27
	3401	**OG614-11**	C3	3.35	5.35	0.3
	3367	**OG614-8**	C3	3.81	-2.57	0.41
	3204	**OG614-5**	C3	2.44	17.41	0.37
	3188	**OG614-6**	C3	4.09	-9.36	0.58

OG235: Homogenous felsic orthogneiss, Rippon Point, border of Napier Complex

A total of 12 zircon grains were U-Pb and Hf-analysed; emplaced and partly metamorphosed during the Archaean and late Proterozoic (Halpin et al 2005) (Table 15). A single T_{DM} peak occurred 3.76-3.54Ga. Th/U ratio was 0.26 – 0.04, with both magmatic and metamorphic Th/U ratios. Magmatic Th/U ratios ≥0.1 in this sample, are categoried as forming from felsic magma between ESZ and LSZ. Th/U ratios < 0.1 are categorized as metamorphic.

Archaean age cluster **aaaa** contained 2 grains, dated 3269±9Ma to 3017±9Ma. εHf ranged from -7.61 to -10.79 recycled and $T_{DM}{}^{c}$ was 4.05Ga. One grain had metamorphic Th/U ratio 0.04.

Age cluster **aaa** contained 8 grains, dated 2930±9Ma to 2504±9Ma. εHf ranged from -13.57 to -22.33 recycled and $T_{DM}{}^{c}$ was 4.38-4.05Ga. Four grains had metamorphic Th/U ratios <0.10.

Proterozoic age cluster **aa'** contained 2 grains, dated 2471±10Ma to 2454±10Ma. εHf ranged from -24.70 to -27.57 recycled and $T_{DM}{}^{c}$ was 4.63-4.47Ga. Th/U ratio was within magmatic range.

Table 15. Sample OG235: Homogenous felsic orthogneiss, Rippon Point, border of Napier Complex

Zircon Age Clusters	Age (Ma)	Sample	Zircon Type	T(DM) crustal (Ga)	εHf	Th/U ratio
aaaa	**3269**	**OG235-18**	C2	4.05	-7.61	**0.04**
(n = 2)	**3017**	**OG235-10**	C2	4.05	-10.79	0.11
aaa	**2930**	**OG235-13**	C2	4.31	-16.18	0.12
(n = 8)	**2798**	**OG235-3**	C2	4.05	-13.57	**0.07**
	2725	**OG235-2**	C4	4.38	-19.98	0.14
	2702	**OG235-1**	C2	4.16	-16.57	**0.09**
	2675	**OG235-23**	C2	4.16	-16.9	**0.07**
	2607	**OG235-14**	C2	4.31	-20.4	0.14
	2516	**OG235-11**	C2	4.34	-22.07	**0.09**
	2504	**OG235-5**	C2	4.35	-22.33	0.12
aa'	**2471**	**OG235-24**	C2	4.47	-24.7	0.27
(n = 2)	**2454**	**OG235-15**	C2	4.63	-27.57	0.13

5. Discussion

5.1 Probability Density Plots

In 90024, a single peak occurs c.950Ma (age cluster **c**) (Figure 11b). At Mawson Station, in the vicinity of Forbes Glacier at 954±12Ma, charnockite was emplaced. (Halpin et al 2005, p. 692). A trend of regional metamorphism combined with igneous charnockitic emplacement was effecting Archaean and Paleaoproterozoic cratonic blocks in east Antarctica during RSE, from Meso-to-Neoproterozoic continental collision (Zhao et al 1997, p.37). This combination of events most likely contributed to the population density peak at c.950Ma, through zircon growth and recrystallisation in the metapelite.

In AC34, the single peak occurs slightly earlier than sample 90024 at c.900Ma (age cluster **c**), but the overall population density curve between both MacRobertson Land samples is extremely similar (Figure 8b). At 910±18Ma at Cape Bruce, metamorphic events formed paragneiss and orthogniess. Pegmatite was also emplaced penecontemporaneously at Cape Bruce (Halpin et al 2005, p.693). It is possible that this combination of events caused the peak in population density within this sample.

The four samples from Stillwell Hills, Kemp Land have more individualistic age population clusters, but share similar aged peaks.

In GS01, peaks occur at c.1525Ma and c.925Ma (Figure 18b). In FS0214, peaks occur at c.1500Ma and 1000Ma (Figure 15b). In FS0223, a single peak occurs at c.950Ma (Figure 24b). In SW54, a single peak also occurs at c.950Ma (Figure 21b). This trend in peak ages may be due to major zircon growth or the resetting of ages during the RSE in Stillwell Hills at c.945Ma (Halpin et al 2007c, p.116). In sample FS0214, this major influx of zircon growth and recrystallisation occurs slightly later at c.1000Ma. RSE is recorded to have occurred in MacRobertson Land between c.1000-980Ma (Harley & Kelly 2007). This event may have provided detritus shed from sources proximal to MacRobertson Land; or from unknown subglacial sources upflow.

The second major peak occurring c.1500-1525Ma in GS01 and FS0214 is harder to trace. Magmatism and metamorphism is recorded in proximal Oygarden Islands c.1600Ma (Halpin et al 2005, p.691). Erosion of some igneous detrital grains may have migrated east from there. Another possibility is Pb-loss from c.1600 Ma zircons from Stillwell Charnockite (SW242A). This might give rise to a major peak at c.1500-1525Ma, from discordant zircon ages displayed in both Concordia diagrams for samples GS01 and FS0214.

5.2 Provenance of the grains: known rock types as potential sources of detrital grains in Kemp and MacRobertson Land metapelite samples (90024, AC34, GS01, FS0214, FS0223, SW54).

To ascertain whether detrital zircon grains contained within the six metapelite samples from Kemp and MacRobertson Lands had been previously eroded from older-to-contemporaneous proximal known rock types, data gathered on both groups were sorted by 207/206Pb age and cross-referenced (Table 16). Known rock types (90030, OG235, OG614, SW268 and SW242A) are highlighted in colour and bold font. Metamorphic Th/U ratios are also highlighted in bold.

To determine whether a detrital zircon grain from a metapelitic sample fitted the profile of contemporaneous zircons from a known rock type, 207/206Pb age (plus 1se) provided a starting point. Zircon grains older and younger than the ages of zircons from known rock types were not considered. This interpretation of data was backed up by T_{DM}^{c}. This crustal model age was extremely useful in sorting provenance. When searching for zircons eroded from known rock types, T_{DM}^{c} was kept within the known crustal model age of this rock. Th/U ratios of known rock types were also considered when selecting zircons of similar provenance.

There were only a few grains from the six metapelite samples that shared a similar geological profile to one of the known rock types in Kemp and MacRobertson Lands. Whenever this occurred, the known rock type was listed beside the specific grain, in the column 'Possible Source' in Table 16. In most cases, however, a potential protolith for each grain was not identifiable and therefore the 'Possible Source' column was left blank.

Table 16. 207/206Pb age-sorted properties from 6 metapelite samples (90024, AC34, FS0214, FS0223, GS01 and SW54) cross-referenced with known rock types from Kemp and MacRobertson Lands (90030, OG235, OG614, SW268, SW242A)

Possible Source	Age Clusters	Age (Ma)	1σ ±	Sample	Location	Zircon Type	T(DM) crustal (Ga)	εHf	Th/U ratio
	aaaa	3594	8	OG614-13	Oygarden Group	C3	3.59	3.81	0.56
	aaaa	3554	9	OG614-3	Oygarden Group	C3	3.47	5.34	0.4
	aaaa	3538	7	BH290-22	Broka & Havstein Is	C3	1.59	34.69	0.22
	aaaa	3490	26	BH290-14	Broka & Havstein Is	C1	3.5	3.93	0.37
	aaaa	3478	8	OG614-19	Oygarden Group	C3	3.56	2.96	0.42
	aaaa	3467	29	SW268-8	Stillwell Hills (south)	C1-bk	3.98	-4.04	0.61
	aaaa	3443	9	OG614-1	Oygarden Group	C3	3.7	0.23	0.54
	aaaa	3441	8	OG614-4	Oygarden Group	C3	3.06	10.43	0.25
	aaaa	3434	8	OG614-16	Oygarden Group	C3	3.64	0.98	0.51
	aaaa	3420	7	OG614-7	Oygarden Group	C3	3.58	1.78	0.27
	aaaa	3401	8	OG614-11	Oygarden Group	C3	3.35	5.35	0.3
	aaaa	3400	27	SW268-12	Stillwell Hills (south)	C1-bk	4.18	-8.15	0.15
	aaaa	3390	9	SW268-14	Stillwell Hills (south)	C1-bk	3.79	-1.9	0.24
	aaaa	3367	8	SW268-2	Stillwell Hills (south)	C1	3.97	-5.09	0.3
	aaaa	3367	9	OG614-8	Oygarden Group	C3	3.81	-2.57	0.41
	aaaa	3362	9	SW268-16	Stillwell Hills (south)	C1	3.86	-3.38	0.26
	aaaa	3355	23	BH290-13	Broka & Havstein Is	C3	3.59	0.9	0.43
	aaaa	3338	8	SW268-3	Stillwell Hills (south)	C1	4.02	-6.35	0.15
	aaaa	3292	26	BH290-7	Broka & Havstein Is	C4	2.58	16.26	0.23
	aaaa	3269	9	OG235-18	Rippon Point, Napier	C2	4.05	-7.61	**0.04**
	aaaa	3204	9	OG614-5	Oygarden Group	C3	2.44	17.41	0.37
	aaaa	3188	21	BH290-19	Broka & Havstein Is	C4	3.29	3.6	0.16
	aaaa	3188	9	OG614-6	Oygarden Group	C3	4.09	-9.36	0.58
	aaaa	3100	8	SW268-5	Stillwell Hills (south)	C1	4.24	-12.97	0.14
	aaaa	3091	26	SW268-22	Stillwell Hills (south)	C1-bk	4.03	-11.45	0.12
	aaaa	3084	28	SW268-24	Stillwell Hills (south)	C1-bk	4.21	-12.69	0.12
	aaaa	3084	26	BH290-16	Broka & Havstein Is	C1	3.56	-1.97	**0.07**
	aaaa	3048	9	SW268-9	Stillwell Hills (south)	C1	3.92	-8.26	0.37

	aaaa	**3017**	9	**OG235-10**	**Rippon Point, Napier**	C2	4.05	-10.79	0.11
	aaaa	**2978**	8	**SW268-4**	**Stillwell Hills (south)**	C1	4.36	-16.36	0.26
	aaa	**2956**	8	**BH290-17**	**Broka & Havstein Is**	C2	4.13	-12.98	**0.06**
	aaa	**2930**	9	**OG235-13**	**Rippon Point, Napier**	C2	4.31	-16.18	0.12
	aaa	**2798**	9	**OG235-3**	**Rippon Point, Napier**	C2	4.05	-13.57	**0.07**
	aaa	**2725**	9	**OG235-2**	**Rippon Point, Napier**	C4	4.38	-19.98	0.14
	aaa	**2706**	26	**BH290-8**	**Broka & Havstein Is**	C2	0.6	40.35	0.19
	aaa	**2702**	9	**OG235-1**	**Rippon Point, Napier**	C2	4.16	-16.57	**0.09**
	aaa	**2675**	10	**OG235-23**	**Rippon Point, Napier**	C2	4.16	-16.9	**0.07**
	aaa	**2650**	40	**AC34-4**	Cape Bruce, Mawson	C1	3.07	0.60	0.46
	aaa	**2637**	34	**FS0214-37A**	Keel Is, Stillwell H	C1	2.52	9.24	0.42
	aaa	**2607**	10	**OG235-14**	**Rippon Point, Napier**	C2	4.31	-20.4	0.14
	aaa	**2583**	46	**FS0214-58A**	Keel Is, Stillwell H	C1	2.52	8.61	0.69
	aaa	**2582**	26	**BH290-1**	**Broka & Havstein Is**	C2	3.85	-13.08	**0.06**
	aaa	**2580**	50	**FS0214-24**	Keel Is, Stillwell H	C1	2.65	6.46	0.34
	aaa	**2580**	29	**BH290-27**	**Broka & Havstein Is**	C2	3.85	-13.01	0.14
	aaa	**2545**	25	**BH290-4**	**Broka & Havstein Is**	C2	3.74	-11.65	**0.07**
	aaa	**2522**	22	**90024-15**	Forbes Glacier, Mawson	C1	2.75	4.10	0.41
	aaa	**2520**	9	**BH290-28**	**Broka & Havstein Is**	C4	0.68	36.82	**0.06**
	aaa	**2516**	9	**OG235-11**	**Rippon Point, Napier**	C2	4.34	-22.07	**0.09**
	aaa	**2504**	9	**OG235-5**	**Rippon Point, Napier**	C2	4.35	-22.33	0.12
BH290	**aa'**	**2488**	32	**90024-42**	Forbes Glacier, Mawson	C2	3.65	-10.96	0.39
	aa'	**2478**	32	**FS0214-10**	Keel Is, Stillwell H	C1	2.75	3.65	0.50
	aa'	**2471**	10	**OG235-24**	**Rippon Point, Napier**	C2	4.47	-24.7	0.27
	aa'	**2454**	10	**OG235-15**	**Rippon Point, Napier**	C2	4.63	-27.57	0.13
	aa'	**2446**	44	**FS0214-23B**	Keel Is, Stillwell H	R2	2.72	3.67	0.30
	aa'	**2393**	8	**BH290-6**	**Broka & Havstein Is**	C3	4	-17.89	0.17
	aa	**2099**	25	**AC34-70**	Cape Bruce, Mawson	C1	2.29	6.24	0.80
	aa	**2078**	33	**AC34-27**	Cape Bruce, Mawson	C3	2.37	4.81	0.51
	aa	**1986**	19	**90024-60**	Forbes Glacier, Mawson	C1	2.04	8.91	0.59
	a	**1792**	44	**AC34-5**	Cape Bruce, Mawson	C1	2.57	-2.10	0.86
	a	**1741**	30	**AC34-68A**	Cape Bruce, Mawson	C3	2.75	-5.57	0.23
	a	**1715**	44	**GS01-42**	Keel Is, Stillwell Hills	C1	2.55	-2.67	0.23
	a	**1706**	46	**GS01-20A**	Keel Is, Stillwell Hills	C1	2.68	-5.00	0.19
	a	**1651**	26	**GS01-86**	Keel Is, Stillwell Hills	C2	2.85	-9.05	0.23
	a	**1648**	78	**GS01-22**	Keel Is, Stillwell Hills	C1	2.71	-6.23	0.23
	a	**1620**	33	**SW54-98A**	Sth of Ives Tongue,SW	C3	2.34	-0.42	0.48
	a	**1615**	44	**90024-83**	Forbes Glacier, Mawson	C3	2.30	0.06	0.46
	a	**1607**	96	**GS01-68/70**	Keel Is, Stillwell Hills	C2	2.61	-4.99	0.34
	a	**1600**	44	**FS0214-36A**	Keel Is, Stillwell H	C2	3.26	-15.82	**0.06**
	a	**1593**	56	**GS01-105**	Keel Is, Stillwell Hills	C3	2.41	-1.94	0.39
	a	**1592**	42	**GS01-14A**	Keel Is, Stillwell Hills	C1-bk	2.48	-3.05	**0.08**

	a	**1582**	21	**GS01-102**	Keel Is, Stillwell Hills	C2	2.41	-2.10	**0.06**
	a	**1578**	58	**GS01-97A**	Keel Is, Stillwell Hills	C1	2.50	-3.70	**0.09**
	a	**1574**	10	**SW242A-7**	**Stillwell Hills**	C1	2.68	-10.51	1.01
	a	**1562**	11	**SW242A-21**	**Stillwell Hills**	C1	2.89	-14.85	2.36
	a	**1540**	34	**GS01-87**	Keel Is, Stillwell Hills	C3	2.74	-8.07	0.28
	a	**1536**	35	**90024-51**	Forbes Glacier, Mawson	C1	1.48	12.42	0.82
	a	**1535**	11	**SW242A-22**	**Stillwell Hills**	C1	2.48	-7.13	4.3
	a	**1522**	44	**FS0214-14**	Keel Is, Stillwell H	C2	3.44	-19.89	**0.05**
	a	**1514**	37	**FS0214-16B**	Keel Is, Stillwell H	R2	3.34	-18.32	**0.03**
	a	**1509**	10	**SW242A-13**	**Stillwell Hills**	C1	2.91	-16.07	0.81
	a	**1509**	64	**FS0214-95**	Keel Is, Stillwell H	C1-C3	3.27	-17.14	0.17
	a	**1499**	12	**SW242A-20**	**Stillwell Hills**	C1	2.68	-11.72	2.3
SW242A	**a**	**1490**	30	**AC34-34**	Cape Bruce, Mawson	C1	2.74	-8.58	0.59
	a	**1490**	11	**SW242A-28**	**Stillwell Hills**	C1	2.72	-12.67	3.41
	a	**1480**	10	**SW242A25**	**Stillwell Hills**	C1	2.4	-6.37	7.22
	a	**1479**	11	**SW242A-16**	**Stillwell Hills**	C1	2.53	-8.9	1.01
	a	**1465**	34	**GS01-10**	Keel Is, Stillwell Hills	C1-bk/C2	2.63	-7.22	**0.07**
	a	**1458**	11	**SW242A-23**	**Stillwell Hills**	C1-bk	2.46	-7.9	2.61
	a	**1457**	82	**FS0223-19**	Ives Tongue, SW	C2	2.42	-3.80	**0.01**
	a	**1454**	51	**FS0214-46**	Keel Is, Stillwell H	C1	3.21	-16.92	**0.08**
	a	**1440**	18	**AC34-78**	Cape Bruce, Mawson	C1	2.44	-4.31	0.55
	a	**1440**	97	**FS0214-69**	Keel Is, Stillwell H	C3	3.40	-20.21	**0.08**
	a	**1437**	35	**GS01-101A**	Keel Is, Stillwell Hills	C1-bk	2.81	-10.51	0.14
	a	**1433**	40	**GS01-17**	Keel Is, Stillwell Hills	C1	2.40	-3.81	**0.06**
	a	**1425**	54	**GS01-85A**	Keel Is, Stillwell Hills	C1	2.22	-0.97	0.34
	a	**1406**	23	**AC34-2A**	Cape Bruce, Mawson	C1	1.74	6.53	0.60
	a	**1406**	19	**SW242A-8**	**Stillwell Hills**	C1	2.77	-14.98	0.53
	a	**1406**	31	**90024-81**	Forbes Glacier, Mawson	C1	2.21	-1.08	0.59
	bb	**1397**	11	**SW242A-3**	**Stillwell Hills**	R1	2.88	-17.24	0.77
	bb	**1396**	28	**AC34-44**	Cape Bruce, Mawson	C1	2.39	-4.17	0.53
	bb	**1380**	10	**SW242A-10**	**Stillwell Hills**	C1	2.67	-13.44	0.48
	bb	**1343**	78	**FS0214-61**	Keel Is, Stillwell H	C2	3.40	-21.45	**0.01**
	bb	**1333**	29	**90024-37**	Forbes Glacier, Mawson	C2	1.79	4.84	0.20
SW242A	**bb**	**1326**	35	**GS01-9**	Keel Is, Stillwell Hills	C2	2.72	-10.35	0.19
SW242A	**bb**	**1316**	33	**GS01-96**	Keel Is, Stillwell Hills	C2	2.70	-10.24	0.15
	bb	**1315**	62	**AC34-85**	Cape Bruce, Mawson	C1	2.05	0.33	0.39
	bb	**1306**	11	**SW242A-27**	**Stillwell Hills**	C1	2.61	-13.42	6.01
	c	**1300**	48	**90024-77**	Forbes Glacier, Mawson	C1-bk	2.15	-1.35	0.26
	c	**1291**	57	**FS0214-102**	Keel Is, Stillwell H	C1-bk	3.37	-21.63	**0.04**
	c	**1283**	10	**SW242A-18**	**Stillwell Hills**	C3	2.89	-19.32	0.75
	c	**1280**	67	**90024-14**	Forbes Glacier, Mawson	C1	2.21	-2.72	0.25
	c	**1269**	127	**FS0214-97**	Keel Is, Stillwell H	C3	3.45	-23.24	0.12

	c	**1251**	27	**90024-3A**	Forbes Glacier, Mawson	C1	2.08	-0.89	0.57
	c	**1235**	69	**FS0214-44**	Keel Is, Stillwell H	C1	3.24	-20.23	**0.05**
	c	**1233**	51	**GS01-101B**	Keel Is, Stillwell Hills	C3	2.86	-13.99	0.45
	c	**1182**	40	**AC34-36**	Cape Bruce, Mawson	C1	2.19	-3.50	0.88
	c	**1167**	26	**AC34-87**	Cape Bruce, Mawson	C1	2.08	-1.91	0.70
	c	**1155**	82	**FS0223-36**	Ives Tongue, SW	C2	2.67	-11.80	**0.07**
	c	**1151**	11	**SW242A-11**	**Stillwell Hills**	C1	2.63	-16.24	0.61
	c	**1150**	73	**90024-75**	Forbes Glacier, Mawson	C1	1.98	-0.54	0.58
	c	**1144**	61	**90024-36**	Forbes Glacier, Mawson	C1	1.85	1.55	0.85
SW242A	**c**	**1141**	68	**SW54-41C**	Sth of Ives Tongue,SW	R1	2.63	-11.28	0.67
	c	**1132**	32	**AC34-3**	Cape Bruce, Mawson	C1	2.06	-2.11	0.72
	c	**1115**	28	**AC34-14**	Cape Bruce, Mawson	C2	1.99	-1.18	0.84
	c	**1105**	47	**90024-63A**	Forbes Glacier, Mawson	C1	1.71	3.28	1.06
	c	**1094**	29	**AC34-23**	Cape Bruce, Mawson	C1	2.00	-1.57	0.78
	c	**1084**	29	**90024-41**	Forbes Glacier, Mawson	C1-bk	2.05	-2.59	0.50
	c	**1084**	62	**90024-22**	Forbes Glacier, Mawson	C1-bk	1.81	1.37	0.42
	c	**1081**	58	**90024-3B**	Forbes Glacier, Mawson	R2	1.88	0.13	0.10
	c	**1072**	30	**AC34-18**	Cape Bruce, Mawson	C1	2.08	-3.11	0.30
	c	**1063**	11	**90030-9**	**Mawson Station**	C1	2.05	-6.2	0.98
	c	**1057**	59	**90024-50A**	Forbes Glacier, Mawson	C1	1.98	-1.67	0.53
	c	**1054**	54	**AC34-48**	Cape Bruce, Mawson	C1	1.88	-0.12	0.69
	c	**1047**	99	**FS0214-79B**	Keel Is, Stillwell H	C4	3.62	-29.05	**0.04**
	c	**1046**	125	**90024-71**	Forbes Glacier, Mawson	C1	2.14	-4.53	0.42
	c	**1034**	10	**SW242A-5**	**Stillwell Hills**	C1-bk	2.84	-22.42	0.74
	c	**1029**	117	**FS0223-88**	Ives Tongue, SW	C2	2.78	-15.22	**0.04**
SW242A	**c**	**1025**	74	**SW54-98B**	Sth of Ives Tongue,SW	C3	2.67	-13.54	0.70
	c	**1012**	34	**AC34-2B**	Cape Bruce, Mawson	R2	1.79	0.86	**0.01**
	c	**1008**	13	**90030-7**	**Mawson Station**	C3	2.09	-7.92	0.75
SW242A	**c**	**1003**	84	**FS0223-89**	Ives Tongue, SW	C2	2.63	-13.16	**0.09**
	c	**996**	13	**90030-11**	**Mawson Station**	C1	2.19	-10.02	0.9
	c	**993**	29	**AC34-26**	Cape Bruce, Mawson	C1	1.82	0.06	1.04
	c	**987**	12	**90030-6**	**Mawson Station**	C3	2.14	-9.25	0.84
	c	**982**	49	**90024-63B**	Forbes Glacier, Mawson	R1	1.99	-2.87	0.70
	c	**979**	87	**FS0223-76**	Ives Tongue, SW	C2	2.71	-14.74	0.10
	c	**978**	84	**GS01-52**	Keel Is, Stillwell Hills	C3	1.60	3.37	0.92
	c	**975**	91	**FS0214-82**	Keel Is, Stillwell H	C2	3.57	-29.16	0.34
	c	**970**	80	**FS0223-10**	Ives Tongue, SW	C2	2.77	-15.80	0.15
	c	**962**	75	**FS0223-56**	Ives Tongue, SW	C2	2.78	-16.17	**0.09**
	c	**961**	13	**90030-18**	**Mawson Station**	C1	2.09	-8.55	0.87
SW242A	**c**	**960**	59	**SW54-89B**	Sth of Ives Tongue,SW	C3	2.76	-15.84	0.65
	c	**957**	90	**FS0214-37B**	Keel Is, Stillwell H	C3	3.32	-25.14	0.60
	c	**956**	44	**AC34-68B**	Cape Bruce, Mawson	R2	1.81	-0.25	**0.01**

	c	953	76	FS0223-92	Ives Tongue, SW	C3	2.74	-15.62	**0.08**
	c	950	109	FS0214-42	Keel Is, Stillwell H	C2	3.32	-25.17	0.43
SW242A	c	948	62	SW54-41D	Sth of Ives Tongue,SW	R2	2.77	-16.06	0.56
	c	948	55	SW54-41B	Sth of Ives Tongue,SW	C1	2.69	-14.73	0.18
	c	945	86	FS0223-5	Ives Tongue, SW	C2	2.67	-14.47	0.20
	c	944	11	BH290-23	**Broka & Havstein Is**	C2	4.12	-38.87	**0.07**
	c	942	58	GS01-31	Keel Is, Stillwell Hills	C3	2.32	-8.75	0.52
SW242A	c	940	60	SW54-25A	Sth of Ives Tongue,SW	C3	2.72	-15.41	0.55
	c	938	65	FS0223-59	Ives Tongue, SW	R2	2.78	-16.47	**0.07**
	c	936	24	GS01-85B	Keel Is, Stillwell Hills	R2	2.24	-7.49	0.23
	c	931	58	90024-23	Forbes Glacier, Mawson	R2	1.97	-3.21	**0.08**
SW242A	c	925	40	SW54-25B	Sth of Ives Tongue,SW	R2	2.69	-15.14	0.48
SW242A	c	924	71	SW54-3	Sth of Ives Tongue,SW	C3	2.85	-17.83	0.60
	c	920	11	90030-10	**Mawson Station**	C1	2.16	-10.71	0.15
	c	915	61	FS0223-35	Ives Tongue, SW	C1-bk/C2	2.87	-18.14	0.14
	c	909	100	FS0214-06	Keel Is, Stillwell H	C1	3.49	-28.70	0.50
	c	908	53	AC34-55	Cape Bruce, Mawson	C3	1.74	0.38	**0.06**
	c	907	53	90024-73	Forbes Glacier, Mawson	R1	1.85	-1.58	0.21
	c	907	21	SW54-89C	Sth of Ives Tongue,SW	R2	2.75	-16.32	**0.07**
	ddd	889	73	90024-50B	Forbes Glacier, Mawson	R1	1.90	-2.58	0.43
	ddd	853	15	90030-13	**Mawson Station**	C3	2.13	-11.12	2.16
	ddd	852	25	GS01-11B	Keel Is, Stillwell Hills	R2	2.00	-4.64	0.21
SW242A	ddd	850	68	SW54-62	Sth of Ives Tongue,SW	C2	2.77	-17.43	0.54
	ddd	846	14	90030-12	**Mawson Station**	C3	2.21	-12.84	0.81
	ddd	836	69	FS0223-91	Ives Tongue, SW	C1-bk/C2	2.71	-16.49	**0.06**
	d+	692	131	90024-20	Forbes Glacier, Mawson	C1	2.39	-13.17	0.32

5.2 Broka and Havstein Islands orthogneiss (BH290) as a potential source for similar detrital grains found within the 6 metapelitic samples

After a detailed comparison of all detrital zircon grains from the six metapelite samples, only one grain aged c.2488Ma matched the U-Pb and Hf-analysis data of BH290 (Table 17).

A felsic grain from a lens in Painted Gneiss (90024), Forbes Glacier, fell within all known parameters of sample BH290.

Table 17. Broka & Havstein Is source-sorted properties of detrital zircon from metapelite samples

Source	Age Clusters	Age (Ma)	1σ ±	Sample	Location	Zircon Type	T(DM) crustal (Ga)	e Hf	Th/U ratio
BH290	aa'	2488	32	90024-42	Forbes Glacier, Mawson	C2	3.65	-10.96	0.39

In sample 90024, the second-oldest felsic grain 42 is dated Proterozoic 2488±32Ma in its C2 patchy-homogenous outercore (Figure 26). This zircon had the second-lowest εHf -10.96, indicating enriched recycled crustal content. It also had the lowest initial Hf, lowest 176Lu/177Hf and 176Yb/177Hf and oldest T_{DM}^{c} of 3.65Ga.

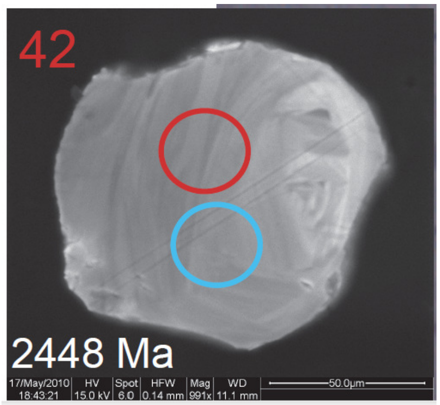

Figure 26. CL image of sample 90024 grain 42: Zircon grain with similar U-Pb and Hf-analysis to zircon grains from Broka and Havstein Islands Homogenous felsic orthogneiss, This grain potentially eroded from this known rock type, to be deposited within a metapelitic lens in Painted Gneiss, Forbes Glacier. (Blue circle shows location of U-Pb analysis ablation. Red circle shows location of Hf-analysis ablation).

5.3 Stillwell Hills Charnockite (SW242A) as a potential source for similar detrital grains found within the 6 metapelitic samples

When comparing detrital grains from the six metapelitic samples and potentially having been eroded and transported from Stillwell Hills Charnockite, consideration was given to the wide range of Th/U ratios shown by zircons from SW242A. T_{DM}^{c}, εHf and age criteria was strictly adhered to. 12 zircon grains spread across four of the metapelitic samples, matched the U-Pb and Hf-analysis profile of Stillwell Hills Charnockite (Table 18). Mostly from Stillwell Hills samples GS01, FS0223 and especially SW54, a single grain from Colbeck Gneiss AC34 also fitted all known parameters of Stillwell Hills Charnockite (Figure 27).

In Colbeck Gneiss sample AC34, grain 34 dated 1490±30, recorded the lowest εHf -8.58, indicating recycled crustal material was instrumental in the granitic igneous growth of this oscillatory core; with the sample's third-oldest T_{DM}^{c} of 2.74Ga.

In Stillwell Hills, sample GS01, Grain 9, dated 1326±35Ma at its homogenous (C2) outer-core, had enriched εHf of -10.35 and a granitic Th/U ratio of 0.59. Grain 96, dated 1316±33Ma at its matching homogenous (C2) outer-core, had εHf -10.24; indicating a provenance containing strikingly similar recycled crustal content. Its lower felsic Th/U ratio might indicate either ESZ or partial metamorphism. T_{DM}^{c} is dated between 2.72-2.70Ga for these two grains.

In sample FS0223, grain 89 has patchy (C2) zonation, ovoid morphology and a metamorphic Th/U ratio of 0.90. It contains the second-youngest T_{DM}^{c} of 2.63Ga.

In sample SW54, grain 25A showed radial-irregular (C3) sector zoning, whilst dark homogenous rim 25B had extremely low CL response.

Grain 41C and D zones were within parameters of zircon sampled from SW242A. 41C homogenous (C2) outer-core, dated c.1141Ma contains patchy concentric zoning (from recrystallising its 41B inner-core). εHf -11.28 recycled crustal content and Th/U ratio 0.67 indicates petrogenesis within a granitic-intermediate igneous protolith. 41C also has recrystallised in contact with homogenous R2 dark rim of 41D.

41D's extremely low-CL response, homogenous zoning, varying thickness and continuity is characteristic of a typical R2 rim. Dated c.948Ma during RSE, this outer-rim records εHf -16.06 recycled crustal content and Th/U ratio of 0.56; possibly lowered by partial metamorphism. The finest bleached R1 rim highlights one end of this ovoid (sub-angular) crystal.

Grain 98B also fell within SW242A parameters. Dated c.1025Ma, this outer-core continued the metamorphic C3 radial sector zoning seen within its inner 98A core. εHf -13.54 dramatically increases the recycled crustal content of this equant (sub-rounded) grain. Th/U ratio 0.70 places this outer-core's petrogenesis within an intermediate igneous event. It is possible that the 207/206Pb date of 98B has been reset to the metamorphic event which gave igneous 98B its sector zonation. A moderate-low CL response R2 rim has begun to homogenously recrystallise the top-right sub-angular corner of 98B.

Grain 89B sector zoned (C3) outer-core is dated 960±59Ma in cluster (**c**). Recycled crustal signature of εHf -15.84 and the third-oldest $T_{DM}{}^{c}$ of 2.76Ga, is typical of the trend of younger crusts having lower εHf enriched crustal content. 89B also has the second-lowest initial Hf, and the third-highest 176Lu/177Hf and 176Yb/177Hf ratios.

Grain 3 dated 924±71, has sub-angular equant morphology and radial-to-irregular sector (C3) zoning, with εHf, $T_{DM}{}^{c}$ and igneous Th/U ratio within SW242A parameters.

Grain 62 core was mostly homogenous (C2) zonation, rounded-angular morphology.

Table 18. Stillwell Hills Charnockite source-sorted properties of detrital zircon from metapelite samples

Source	Age Clusters	Age (Ma)	1σ ±	Sample	Location	Zircon Type	T(DM) crustal (Ga)	εHf	Th/U ratio
SW242A	**a**	**1490**	30	**AC34-34**	Cape Bruce, Mawson	C1	2.74	-8.58	0.59
SW242A	**bb**	**1326**	35	**GS01-9**	Keel Is, Stillwell Hills	C2	2.72	-10.35	0.19
SW242A	**bb**	**1316**	33	**GS01-96**	Keel Is, Stillwell Hills	C2	2.70	-10.24	0.15
SW242A	**c**	**1141**	68	**SW54-41C**	Sth of Ives Tongue,SW	R1	2.63	-11.28	0.67
SW242A	**c**	**1025**	74	**SW54-98B**	Sth of Ives Tongue,SW	C3	2.67	-13.54	0.70
SW242A	**c**	**1003**	84	**FS0223-89**	Ives Tongue, SW	C2	2.63	-13.16	**0.09**
SW242A	**c**	**960**	59	**SW54-89B**	Sth of Ives Tongue,SW	C3	2.76	-15.84	0.65
SW242A	**c**	**948**	62	**SW54-41D**	Sth of Ives Tongue,SW	R2	2.77	-16.06	0.56
SW242A	**c**	**940**	60	**SW54-25A**	Sth of Ives Tongue,SW	C3	2.72	-15.41	0.55
SW242A	**c**	**925**	40	**SW54-25B**	Sth of Ives Tongue,SW	R2	2.69	-15.14	0.48
SW242A	**c**	**924**	71	**SW54-3**	Sth of Ives Tongue,SW	C3	2.85	-17.83	0.60
SW242A	**ddd**	**850**	68	**SW54-62**	Sth of Ives Tongue,SW	C2	2.77	-17.43	0.54

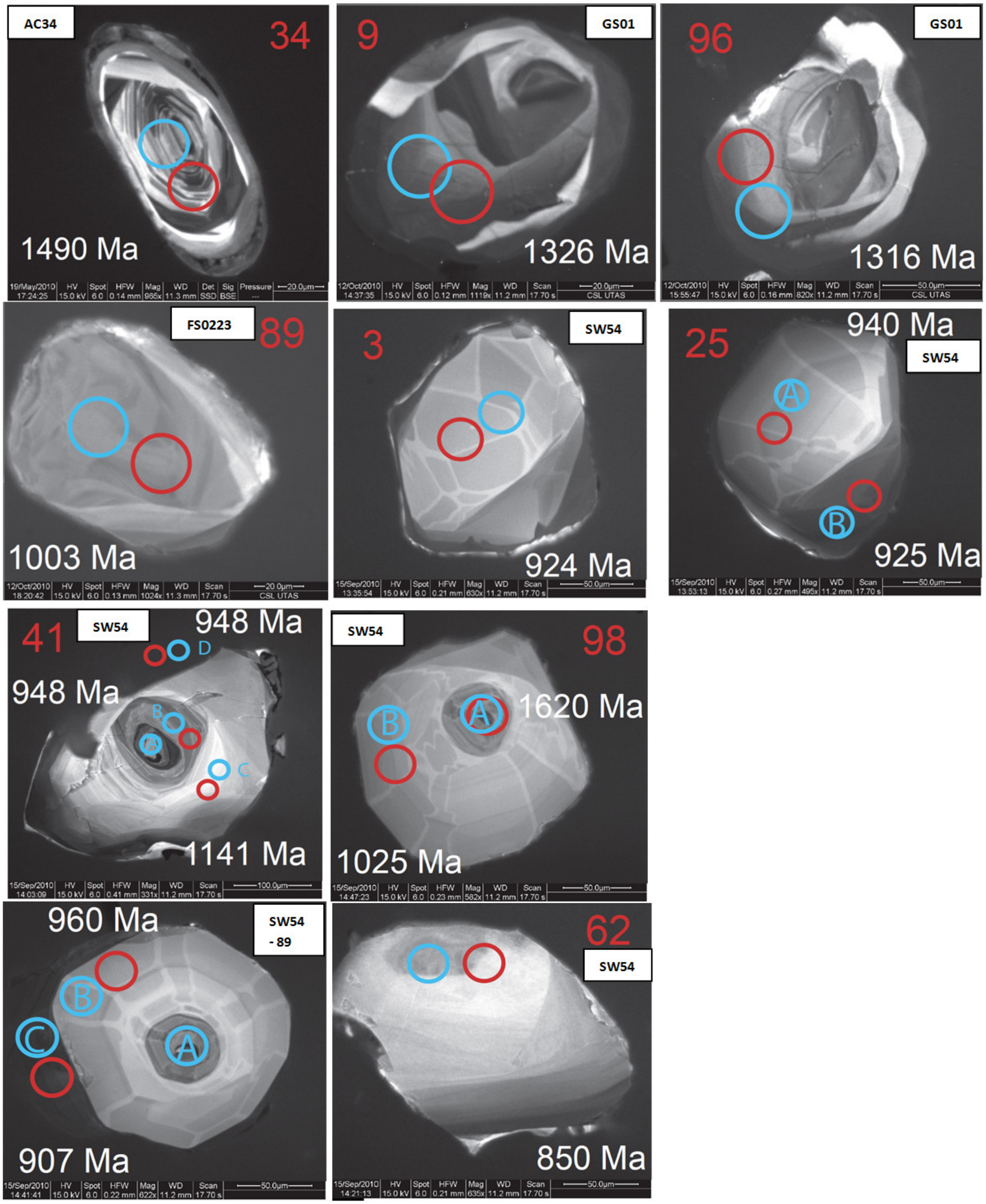

Figure 27. Zircon grains with zones of similar provenance to Stillwell Hills Charnockite (SW242A); CL imagery of detrital grains from metapelitic samples AC34, GS01, FS0223 and SW54. (Blue circle shows location of U-Pb analysis ablation. Red circle shows location of Hf-analysis ablation).

5.4 Possible location of distal unknown sources in Gamburtsev Subglacial Mountains - Vostok Subglacial Highlands craton, east Antarctica.

Veevers and Saeed (2011) published the currently known properties of detrital zircon from the sub-glacial bedrock of Gamburtsev Subglacial Mountains - Vostok Subglacial Highlands craton (GSM-VSH), east Antarctica (Figure 28).

A distal source like GSM-VSH craton is ideally located to provide a widening fan of detritus to both Kemp and MacRobertson Lands' metapelite samples. A large and ancient ice drainage basin, it is possible that the sources of some of the unknown detrital zircon within metapelite samples from Kemp and MacRobertson Lands are contained within this craton under the ice (Refer to figure 4).

However, the properties of detrital zircon collected from GSM-VSH are not entirely within the same U-Pb and Hf-analysis parameters of the six metapelitic samples. It may be that data collected in this study enlarges the previously published range of detrital zircon from subglacial GSM-VSH rock units, in the same way that the known age clusters of detrital zircon in east Antarctica were expanded to account for the wider range of 207/206Pb ages.

It is equally plausible that unknown sources for detrial zircon in the six metapelitic samples originated from other continents attached to east Antarctica at different times during Gondwanaland's geohistory.

	GSM-VSH
T_{DM} peaks	1.6-1.0 Ga 2.4-1.6 3.7-2.4
d+	mafic granitoid low-HREE-c hosts εHf 9 to -28 fertile-recycled $T_{DM}{}^{C}$ 2.5-1.3 Ga
c	mafic granitoid low-HREE-c hosts εHf 11 to -28 fertile-recycled $T_{DM}{}^{C}$ 1.8-1.3 Ga
aa	mafic granitoid εHf 0 to -20 recycled T_{DM} 2.7-2.5 Ga
aaa	granitoids εHf 1 to -8 T_{DM} 3.2 Ga
aaaa	mafic granitoid εHf 0 to -20 recycled T_{DM} 3.6-3.5 Ga

Figure 28. Known properties of bedrock of subglacial GSM-VSH complex, directly upflow from Kemp and MacRobertson Lands, east Antarctica; from studies of detrital zircon. (Veevers & Saeed 2008; 2011).

6. Conclusion

1. Analysis of 207/206Pb-dated detrital and metamorphic zircon grains gave a maximum age of deposition for Colbeck Gneiss (AC34) at Cape Bruce, MacRobertson Land as 1258±23 Ma.

2. Maximum age of deposition for the younger Painted Gneiss (90024) at Forbes Glacier, MacRobertson Land, was 1251±27 Ma.

3. The order and maximum age of deposition of four metapelitic layers at Stillwell Hills is as follows: The oldest of the Stillwell Hills metapelitic samples, Pink Gneiss (FS0214) maximum depositional age was interpreted as having occurred 1317±51 Ma. This was followed by Green layered sequence (GS01) at 1316±33 Ma, Garnet-sillimanite metapelite (SW54) at 1260±47 Ma and Rusty gneiss (FS0223) the youngest at 1178±84 Ma.

4. Detrital zircon from all six metapelitic samples overwhelmingly originated from felsic igneous events. Metamorphism could be traced to peak regional metamorphic events occurring proximal to their place of deposition in Kemp or MacRobertson Lands.

5. Two known rock types from Kemp and MacRobertson Land, Broka and Havstein Islands homogenous felsic orthogneiss and Stillwell Hills orthogneiss, may have contributed detrital zircon grains to some of the metapelite samples.

6. It is possible that unknown sub-glacial (or already eroded) sources proximal either to Kemp or MacRobertson Lands or from distal GSM-VSH sub-glacial craton provided detrital zircon to the 6 metapelitic samples. However, it is equally plausible that the source of these detrital grains came not from the interior of Antarctica, but upflow from neighouring continents adjoining east Antarctica in Archaean and proterozoic times, as part of the Gondwanaland supercontinent.

Acknowledgements

To Dr.Nathan Daczko and Dr.Jacqueline Halpin, thank you for teaching me everything I ever wanted to know about CL-imaging, U-Pb and Hf-analysis of zircon. Thank you for your patience, kindness and generosity of time and knowledge. Thanks also to Jacqui for sharing all the samples mentioned in this paper, which she personally collected from east Antarctica.

To my husband, Cameron, thanks for doing the work of two parents whilst I worked on this; and for staying up to keep me company all the times I worked late.

To my mum, Patricia Myers, thanks for giving me the courage and determination to pursue an opportunity you never had.

To my kids, Aiden, Heath, Kyle and Neve, here’s to the good times ahead!

Appendix A. Summary of U-Pb and Hf data for AC34, 90024, FS0213, GS01, SW54 and FS0223.

Appendix A: Table 2: Sample AC34

Sample	Analysis no.	CL zoning	Th	U	Th/U	Ratios for concordia 238U/206Pb	+/-1 std err	207Pb/206Pb	+/-1 std err	Common Pb 207Pb/206Pb	206Pb/238U 207 corr	1s	206/238 age	+/-1s	207/206 age	+/-1s	conc.
AC34-4 **aaa**	my27a125	ghost oscillatory	49	107	0.46	2.08	0.04	0.1797	0.0044	1.058	2487.3	56.0	2526	52	2650	40	95
AC34-70 **aa**	my27a195	oscillatory	135	169	0.80	2.62	0.03	0.1301	0.0018	1.011	2084.5	22.7	2087	22	2099	25	99
AC34-27	my27a150	sector	47	92	0.51	2.63	0.03	0.1286	0.0024	1.010	2079.4	25.7	2079	25	2078	33	100
AC34-42	my27a165	ghost oscillatory	123	189	0.65	2.62	0.03	0.1273	0.0017	1.011	2090.8	20.7	2086	20	2062	24	101
AC34-64	my27a185	ghost oscillatory	161	210	0.77	2.85	0.05	0.1224	0.0026	0.996	1933.5	31.4	1941	31	1992	38	97
AC34-52	my27a176	oscillatory	168	623	0.27	3.13	0.04	0.1160	0.0017	0.981	1776.5	20.2	1790	21	1895	26	94
AC34-5 **a**	my27a126	ghost oscillatory	30	35	0.86	3.31	0.05	0.1096	0.0026	0.972	1692.8	24.0	1703	24	1792	44	95
AC34-68A	my27a188	ghost oscillatory	38	164	0.23	3.46	0.04	0.1066	0.0017	0.966	1623.9	17.0	1635	17	1741	30	94
AC34-34	my27a158	oscillatory	110	186	0.59	3.91	0.04	0.0931	0.0015	0.950	1467.4	14.8	1469	15	1490	30	99
AC34-78	my27a204	oscillatory	321	583	0.55	3.97	0.04	0.0907	0.0009	0.948	1449.2	12.6	1448	13	1440	18	101
AC34-2A	my27a122	oscillatory	166	277	0.60	4.01	0.04	0.0891	0.0010	0.947	1438.1	13.0	1436	13	1406	23	102
AC34-44 **bb**	my27a166	ghost oscillatory	326	616	0.53	4.01	0.04	0.0886	0.0013	0.947	1438.3	14.2	1435	15	1396	28	103
AC34-85	my27a210	ghost oscillatory	88	227	0.39	4.25	0.07	0.0850	0.0027	0.940	1365.1	23.4	1362	24	1315	62	104
AC34-6A **c**	my27a127	homogenous	183	392	0.47	4.42	0.04	0.0825	0.0010	0.936	1317.6	11.7	1314	12	1258	23	104
AC34-74A	my27a199	ghost oscillatory	54	108	0.50	4.84	0.07	0.0801	0.0022	0.927	1210.5	16.5	1210	17	1198	55	101
AC34-36	my27a160	oscillatory	172	196	0.88	4.98	0.06	0.0794	0.0016	0.924	1179.8	13.5	1180	14	1182	40	100
AC34-79	my27a205	homogenous	46	121	0.38	5.78	0.08	0.0790	0.0023	0.911	1023.0	13.6	1029	14	1171	57	88
AC34-21	my27a145	oscillatory	73	135	0.54	5.36	0.11	0.0788	0.0037	0.917	1099.3	22.0	1102	22	1168	94	94
AC34-87	my27a216	oscillatory	341	487	0.70	5.16	0.05	0.0788	0.0010	0.921	1140.9	11.3	1142	12	1167	26	98
AC34-38A	my27a161	chaotic	82	305	0.27	4.85	0.05	0.0781	0.0013	0.927	1212.9	12.3	1210	13	1149	33	105
AC34-39	my27a163	chaotic	170	434	0.39	5.11	0.05	0.0776	0.0010	0.922	1152.2	10.5	1151	11	1136	26	101
AC34-3	my27a124	chaotic	131	183	0.72	5.07	0.05	0.0774	0.0012	0.922	1160.9	11.2	1159	11	1132	32	102
AC34-66	my27a187	oscillatory	136	268	0.51	5.13	0.05	0.0771	0.0013	0.921	1150.3	11.6	1149	12	1124	35	102
AC34-14	my27a139	oscillatory	400	473	0.84	5.11	0.05	0.0768	0.0011	0.922	1153.7	10.7	1152	11	1115	28	103
AC34-15A	my27a140	oscillatory	75	185	0.40	5.25	0.06	0.0768	0.0017	0.919	1124.9	13.2	1124	13	1115	44	101
AC34-22	my27a146	oscillatory	144	314	0.46	4.87	0.06	0.0762	0.0019	0.926	1208.6	14.6	1203	15	1100	49	109
AC34-23	my27a147	oscillatory	318	408	0.78	5.39	0.05	0.0760	0.0011	0.917	1096.8	10.1	1097	10	1094	29	100
AC34-81	my27a207	chaotic	72	391	0.18	5.92	0.07	0.0755	0.0014	0.909	1002.1	12.1	1005	12	1083	38	93
AC34-75	my27a201	chaotic	39	95	0.41	5.78	0.13	0.0755	0.0035	0.911	1027.2	22.5	1029	23	1082	94	95
AC34-18	my27a143	oscillatory	151	499	0.30	5.38	0.05	0.0751	0.0011	0.917	1099.4	9.8	1098	10	1072	30	102
AC34-77	my27a203	homogenous	829	848	0.98	5.22	0.05	0.0748	0.0008	0.920	1133.4	10.8	1130	11	1063	22	106
AC34-11B	my27a136	chaotic	3	265	0.01	6.25	0.06	0.0746	0.0015	0.905	952.2	9.3	956	10	1057	40	90
AC34-48	my27a168	oscillatory	261	379	0.69	5.64	0.08	0.0745	0.0020	0.913	1052.7	14.3	1053	15	1054	54	100
AC34-11A	my27a135	oscillatory	212	386	0.55	5.85	0.07	0.0745	0.0018	0.910	1016.4	12.7	1018	13	1054	50	97
AC34-40	my27a164	oscillatory	68	257	0.27	6.04	0.06	0.0741	0.0013	0.908	984.8	10.1	987	10	1045	36	94
AC34-6B	my27a128	patchy	5	220	0.02	5.93	0.06	0.0738	0.0013	0.909	1003.5	9.5	1005	10	1037	34	97
AC34-17	my27a142	ghost oscillatory	99	185	0.54	5.87	0.06	0.0729	0.0017	0.910	1014.6	10.5	1015	11	1012	48	100
AC34-2B	my27a123	chaotic	2	228	0.01	5.90	0.06	0.0729	0.0012	0.909	1009.1	10.1	1009	10	1012	34	100
AC34-38B	my27a162	chaotic	3	291	0.01	6.04	0.07	0.0727	0.0014	0.908	986.8	10.7	988	11	1005	40	98

Appendix A: Table 2: Sample AC34

Sample	Analysis no.	CL zoning	Th	U	Th/U	Ratios for concordia 238U/206Pb	+/-1 std err	207Pb/206Pb	+/-1 std err	Common Pb 207Pb/206Pb	206Pb/238U 207 corr	1s	206/238 age	+/-1s	207/206 age	+/-1s	conc.
AC34-61	my27a183	patchy	46	401	0.11	6.21	0.06	0.0724	0.0011	0.906	961.9	9.3	963	10	996	32	97
AC34-60	my27a182	sector	43	658	0.07	6.29	0.06	0.0723	0.0009	0.905	949.2	8.5	951	9	993	26	96
AC34-26	my27a149	ghost oscillatory	442	423	1.04	5.73	0.06	0.0722	0.0010	0.912	1038.6	10.3	1037	11	993	29	104
AC34-69	my27a190	sector	97	222	0.44	5.71	0.07	0.0720	0.0017	0.912	1043.0	12.5	1041	13	986	49	105
AC34-50	my27a170	sector	34	526	0.06	6.23	0.06	0.0720	0.0009	0.905	958.3	9.0	959	9	985	27	97
AC34-94A	my27a224	ghost oscillatory	12	474	0.03	5.85	0.06	0.0718	0.0010	0.910	1018.6	9.5	1017	10	980	29	104
AC34-54	my27a177	sector	23	511	0.05	6.15	0.07	0.0716	0.0015	0.906	971.0	10.6	971	11	975	43	100
AC34-91A	my27a220	oscillatory	160	573	0.28	5.92	0.06	0.0716	0.0012	0.909	1007.8	9.8	1006	10	973	35	103
AC34-90A	my27a218	sector	24	346	0.07	6.15	0.06	0.0714	0.0013	0.906	970.6	9.8	971	10	969	36	100
AC34-56	my27a179	chaotic	36	603	0.06	6.19	0.06	0.0711	0.0009	0.906	965.1	8.7	965	9	961	26	100
AC34-71B	my27a197	homogenous	43	437	0.10	6.37	0.06	0.0711	0.0013	0.904	939.0	8.5	940	9	960	36	98
AC34-9	my27a129	chaotic	29	510	0.06	6.28	0.06	0.0710	0.0008	0.905	952.5	8.3	953	9	958	24	99
AC34-10	my27a130	homogenous	21	358	0.06	6.14	0.06	0.0710	0.0011	0.906	972.5	9.2	972	9	958	31	101
AC34-68B	my27a189	patchy	3	246	0.01	6.10	0.07	0.0710	0.0015	0.907	979.6	10.8	979	11	956	44	102
AC34-33	my27a157	homogenous	35	589	0.06	6.35	0.06	0.0709	0.0009	0.904	942.6	8.4	943	9	955	26	99
AC34-15B	my27a141	chaotic	27	480	0.06	6.50	0.06	0.0709	0.0010	0.902	920.8	8.3	922	9	954	30	97
AC34-12	my27a137	sector	38	681	0.06	6.29	0.06	0.0708	0.0008	0.905	950.4	8.2	950	8	950	23	100
AC34-95	my27a226	patchy	33	488	0.07	6.27	0.06	0.0707	0.0010	0.905	953.6	8.6	953	9	948	30	101
AC34-97	my27a228		42	469	0.09	6.26	0.06	0.0706	0.0011	0.905	955.1	8.5	955	9	946	31	101
AC34-74B	my27a200	patchy	3	312	0.01	6.18	0.07	0.0706	0.0015	0.906	967.8	10.1	967	10	944	44	102
AC34-24	my27a148	sector	37	629	0.06	6.30	0.06	0.0705	0.0010	0.905	950.4	8.8	950	9	942	28	101
AC34-65	my27a186	chaotic	47	545	0.09	6.38	0.06	0.0705	0.0009	0.904	937.9	8.3	938	8	942	28	100
AC34-49	my27a169	ghost oscillatory	29	574	0.05	6.42	0.06	0.0704	0.0011	0.903	932.4	8.7	933	9	940	31	99
AC34-90B	my27a219	sector	55	766	0.07	6.27	0.06	0.0703	0.0010	0.905	954.1	8.3	953	9	938	28	102
AC34-76	my27a202	chaotic	34	558	0.06	6.48	0.07	0.0703	0.0011	0.902	924.1	9.0	925	9	937	33	99
AC34-93	my27a223	sector	30	662	0.04	6.24	0.08	0.0702	0.0013	0.905	959.1	11.9	958	12	934	39	103
AC34-73	my27a198	sector	47	681	0.07	6.39	0.06	0.0702	0.0010	0.904	937.5	8.3	937	9	933	30	100
AC34-71A	my27a196	sector	79	666	0.12	6.28	0.06	0.0702	0.0013	0.905	952.9	8.8	952	9	933	38	102
AC34-94B	my27a225	homogenous	36	520	0.07	6.46	0.06	0.0701	0.0011	0.903	927.5	8.3	928	8	930	31	100
AC34-89	my27a217	sector	49	534	0.09	6.38	0.06	0.0700	0.0011	0.904	939.7	9.0	939	9	929	31	101
AC34-96	my27a227	chaotic	35	597	0.06	6.32	0.06	0.0700	0.0011	0.904	947.8	8.9	947	9	929	32	102
AC34-32	my27a156	sector	50	448	0.11	6.41	0.06	0.0700	0.0011	0.903	934.2	8.7	934	9	928	32	101
AC34-86	my27a215	sector	23	582	0.04	5.99	0.07	0.0699	0.0009	0.908	997.6	11.0	995	11	925	26	108
AC34-91B	my27a221	homogenous	29	884	0.03	6.18	0.06	0.0698	0.0008	0.906	968.1	8.5	966	9	922	23	105
AC34-35	my27a159	sector	44	392	0.11	6.25	0.06	0.0697	0.0011	0.905	958.2	9.2	957	9	921	31	104
AC34-51	my27a175	oscillatory	8	365	0.02	6.08	0.06	0.0697	0.0011	0.907	983.2	9.8	981	10	920	32	107
AC34-1	my27a121	sector	28	416	0.07	6.06	0.05	0.0697	0.0009	0.907	987.3	8.7	985	9	919	28	107
AC34-30	my27a155	sector	35	483	0.07	6.36	0.06	0.0696	0.0010	0.904	941.7	8.5	941	9	918	31	103
AC34-57	my27a180	sector	38	689	0.06	6.31	0.06	0.0696	0.0008	0.904	950.1	8.5	949	9	916	24	104

Appendix A: Table 2: Sample AC34

Sample	Analysis no.	CL zoning	Th	U	Th/U	Ratios for concordia 238U/206Pb	+/-1 std err	207Pb/206Pb	+/-1 std err	Common Pb 207Pb/206Pb	206Pb/238U 207 corr	1s	206/238 age	+/-1s	207/206 age	+/-1s	conc.
AC34-80	my27a206	chaotic	31	501	0.06	6.43	0.07	0.0696	0.0010	0.903	932.5	9.2	932	9	915	30	102
AC34-92	my27a222	homogenous	33	664	0.05	6.36	0.06	0.0695	0.0009	0.904	942.4	8.2	941	8	912	27	103
AC34-19	my27a144	sector	46	993	0.05	6.41	0.06	0.0694	0.0007	0.903	935.4	7.9	935	8	912	21	103
AC34-46	my27a167	patchy	20	370	0.05	6.22	0.06	0.0694	0.0012	0.905	963.3	9.4	961	10	910	34	106
AC34-55	my27a178	ghost oscillatory	26	465	0.06	6.70	0.08	0.0693	0.0018	0.900	896.8	10.9	897	11	908	53	99
AC34-63	my27a184	sector	44	519	0.08	6.44	0.06	0.0693	0.0011	0.903	930.7	8.7	930	9	906	31	103
AC34-13	my27a138	sector	38	569	0.07	6.41	0.06	0.0692	0.0008	0.903	935.0	8.0	934	8	904	25	103
AC34-58	my27a181	homogenous	22	1191	0.02	5.76	0.06	0.0692	0.0013	0.911	1037.2	10.9	1032	11	903	39	114
AC34-82 ddd	my27a208	oscillatory	32	451	0.07	6.77	0.07	0.0685	0.0013	0.900	888.4	9.0	888	9	883	39	101
AC34-84	my27a209	sector	44	516	0.09	7.44	0.07	0.0670	0.0010	0.894	812.0	7.8	813	8	838	30	97

Sample		Analysis no.	CL zoning	Th	U	Th/U Ratio	Ratios for concordia 238U/206Pb	+/-1 std err	207Pb/206Pb	+/-1 std err	Common Pb 207Pb/206Pb	206Pb/238U 207 corr	1s	206/238 age	+/-1s	207/206 age	+/-1s	conc.
		Appendix A: Table 1: Sample 90024																
90024-15	**aaa**	my27a029	chaotic	55	132	0.41	2.13	0.02	0.1665	0.0022	1.053	2465.5	27.8	2478	26	2522	22	98
90024-42	**aa'**	my27a060	homogenous unzc	24	62	0.39	2.13	0.05	0.1631	0.0031	1.053	2475.4	63.6	2478	59	2488	32	100
90024-60	**aa**	my27a078	oscillatory zoning	445	759	0.59	2.63	0.03	0.1220	0.0013	1.010	2090.8	21.1	2076	21	1986	19	105
90024-83	**a**	my27a105	irregular concentr	149	320	0.46	3.81	0.05	0.0995	0.0023	0.953	1492.3	19.9	1502	20	1615	44	93
90024-51		my27a070	chaotic	154	188	0.82	3.83	0.04	0.0954	0.0018	0.952	1492.0	16.7	1495	17	1536	35	97
90024-45A		my27a062	patchy	108	658	0.16	5.48	0.06	0.0893	0.0012	0.916	1064.3	10.6	1081	11	1410	26	77
90024-81		my27a103	oscillatory zoning	409	693	0.59	4.36	0.07	0.0891	0.0015	0.937	1326.3	20.3	1331	21	1406	31	95
90024-37	**bb**	my27a056	oscillatory & trans	124	619	0.20	4.51	0.05	0.0858	0.0013	0.934	1288.6	14.9	1291	15	1333	29	97
90024-77		my27a099	oscillatory zoning	206	779	0.26	4.77	0.07	0.0843	0.0021	0.928	1223.1	18.1	1227	19	1300	48	94
90024-14	**c**	my27a028	oscillatory zoning	52	204	0.25	4.75	0.08	0.0835	0.0029	0.929	1229.3	19.9	1232	20	1280	67	96
90024-3A		my27a017	oscillatory	245	432	0.57	4.77	0.04	0.0822	0.0011	0.928	1225.1	10.8	1227	11	1251	27	98
90024-44		my27a061	ghost oscillatory	62	74	0.83	6.33	0.10	0.0784	0.0031	0.904	937.0	14.3	946	14	1157	79	82
90024-75		my27a097	oscillatory	158	271	0.58	5.22	0.08	0.0781	0.0029	0.920	1129.1	16.4	1130	17	1150	73	98
90024-36		my27a055	oscillatory	138	163	0.85	5.17	0.08	0.0779	0.0024	0.921	1139.7	18.1	1140	19	1144	61	100
90024-35A		my27a049	sector	43	116	0.37	6.28	0.09	0.0764	0.0028	0.905	946.8	13.7	953	14	1106	73	86
90024-63A		my27a081	oscillatory zoning	255	241	1.06	5.96	0.07	0.0764	0.0018	0.909	994.8	10.9	999	11	1105	47	90
90024-67		my27a085	patchy	768	2666	0.29	5.42	0.06	0.0759	0.0014	0.916	1091.3	12.0	1091	12	1093	37	100
90024-35B		my27a050	sector	42	102	0.41	6.32	0.09	0.0758	0.0024	0.904	941.5	12.9	947	13	1091	64	87
90024-41		my27a059	oscillatory zoning	276	553	0.50	5.36	0.05	0.0756	0.0011	0.917	1104.1	10.2	1103	10	1084	29	102
90024-22		my27a039	chaotic	47	112	0.42	5.84	0.08	0.0756	0.0023	0.910	1016.8	14.2	1020	15	1084	62	94
90024-3B		my27a018	ghost oscillatory/s	33	321	0.10	5.80	0.08	0.0755	0.0022	0.911	1022.4	13.7	1025	14	1081	58	95
90024-84		my27a106	chaotic	33	176	0.19	6.52	0.08	0.0752	0.0019	0.902	913.6	11.1	919	11	1073	50	86
90024-85		my27a107	oscillatory zoning	247	733	0.34	5.46	0.05	0.0751	0.0009	0.916	1085.0	10.1	1084	10	1072	24	101
90024-33		my27a047	ghost irregular co	35	96	0.36	6.34	0.09	0.0749	0.0025	0.904	939.5	13.0	944	13	1065	66	89
90024-10A		my27a022	chaotic	24	234	0.10	4.79	0.09	0.0748	0.0036	0.928	1230.9	23.5	1222	24	1063	97	115
90024-69		my27a087	irregular concentr	30	112	0.27	6.47	0.10	0.0747	0.0025	0.903	921.9	13.6	927	14	1059	68	88
90024-50A		my27a068	oscillatory zoning	264	494	0.53	5.93	0.08	0.0746	0.0022	0.909	1001.9	13.7	1004	14	1057	59	95
90024-74		my27a096	homogenous unzc	43	148	0.29	6.46	0.08	0.0745	0.0020	0.903	922.3	11.0	927	11	1056	55	88
90024-46A		my27a064	ghost oscillatory	30	113	0.26	6.16	0.09	0.0745	0.0021	0.906	966.5	13.1	970	13	1056	58	92
90024-17B		my27a035	sector	35	139	0.25	6.37	0.09	0.0743	0.0027	0.904	935.5	13.2	940	13	1048	74	90
90024-71		my27a089	oscillatory zoning	72	168	0.43	5.84	0.17	0.0742	0.0046	0.910	1017.4	28.8	1019	29	1046	125	97
90024-58		my27a076	homogenous unzc	42	93	0.45	6.40	0.09	0.0740	0.0025	0.903	932.4	13.2	936	13	1043	68	90
90024-92		my27a118	homogenous unzc	19	91	0.21	6.12	0.08	0.0740	0.0019	0.907	973.0	12.5	976	13	1042	52	94
90024-1		my27a015	oscillatory	218	304	0.72	5.60	0.05	0.0734	0.0014	0.914	1059.9	10.2	1058	10	1026	38	103
90024-29		my27a044	homogenous unzc	19	139	0.14	6.42	0.08	0.0733	0.0024	0.903	929.6	12.0	933	12	1021	65	91
90024-39		my27a057	chaotic	43	123	0.35	6.35	0.08	0.0731	0.0023	0.904	939.3	12.2	942	12	1016	64	93
90024-34		my27a048	patchy	26	159	0.17	6.37	0.07	0.0730	0.0020	0.904	936.8	10.5	940	11	1013	56	93
90024-82		my27a104	sector	36	195	0.19	6.37	0.09	0.0729	0.0020	0.904	937.5	12.7	940	13	1010	56	93
90024-62		my27a080	sector	43	170	0.25	6.43	0.08	0.0728	0.0017	0.903	929.6	11.2	932	11	1009	48	92
90024-90		my27a117	chaotic	20	63	0.31	6.28	0.09	0.0728	0.0023	0.905	951.1	12.8	953	13	1008	64	95
90024-59		my27a077	sector	53	118	0.45	6.29	0.09	0.0727	0.0023	0.905	949.7	12.8	952	13	1006	64	95
90024-49		my27a067	chaotic	33	124	0.26	5.99	0.08	0.0725	0.0020	0.908	994.5	13.2	995	13	999	56	100

Appendix A: Table 1: Sample 90024

Sample	Analysis no.	CL zoning	Th	U	Th/U Ratio	Ratios for concordia 238U/206Pb	+/-1 std err	207Pb/206Pb	+/-1 std err	Common Pb 207Pb/206Pb	206Pb/238U 207 corr	1s	206/238 age	+/-1s	207/206 age	+/-1s	conc.
90024-46B	my27a065	chaotic	23	179	0.13	6.29	0.07	0.0724	0.0019	0.905	949.3	11.1	951	11	997	52	95
90024-18	my27a036	chaotic	42	94	0.45	6.21	0.09	0.0721	0.0025	0.906	961.2	13.7	962	14	990	72	97
90024-26	my27a042	chaotic	40	86	0.46	6.39	0.10	0.0720	0.0023	0.904	935.2	14.0	937	14	986	66	95
90024-63B	my27a082	irregular concentr	212	303	0.70	6.20	0.07	0.0719	0.0017	0.906	963.8	11.3	965	12	982	49	98
90024-94	my27a120	chaotic	15	91	0.17	6.06	0.07	0.0719	0.0022	0.907	984.8	12.0	985	12	982	62	100
90024-64	my27a083	chaotic	48	99	0.48	6.29	0.09	0.0718	0.0023	0.905	950.2	13.3	951	14	980	65	97
90024-6	my27a020	ghost oscillatory	32	89	0.36	6.25	0.09	0.0717	0.0026	0.905	956.4	14.3	957	15	977	75	98
90024-88	my27a110	irregular concentr	39	152	0.25	6.48	0.09	0.0717	0.0021	0.903	922.8	12.0	925	12	977	59	95
90024-10B	my27a023	chaotic	31	174	0.18	6.28	0.07	0.0717	0.0019	0.905	951.7	11.1	953	11	976	53	98
90024-61	my27a079	chaotic	35	118	0.29	6.22	0.09	0.0716	0.0024	0.905	960.5	13.1	961	13	974	68	99
90024-11	my27a024	sector	38	188	0.20	6.07	0.09	0.0715	0.0028	0.907	984.2	15.0	984	15	972	80	101
90024-12A	my27a025	sector	36	121	0.30	6.31	0.08	0.0714	0.0023	0.904	947.7	12.1	949	12	970	65	98
90024-72	my27a090	chaotic	28	176	0.16	6.21	0.14	0.0713	0.0034	0.906	963.1	21.9	963	22	967	96	100
90024-40	my27a058	sector	49	209	0.23	6.47	0.08	0.0713	0.0018	0.903	925.4	10.8	927	11	965	51	96
90024-7	my27a021	ghost oscillatory	28	116	0.24	6.22	0.08	0.0712	0.0020	0.905	961.1	12.1	961	12	964	56	100
90024-66	my27a084	sector	46	126	0.37	6.37	0.09	0.0712	0.0022	0.904	939.8	12.5	941	13	963	64	98
90024-78	my27a100	homogenous unzc	28	192	0.15	6.43	0.07	0.0712	0.0017	0.903	930.8	10.1	932	10	963	50	97
90024-13	my27a027	chaotic	33	106	0.31	6.18	0.09	0.0709	0.0025	0.906	967.6	13.1	967	13	954	71	101
90024-76	my27a098	sector	39	146	0.27	6.44	0.08	0.0708	0.0020	0.903	930.3	11.4	931	12	952	57	98
90024-27	my27a043	oscillatory	146	397	0.37	5.98	0.06	0.0708	0.0014	0.908	998.8	9.9	997	10	950	40	105
90024-47	my27a066	sector	42	129	0.32	6.47	0.09	0.0702	0.0022	0.903	926.1	12.2	926	12	934	63	99
90024-23	my27a040	chaotic	13	164	0.08	6.41	0.08	0.0701	0.0020	0.903	934.3	11.5	934	12	931	58	100
90024-17A	my27a030	ghost oscillatory	62	452	0.14	6.13	0.06	0.0701	0.0012	0.907	975.5	9.4	974	10	930	35	105
90024-31	my27a045	sector	37	90	0.41	6.22	0.09	0.0700	0.0027	0.906	962.8	13.7	962	14	930	78	103
90024-32	my27a046	chaotic	33	156	0.21	6.40	0.08	0.0697	0.0022	0.903	937.1	11.3	937	11	920	64	102
90024-93	my27a119	homogenous unzc	4	89	0.05	6.16	0.08	0.0696	0.0020	0.906	971.3	12.0	969	12	916	58	106
90024-2	my27a016	sector	61	140	0.44	6.25	0.08	0.0696	0.0019	0.905	957.8	11.7	956	12	916	57	104
90024-19	my27a037	chaotic	47	137	0.34	6.29	0.08	0.0696	0.0023	0.905	952.6	12.0	951	12	915	67	104
90024-79	my27a101	chaotic	33	128	0.26	6.48	0.09	0.0694	0.0022	0.903	925.6	12.4	925	13	911	65	102
90024-25	my27a041	chaotic	34	113	0.30	6.30	0.09	0.0694	0.0022	0.904	950.6	13.0	949	13	911	64	104
90024-73	my27a095	sector	44	209	0.21	6.45	0.07	0.0693	0.0018	0.903	929.4	10.1	929	10	907	53	102
90024-5	my27a019	patchy	26	105	0.25	6.13	0.08	0.0692	0.0023	0.906	976.2	12.7	973	13	904	70	108
90024-56	my27a075	chaotic	44	101	0.44	6.46	0.09	0.0691	0.0025	0.903	929.0	12.7	928	13	902	74	103
90024-68	my27a086	chaotic	40	162	0.24	6.17	0.08	0.0691	0.0018	0.906	971.1	12.2	969	12	901	53	107
90024-70	my27a088	chaotic	28	127	0.22	6.10	0.19	0.0691	0.0047	0.907	981.3	30.3	978	31	901	141	109
90024-89A ddd	my27a115	oscillatory zoning	37	254	0.15	6.48	0.07	0.0687	0.0015	0.903	927.0	9.4	926	10	891	46	104
90024-50B	my27a069	chaotic	40	95	0.43	6.44	0.10	0.0687	0.0024	0.903	931.7	14.3	930	15	889	73	105
90024-80	my27a102	sector	42	122	0.35	6.27	0.10	0.0680	0.0022	0.905	956.8	14.6	954	15	869	66	110
90024-86	my27a108	chaotic	32	174	0.19	6.57	0.08	0.0680	0.0017	0.902	915.2	10.5	914	11	867	52	105
90024-89B	my27a116	chaotic	12	91	0.13	5.89	0.07	0.0678	0.0018	0.910	1017.1	11.8	1011	12	861	56	117
90024-87	my27a109	chaotic	36	92	0.40	6.31	0.09	0.0674	0.0027	0.904	951.7	13.5	948	14	850	85	112
90024-45B	my27a063	chaotic	34	212	0.16	6.19	0.07	0.0672	0.0015	0.906	970.6	10.4	966	11	843	46	115

	Appendix A: Table 1: Sample 90024				Th/U	Ratios for concordia											
Sample	Analysis no.	CL zoning	Th	U	Ratio	238U/206Pb	+/-1 std err	207Pb/206P	+/-1 std err	Common Pb 207Pb/206Pb	206Pb/238U 207 corr	1s	206/238 age	+/-1s	207/206 age	+/-1s	conc.
90024-12B	my27a026	chaotic	39	94	0.41	6.20	0.13	0.0670	0.0034	0.906	968.1	20.1	963	20	838	107	115
90024-20 **d+**	my27a038	oscillatory zoning	37	116	0.32	8.12	0.17	0.0625	0.0038	0.888	750.0	15.9	749	16	692	131	108

Sample	Appendix A: Table 4: Sample FS0214					Ratios for concordia											
Sample	Analysis no	CL zoning	Th	U	Th/U	238U/206Pb	+/-1 std err	207Pb/206Pb	+/-1 std err	Common Pb 207Pb/206Pb	206Pb/238U 207 corr	1s	206/238 age	+/-1s	207/206 age	+/-1s	conc.
FS0214-10 aa'	OC27b019	oscillatory	99	198	0.50	2.17	0.09	0.1621	0.0031	1.050	2437.3	102.4	2446	97	2478	32	99
FS0214-20	OC27b029	oscillatory	121	212	0.57	2.52	0.09	0.1594	0.0027	1.019	2096.5	79.4	2158	81	2450	29	88
FS0214-23B	OC27b039	homogenous	66	219	0.30	2.20	0.06	0.1591	0.0042	1.046	2401.9	65.8	2411	62	2446	44	99
FS0214-57	OC27b069	homogenous	89	107	0.83	2.58	0.05	0.1511	0.0050	1.014	2061.5	44.3	2110	44	2358	57	89
FS0214-23A	OC27b038	oscillatory	72	208	0.34	2.74	0.06	0.1496	0.0031	1.002	1943.0	41.7	2003	43	2341	35	86
FS0214-74A	OC27b085	chaotic	65	118	0.55	2.84	0.05	0.1465	0.0046	0.996	1883.6	35.3	1943	35	2306	54	84
FS0214-16A	OC27b026	oscillatory	77	271	0.28	2.87	0.11	0.1427	0.0025	0.995	1872.4	72.9	1926	76	2261	30	85
FS0214-103	OC27b124	oscillatory	83	163	0.51	3.35	0.07	0.1384	0.0039	0.970	1616.5	33.6	1683	35	2207	50	76
FS0214-40 aa	OC27b049	chaotic	142	390	0.36	3.70	0.06	0.1298	0.0021	0.957	1483.8	22.6	1543	24	2096	28	74
FS0214-81	OC27b093	oscillatory	161	384	0.42	3.95	0.08	0.1196	0.0024	0.949	1409.9	27.9	1456	30	1951	36	75
FS0214-87	OC27b103	oscillatory	39	275	0.14	3.36	0.18	0.1182	0.0035	0.970	1650.4	87.6	1679	91	1929	53	87
FS0214-70 a	OC27b081	homogenous	9	215	0.04	4.10	0.10	0.1010	0.0040	0.944	1388.7	33.0	1408	34	1643	74	86
FS0214-99	OC27b121	oscillatory	195	167	1.17	5.01	0.09	0.0989	0.0037	0.923	1146.8	19.5	1173	20	1603	70	73
FS0214-36A	OC27b045	chaotic	17	277	0.06	3.96	0.07	0.0987	0.0023	0.948	1438.1	23.4	1450	24	1600	44	91
FS0214-14	OC27b024	patchy	15	313	0.05	3.90	0.15	0.0947	0.0022	0.950	1467.7	54.6	1472	57	1522	44	97
FS0214-16B	OC27b027	chaotic	14	437	0.03	3.87	0.15	0.0943	0.0019	0.951	1480.4	54.4	1483	56	1514	37	98
FS0214-93B	OC27b109	chaotic	31	212	0.14	4.29	0.07	0.0943	0.0027	0.939	1338.5	20.0	1350	21	1514	54	89
FS0214-95	OC27b111	chaotic	59	353	0.17	3.94	0.07	0.0940	0.0032	0.949	1455.2	27.0	1459	28	1509	64	97
FS0214-85	OC27b101	homogenous	10	247	0.04	4.48	0.12	0.0940	0.0055	0.934	1283.3	33.7	1298	34	1509	110	86
FS0214-77A	OC27b088	ghost oscillatory	5	277	0.02	4.33	0.09	0.0932	0.0047	0.938	1328.1	28.9	1339	29	1493	95	90
FS0214-91	OC27b107	homogenous	80	290	0.28	4.67	0.08	0.0926	0.0025	0.930	1235.9	20.4	1251	21	1479	52	85
FS0214-76	OC27b087	chaotic	11	295	0.04	4.18	0.08	0.0918	0.0033	0.942	1376.9	25.3	1383	26	1464	69	94
FS0214-46	OC27b059	chaotic	27	349	0.08	3.99	0.08	0.0913	0.0025	0.948	1441.6	27.3	1443	28	1454	51	99
FS0214-88	OC27b104	homogenous	6	287	0.02	4.25	0.13	0.0910	0.0037	0.940	1357.1	39.2	1363	40	1446	77	94
FS0214-56A	OC27b067	sector	11	265	0.04	4.48	0.08	0.0910	0.0023	0.934	1289.3	21.2	1299	22	1446	48	90
FS0214-69	OC27b080	homogenous	18	231	0.08	4.06	0.11	0.0907	0.0046	0.945	1419.3	38.4	1421	39	1440	97	99
FS0214-41	OC27b050	chaotic	33	304	0.11	3.92	0.06	0.0904	0.0021	0.950	1467.4	23.3	1465	24	1435	44	102
FS0214-73	OC27b084	homogenous	19	231	0.08	5.25	0.11	0.0903	0.0028	0.919	1107.8	23.5	1125	24	1432	60	79
FS0214-71	OC27b082	ghost oscillatory	14	275	0.05	4.52	0.07	0.0898	0.0024	0.934	1280.1	20.3	1289	21	1422	50	91
FS0214-15 bb	OC27b025	oscillatory	73	203	0.36	5.89	0.23	0.0864	0.0028	0.910	995.3	37.1	1011	39	1348	62	75
FS0214-61	OC27b073	homogenous	2	255	0.01	4.46	0.11	0.0862	0.0035	0.935	1302.8	30.3	1305	31	1343	78	97
FS0214-79A	OC27b091	chaotic	18	233	0.08	4.94	0.09	0.0857	0.0031	0.925	1180.7	21.8	1189	22	1332	71	89
FS0214-96	OC27b112	chaotic	14	286	0.05	4.90	0.09	0.0852	0.0029	0.926	1190.5	21.8	1198	22	1321	66	91
FS0214-30	OC27b043	ghost oscillatory	101	435	0.23	4.78	0.08	0.0851	0.0022	0.928	1218.6	18.7	1224	19	1317	51	93
FS0214-102 c	OC27b123	homogenous	16	441	0.04	4.40	0.09	0.0839	0.0025	0.936	1321.1	26.0	1319	27	1291	57	102
FS0214-97	OC27b113	chaotic	22	189	0.12	4.86	0.13	0.0830	0.0054	0.926	1202.1	31.5	1206	32	1269	127	95
FS0214-106	OC27b126	patchy	13	366	0.03	5.51	0.10	0.0817	0.0023	0.915	1066.4	19.2	1074	20	1239	54	87
FS0214-44	OC27b058	chaotic	15	308	0.05	5.12	0.11	0.0816	0.0029	0.921	1145.7	25.0	1150	26	1235	69	93
FS0214-90	OC27b106	patchy	10	175	0.06	5.89	0.13	0.0811	0.0037	0.910	1001.1	21.7	1011	22	1224	90	83
FS0214-77B	OC27b089	chaotic	56	108	0.52	6.45	0.12	0.0809	0.0041	0.903	917.9	17.6	930	18	1219	100	76
FS0214-58B	OC27b071	chaotic	46	117	0.39	6.54	0.15	0.0783	0.0036	0.902	907.6	19.9	917	20	1153	92	79
FS0214-47	OC27b060	chaotic	42	145	0.29	6.42	0.12	0.0772	0.0035	0.903	925.4	17.6	933	18	1126	91	83

Sample	Appendix A: Table 4: Sample FS0214 Analysis no	CL zoning	Th	U	Th/U	Ratios for concordia 238U/206Pb	+/-1 std err	207Pb/206Pb	+/-1 std err	Common Pb 207Pb/206Pb	206Pb/238U 207 corr	1s	206/238 age	+/-1s	207/206 age	+/-1s	conc.
FS0214-74B	OC27b086	chaotic	54	109	0.49	6.69	0.14	0.0769	0.0042	0.900	889.5	18.4	898	19	1118	109	80
FS0214-84B	OC27b100	chaotic	76	151	0.50	6.80	0.14	0.0766	0.0033	0.899	875.6	18.0	884	18	1111	87	80
FS0214-54	OC27b066	ghost oscillatory	52	144	0.36	6.70	0.15	0.0758	0.0038	0.900	889.3	19.1	896	20	1089	100	82
FS0214-7	OC27b018	chaotic	42	158	0.27	6.46	0.27	0.0755	0.0033	0.903	921.9	37.1	928	39	1081	87	86
FS0214-43B	OC27b053	chaotic	109	184	0.59	6.72	0.13	0.0743	0.0033	0.900	888.0	16.5	894	17	1050	89	85
FS0214-79B	OC27b092	oscillatory	8	175	0.04	6.26	0.13	0.0742	0.0037	0.905	951.4	18.8	955	19	1047	99	91
FS0214-98A	OC27b119	chaotic	74	172	0.43	6.29	0.10	0.0735	0.0028	0.905	947.5	15.1	951	15	1028	76	92
FS0214-65	OC27b078		24	151	0.16	6.37	0.13	0.0734	0.0029	0.904	937.1	18.9	940	19	1026	80	92
FS0214-36B	OC27b046	homogenous	39	135	0.29	6.59	0.14	0.0733	0.0033	0.901	907.0	18.3	911	19	1022	92	89
FS0214-67	OC27b079	homogenous	40	126	0.32	6.41	0.14	0.0732	0.0033	0.903	931.8	19.4	935	20	1021	91	92
FS0214-5	OC27b016	sector	65	130	0.50	6.53	0.26	0.0732	0.0034	0.902	914.3	35.4	918	37	1020	95	90
FS0214-98B	OC27b120	sector	64	127	0.50	6.49	0.14	0.0728	0.0033	0.902	920.0	19.0	923	19	1009	91	92
FS0214-25	OC27b041	chaotic	176	375	0.47	6.49	0.11	0.0726	0.0022	0.902	921.1	14.7	924	15	1003	63	92
FS0214-56B	OC27b068	ghost oscillatory	95	170	0.56	6.44	0.13	0.0719	0.0029	0.903	928.6	18.4	931	19	982	83	95
FS0214-82	OC27b098	chaotic	39	116	0.34	6.10	0.15	0.0716	0.0032	0.907	978.3	22.9	978	23	975	91	100
FS0214-89	OC27b105	ghost oscillatory	55	115	0.47	6.58	0.15	0.0713	0.0032	0.902	910.6	19.9	913	20	965	91	95
FS0214-50	OC27b064	chaotic	64	126	0.51	6.46	0.14	0.0712	0.0033	0.903	926.5	20.1	928	20	964	95	96
FS0214-72	OC27b083	sector	84	144	0.58	6.62	0.14	0.0711	0.0032	0.901	904.8	18.9	907	19	960	93	94
FS0214-37B	OC27b048	homogenous	91	152	0.60	6.55	0.16	0.0710	0.0031	0.902	914.4	22.5	916	23	957	90	96
FS0214-49B	OC27b063	sector	35	174	0.20	6.59	0.19	0.0710	0.0039	0.901	909.4	25.4	911	26	957	114	95
FS0214-19	OC27b028	homogenous	23	140	0.16	6.37	0.26	0.0709	0.0031	0.904	939.5	37.3	940	38	953	90	99
FS0214-35	OC27b044	patchy	55	136	0.41	6.48	0.14	0.0708	0.0036	0.902	923.6	19.6	925	20	952	104	97
FS0214-42	OC27b051	chaotic	48	110	0.43	6.26	0.15	0.0708	0.0038	0.905	955.1	22.2	955	23	950	109	100
FS0214-1	OC27b014	sector	47	170	0.28	6.48	0.25	0.0704	0.0028	0.902	924.1	34.8	925	36	940	81	98
FS0214-12B	OC27b022	ghost oscillatory	103	175	0.59	6.45	0.26	0.0701	0.0025	0.903	928.5	35.7	929	37	931	73	100
FS0214-53	OC27b065	ghost sector	27	126	0.22	6.46	0.18	0.0696	0.0060	0.903	928.0	25.3	928	25	917	177	101
FS0214-6	OC27b017	irregular concentr	57	114	0.50	6.51	0.27	0.0694	0.0034	0.902	921.4	36.5	921	38	909	100	101
FS0214-60	OC27b072	chaotic	39	151	0.26	6.35	0.12	0.0692	0.0031	0.904	944.7	17.0	943	17	904	93	104
FS0214-48 ddd	OC27b061	chaotic	50	134	0.37	6.43	0.13	0.0686	0.0031	0.903	934.1	18.3	932	19	887	93	105
FS0214-11	OC27b020	chaotic	105	178	0.59	6.73	0.27	0.0677	0.0027	0.900	894.2	34.7	893	36	858	82	104

	Appendix A: Table 3: Sample GS01					Ratios for concordia											
Sample	Analysis no.	CL zoning	Th	U	Th/U	238U/206Pb	+/-1 std err	207Pb/206Pb	+/-1 std err	Common Pb 207Pb/206Pb	206Pb/238U 207 corr	1s	206/238 age	+/-1s	207/206 age	+/-1s	conc.
GS01-42 a	NV05a058	chaotic	33	141	0.23	3.25	0.04	0.1050	0.0025	0.975	1729.6	23.4	1728	23	1715	44	101
GS01-20A	NV05a038	chaotic	42	226	0.19	3.26	0.05	0.1045	0.0026	0.974	1727.0	26.6	1725	27	1706	46	101
GS01-66	NV05a074	sector	34	276	0.12	3.11	0.04	0.1043	0.0019	0.982	1809.5	22.5	1798	22	1702	33	106
GS01-13A	NV05a024	sector	17	292	0.06	3.41	0.04	0.1024	0.0013	0.968	1658.1	21.1	1659	22	1668	24	99
GS01-25	NV05a043	sector	32	99	0.32	3.85	0.07	0.1016	0.0035	0.952	1473.1	25.8	1487	26	1653	64	90
GS01-86	NV05a087	homogenous	65	277	0.23	3.18	0.07	0.1015	0.0014	0.978	1776.8	36.9	1764	37	1651	26	107
GS01-91	NV05a095	homogenous	43	318	0.13	3.22	0.04	0.1013	0.0016	0.976	1751.4	19.1	1741	19	1649	29	106
GS01-22	NV05a040	chaotic	41	175	0.23	3.62	0.08	0.1013	0.0043	0.960	1566.2	33.3	1573	34	1648	78	95
GS01-93	NV05a097	sector	37	507	0.07	3.36	0.03	0.0992	0.0011	0.970	1687.0	15.8	1680	16	1610	21	104
GS01-70	NV05a075	homogenous	30	86	0.34	3.59	0.08	0.0991	0.0051	0.961	1583.0	35.1	1585	35	1607	96	99
GS01-105	NV05a116	sector	39	99	0.39	3.83	0.06	0.0984	0.0029	0.952	1487.6	22.6	1496	23	1593	56	94
GS01-14A	NV05a026	sector	58	709	0.08	3.57	0.05	0.0983	0.0022	0.962	1592.0	23.8	1592	24	1592	42	100
GS01-61	NV05a068	sector	26	151	0.17	4.60	0.16	0.0979	0.0042	0.932	1245.3	41.3	1267	43	1584	79	80
GS01-102	NV05a108	sector	30	521	0.06	3.65	0.05	0.0978	0.0011	0.959	1558.3	20.0	1560	21	1582	21	99
GS01-97A	NV05a101	sector	25	270	0.09	3.64	0.06	0.0975	0.0030	0.959	1565.2	26.4	1566	27	1578	58	99
GS01-71	NV05a076	sector	39	105	0.37	3.99	0.05	0.0968	0.0027	0.947	1432.3	17.9	1442	18	1562	53	92
GS01-15	NV05a028	sector	51	477	0.11	3.43	0.04	0.0959	0.0019	0.967	1660.0	21.2	1650	21	1546	38	107
GS01-87	NV05a088	sector	44	154	0.28	3.72	0.05	0.0956	0.0017	0.956	1534.5	19.0	1535	19	1540	34	100
GS01-18A	NV05a035	homogenous	29	73	0.39	3.86	0.13	0.0954	0.0062	0.951	1479.9	51.0	1484	52	1535	121	97
GS01-36	NV05a054	sector	61	372	0.16	4.06	0.05	0.0950	0.0017	0.945	1411.5	18.4	1420	19	1529	33	93
GS01-58	NV05a067	sector	57	617	0.09	3.93	0.04	0.0948	0.0011	0.949	1457.0	13.7	1462	14	1524	22	96
GS01-8	NV05a018	sector	66	690	0.10	3.97	0.04	0.0943	0.0013	0.948	1441.9	15.6	1447	16	1514	27	96
GS01-104B	NV05a115	patchy	167	845	0.20	3.76	0.03	0.0942	0.0009	0.955	1519.2	13.7	1519	14	1512	17	100
GS01-48	NV05a060	patchy	44	129	0.34	4.08	0.07	0.0937	0.0029	0.945	1407.7	22.9	1414	23	1501	59	94
GS01-95	NV05a099	sector	45	97	0.46	4.29	0.08	0.0924	0.0034	0.939	1342.6	25.0	1351	26	1475	69	92
GS01-10	NV05a020	sector	76	1113	0.07	3.81	0.07	0.0919	0.0016	0.953	1504.8	26.9	1502	28	1465	34	102
GS01-54	NV05a063	sector	40	95	0.42	4.50	0.06	0.0913	0.0022	0.934	1283.0	17.0	1294	18	1453	46	89
GS01-41	NV05a057	sector	37	459	0.08	4.37	0.06	0.0909	0.0014	0.937	1318.9	16.5	1327	17	1445	30	92
GS01-101A	NV05a106	ghost sector	48	346	0.14	4.28	0.05	0.0906	0.0017	0.939	1347.8	16.2	1354	17	1437	35	94
GS01-17	NV05a034	oscillatory	30	483	0.06	4.06	0.06	0.0904	0.0019	0.945	1419.0	19.9	1420	20	1433	40	99
GS01-85A	NV05a085	chaotic	42	123	0.34	4.05	0.07	0.0900	0.0026	0.946	1421.4	23.5	1422	24	1425	54	100
GS01-13B bb	NV05a025	chaotic	44	471	0.09	4.54	0.05	0.0874	0.0015	0.933	1276.6	12.7	1282	13	1370	33	94
GS01-97B	NV05a102	homogenous	21	1432	0.01	4.65	0.04	0.0868	0.0007	0.931	1249.5	10.4	1256	11	1356	16	93
GS01-34	NV05a053	sector	48	136	0.35	4.59	0.06	0.0866	0.0025	0.932	1264.4	17.3	1270	18	1352	55	94
GS01-30	NV05a047	chaotic	30	280	0.11	4.82	0.05	0.0864	0.0015	0.927	1208.1	13.1	1216	13	1347	33	90
GS01-63	NV05a073	sector	42	110	0.38	4.78	0.06	0.0858	0.0023	0.928	1217.0	15.8	1224	16	1333	52	92
GS01-18B	NV05a036	oscillatory	56	231	0.24	4.96	0.05	0.0857	0.0016	0.924	1176.5	12.3	1185	13	1332	36	89
GS01-9	NV05a019	chaotic	52	269	0.19	4.55	0.05	0.0855	0.0015	0.933	1276.6	14.1	1279	14	1326	35	97
GS01-96	NV05a100	chaotic	44	290	0.15	4.55	0.05	0.0850	0.0014	0.933	1277.2	14.3	1280	15	1316	33	97
GS01-4	NV05a014	sector	35	444	0.08	4.62	0.05	0.0847	0.0018	0.931	1260.6	13.4	1263	14	1308	41	97
GS01-6	NV05a016	sector	29	318	0.09	4.65	0.05	0.0846	0.0013	0.931	1253.8	11.9	1257	12	1306	29	96

	Appendix A: Table 3: Sample GS01					Ratios for concordia											
Sample	Analysis no.	CL zoning	Th	U	Th/U	238U/206Pb	+/-1 std err	207Pb/206Pb	+/-1 std err	Common Pb 207Pb/206Pb	206Pb/238U 207 corr	1s	206/238 age	+/-1s	207/206 age	+/-1s	conc.
GS01-103 c	NV05a114	sector	74	413	0.18	5.17	0.05	0.0842	0.0013	0.921	1131.9	9.8	1140	10	1297	30	88
GS01-76A	NV05a078	chaotic	45	184	0.24	5.09	0.09	0.0840	0.0022	0.922	1149.2	19.2	1157	20	1293	52	89
GS01-101B	NV05a107	sector	53	116	0.45	5.32	0.07	0.0815	0.0021	0.918	1104.3	14.1	1110	14	1233	51	90
GS01-3	NV05a013	sector	37	434	0.09	5.42	0.06	0.0802	0.0011	0.916	1086.6	11.5	1092	12	1202	27	91
GS01-79A	NV05a080	patchy	66	134	0.49	6.05	0.10	0.0784	0.0028	0.907	978.3	15.5	986	16	1156	70	85
GS01-11A	NV05a021	sector	36	225	0.16	5.45	0.06	0.0776	0.0015	0.916	1083.0	11.2	1085	11	1137	38	95
GS01-19	NV05a037	homogenous	54	254	0.21	5.81	0.09	0.0776	0.0022	0.911	1018.6	15.0	1024	15	1136	57	90
GS01-57	NV05a066	sector	28	90	0.32	5.78	0.08	0.0774	0.0023	0.911	1023.4	14.0	1028	14	1133	59	91
GS01-56	NV05a065	chaotic	30	106	0.28	5.87	0.09	0.0762	0.0023	0.910	1010.6	14.8	1014	15	1101	60	92
GS01-92	NV05a096	ghost oscillatory	28	98	0.29	6.21	0.09	0.0762	0.0027	0.906	956.5	13.5	962	14	1100	71	87
GS01-90	NV05a094	patchy	35	107	0.32	5.99	0.07	0.0760	0.0020	0.908	990.6	12.2	995	12	1095	54	91
GS01-29	NV05a046	sector	53	156	0.34	5.69	0.13	0.0749	0.0049	0.912	1042.7	24.5	1044	25	1066	131	98
GS01-50	NV05a061	sector	39	103	0.38	5.96	0.08	0.0749	0.0022	0.909	996.6	13.3	999	14	1065	59	94
GS01-38	NV05a056	homogenous	29	55	0.54	5.99	0.10	0.0737	0.0029	0.908	994.1	16.5	996	17	1033	79	96
GS01-26	NV05a044	chaotic	62	231	0.27	6.11	0.06	0.0732	0.0015	0.907	975.3	9.8	977	10	1019	41	96
GS01-24A	NV05a041	patchy	74	351	0.21	6.53	0.06	0.0725	0.0014	0.902	915.6	8.7	919	9	1001	39	92
GS01-72	NV05a077	homogenous	195	944	0.21	6.08	0.06	0.0724	0.0009	0.907	981.5	8.7	982	9	998	26	98
GS01-52	NV05a062	sector	53	57	0.92	6.13	0.10	0.0717	0.0030	0.907	974.5	15.9	975	16	978	84	100
GS01-12	NV05a023	sector	36	101	0.35	5.67	0.13	0.0713	0.0031	0.913	1051.3	24.4	1048	25	965	88	109
GS01-79B	NV05a081	homogenous	302	1639	0.18	6.14	0.06	0.0709	0.0007	0.906	974.1	8.7	973	9	954	20	102
GS01-98	NV05a103	homogenous	143	1016	0.14	6.40	0.05	0.0705	0.0009	0.903	935.9	7.6	936	8	944	26	99
GS01-20B	NV05a039	homogenous	70	221	0.32	5.96	0.07	0.0705	0.0014	0.909	1003.0	11.1	1001	11	943	42	106
GS01-31	NV05a048	sector	70	133	0.52	6.36	0.08	0.0705	0.0020	0.904	941.4	12.0	941	12	942	58	100
GS01-37	NV05a055	sector	35	114	0.30	6.16	0.08	0.0705	0.0024	0.906	971.4	12.7	970	13	942	69	103
GS01-80	NV05a082	sector	138	244	0.57	6.06	0.06	0.0704	0.0014	0.907	985.7	10.0	984	10	939	42	105
GS01-14B	NV05a027	homogenous	162	953	0.17	6.09	0.10	0.0703	0.0019	0.907	981.6	15.8	980	16	936	56	105
GS01-85B	NV05a086	homogenous	260	1116	0.23	6.45	0.05	0.0702	0.0008	0.903	928.9	7.5	929	8	936	24	99
GS01-24B	NV05a042	homogenous	269	1778	0.15	6.35	0.05	0.0700	0.0006	0.904	942.9	7.7	942	8	930	19	101
GS01-7	NV05a017	sector	38	108	0.35	6.02	0.08	0.0700	0.0020	0.908	993.6	13.0	991	13	930	60	107
GS01-81	NV05a083	homogenous	211	871	0.24	6.44	0.06	0.0700	0.0009	0.903	930.3	7.8	930	8	928	26	100
GS01-55	NV05a064	ghost sector	251	1208	0.21	6.42	0.05	0.0700	0.0007	0.903	932.9	6.9	933	7	928	22	101
GS01-83	NV05a084	sector	104	973	0.11	6.08	0.05	0.0695	0.0007	0.907	985.0	8.2	982	8	914	22	107
GS01-99	NV05a104	sector	170	846	0.20	6.37	0.05	0.0693	0.0008	0.904	941.2	7.7	940	8	908	25	103
GS01-5	NV05a015	homogenous	58	701	0.08	6.52	0.06	0.0692	0.0009	0.902	920.6	8.4	920	9	905	28	102
GS01-16 ddd	NV05a033	patchy	139	308	0.45	6.50	0.07	0.0689	0.0015	0.902	922.8	10.2	922	10	897	43	103
GS01-76B	NV05a079	homogenous	177	988	0.18	6.50	0.06	0.0688	0.0008	0.902	923.4	7.6	922	8	892	23	103
GS01-88	NV05a093	chaotic	50	316	0.16	6.43	0.06	0.0680	0.0013	0.903	933.8	8.9	932	9	869	39	107
GS01-27	NV05a045	homogenous	57	106	0.54	6.15	0.07	0.0676	0.0022	0.906	975.5	11.6	971	12	858	66	113
GS01-11B	NV05a022	homogenous	187	878	0.21	6.50	0.05	0.0675	0.0008	0.902	925.4	7.5	923	8	852	25	108
GS01-47	NV05a059	sector	50	161	0.31	6.29	0.07	0.0667	0.0018	0.905	954.9	10.7	950	11	829	56	115

Appendix A: Table 6: SW54

Sample	Analysis no.	CL zoning	Th	U	Th/U	Ratios for concordia 238U/206Pb	+/-1 std err	207Pb/206Pb	+/-1 std err	Common Pb 207Pb/206Pb	206Pb/238U 207 corr	1s	206/238 age	+/-1s	207/206 age	+/-1s	conc.
SW54-86 **aa**	oc05a096	chaotic	55	669	0.08	4.42	0.07	0.1300	0.0021	0.936	1246.9	19.3	1314	21	2097	28	63
SW54-98A **a**	oc05a101	sector	285	595	0.48	3.92	0.07	0.0998	0.0018	0.950	1451.5	23.9	1465	25	1620	33	90
SW54-89A **bb**	oc05a097	sector	83	452	0.18	5.20	0.08	0.0861	0.0015	0.920	1123.6	16.2	1135	17	1341	33	85
SW54-48A **c**	oc05a068	sector	62	559	0.11	5.03	0.10	0.0826	0.0020	0.923	1163.6	21.7	1169	22	1260	47	93
SW54-64	oc05a084	homogenous	65	99	0.66	6.54	0.11	0.0808	0.0028	0.902	905.7	14.8	918	15	1217	68	75
SW54-28	oc05a048	chaotic	157	732	0.21	6.06	0.12	0.0803	0.0018	0.907	974.8	18.9	984	20	1205	44	82
SW54-41C	oc05a063	chaotic	57	86	0.67	6.37	0.10	0.0778	0.0027	0.904	932.5	14.8	940	15	1141	68	82
SW54-29	oc05a049	sector	70	100	0.70	6.56	0.11	0.0748	0.0026	0.902	909.4	15.3	915	16	1064	69	86
SW54-17	oc05a035	sector	63	84	0.74	6.44	0.12	0.0747	0.0028	0.903	925.8	17.5	931	18	1061	76	88
SW54-9	oc05a024	sector	55	84	0.66	6.55	0.13	0.0736	0.0034	0.902	911.0	18.4	915	19	1030	92	89
SW54-37	oc05a058	sector	56	82	0.69	6.72	0.12	0.0736	0.0032	0.900	889.7	16.1	895	16	1029	89	87
SW54-12	oc05a027	sector	79	105	0.75	6.53	0.10	0.0734	0.0023	0.902	914.4	13.5	918	14	1026	65	90
SW54-98B	oc05a102	sector	66	95	0.70	6.27	0.10	0.0734	0.0027	0.905	951.4	15.6	954	16	1025	74	93
SW54-59	oc05a082	chaotic	61	74	0.82	6.31	0.10	0.0734	0.0028	0.904	945.7	15.2	949	15	1025	78	93
SW54-75	oc05a088	sector	61	82	0.74	6.59	0.11	0.0734	0.0033	0.901	906.9	15.5	911	16	1024	90	89
SW54-8	oc05a023	sector	78	88	0.88	6.25	0.14	0.0732	0.0039	0.905	953.8	21.4	956	22	1021	108	94
SW54-18	oc05a036		63	80	0.79	6.51	0.11	0.0729	0.0025	0.902	917.8	15.3	921	16	1011	70	91
SW54-52B	oc05a079	chaotic	70	102	0.69	6.66	0.12	0.0727	0.0025	0.901	898.2	16.3	902	17	1007	70	90
SW54-57	oc05a080	sector	98	179	0.55	6.65	0.10	0.0725	0.0020	0.901	899.8	13.1	903	13	1001	55	90
SW54-23	oc05a041	sector	60	95	0.63	6.66	0.13	0.0725	0.0031	0.901	898.3	17.6	902	18	999	87	90
SW54-11	oc05a026	sector	85	160	0.53	6.52	0.09	0.0725	0.0020	0.902	917.0	12.2	920	12	999	56	92
SW54-16	oc05a030		60	83	0.73	6.59	0.12	0.0724	0.0028	0.901	907.2	16.4	910	17	998	80	91
SW54-1	oc05a015	sector	59	82	0.72	6.52	0.13	0.0722	0.0029	0.902	917.4	17.9	920	18	990	81	93
SW54-33	oc05a056	sector	57	83	0.69	6.71	0.14	0.0721	0.0035	0.900	892.7	18.0	896	18	990	100	91
SW54-24B	oc05a043	homogenous	156	311	0.50	6.54	0.09	0.0721	0.0016	0.902	914.5	12.3	917	13	989	44	93
SW54-48B	oc05a069	sector	78	120	0.65	6.55	0.11	0.0719	0.0025	0.902	913.1	14.6	916	15	984	70	93
SW54-5	oc05a020	sector	72	108	0.67	6.81	0.12	0.0718	0.0023	0.899	879.7	15.2	883	16	981	66	90
SW54-35	oc05a057	sector	61	81	0.75	6.53	0.12	0.0718	0.0027	0.902	916.4	16.3	919	17	980	76	94
SW54-21	oc05a038	sector	102	161	0.63	6.46	0.10	0.0717	0.0020	0.903	926.2	14.4	928	15	979	56	95
SW54-20	oc05a037	sector	86	153	0.56	6.73	0.10	0.0717	0.0020	0.900	890.4	12.9	893	13	978	57	91
SW54-2B	oc05a017	homogenous	173	815	0.21	6.68	0.08	0.0717	0.0011	0.900	896.0	10.1	899	10	977	31	92
SW54-82B	oc05a090	chaotic	64	86	0.75	6.42	0.12	0.0716	0.0027	0.903	930.9	17.5	933	18	975	77	96
SW54-4	oc05a019	oscillatory	52	81	0.64	6.37	0.12	0.0716	0.0027	0.904	939.4	16.7	941	17	975	77	97
SW54-71	oc05a087	sector	108	109	0.99	6.68	0.10	0.0716	0.0023	0.900	896.4	13.3	899	14	974	67	92
SW54-15	oc05a029	sector	76	124	0.61	6.41	0.10	0.0716	0.0022	0.903	933.6	14.6	935	15	974	64	96
SW54-6	oc05a021	chaotic	62	94	0.66	6.55	0.11	0.0716	0.0026	0.902	914.4	15.2	917	16	974	75	94
SW54-100B	oc05a106	sector	54	77	0.70	6.34	0.11	0.0714	0.0027	0.904	943.1	15.6	944	16	970	78	97
SW54-50	oc05a075	oscillatory	61	92	0.66	6.39	0.11	0.0714	0.0023	0.904	936.1	15.5	937	16	969	66	97
SW54-47B	oc05a067	sector	64	80	0.79	6.42	0.11	0.0713	0.0024	0.903	931.4	16.1	933	16	966	68	97

Appendix A: Table 6: SW54

Sample	Analysis no.	CL zoning	Th	U	Th/U	Ratios for concordia 238U/206Pb	+/-1 std err	207Pb/206Pb	+/-1 std err	Common Pb 207Pb/206Pb	206Pb/238U 207 corr	1s	206/238 age	+/-1s	207/206 age	+/-1s	conc.
SW54-7	oc05a022	sector	66	87	0.75	6.82	0.12	0.0713	0.0026	0.899	879.2	14.6	882	15	965	74	91
SW54-27	oc05a047		78	122	0.63	6.47	0.11	0.0712	0.0021	0.903	925.3	15.0	927	15	962	62	96
SW54-115A	oc05a110	chaotic	54	213	0.25	6.37	0.09	0.0711	0.0021	0.904	939.3	13.2	940	13	961	61	98
SW54-89B	oc05a098	sector	81	125	0.65	6.46	0.10	0.0711	0.0021	0.903	926.8	14.1	928	14	960	59	97
SW54-99A	oc05a103	chaotic	63	88	0.72	6.63	0.11	0.0709	0.0025	0.901	903.2	14.7	905	15	955	73	95
SW54-46	oc05a065	sector	70	94	0.74	6.58	0.10	0.0708	0.0024	0.901	910.9	13.6	912	14	953	70	96
SW54-41D	oc05a064	homogenous	95	172	0.56	6.52	0.10	0.0707	0.0021	0.902	918.8	13.7	920	14	948	62	97
SW54-41B	oc05a062	chaotic	38	214	0.18	6.06	0.10	0.0707	0.0019	0.907	986.5	15.7	985	16	948	55	104
SW54-70	oc05a086	sector	42	243	0.17	6.60	0.09	0.0707	0.0016	0.901	908.5	11.8	910	12	947	47	96
SW54-2A	oc05a016	sector	82	138	0.59	6.66	0.10	0.0706	0.0021	0.901	900.4	13.3	902	14	946	62	95
SW54-117	oc05a116	sector	85	130	0.66	6.45	0.10	0.0705	0.0021	0.903	929.1	14.1	930	14	944	62	99
SW54-107	oc05a109	sector	66	92	0.72	6.90	0.12	0.0704	0.0025	0.898	870.3	14.6	873	15	941	73	93
SW54-25A	oc05a044	sector	89	163	0.55	6.60	0.10	0.0704	0.0021	0.901	908.2	13.0	909	13	940	60	97
SW54-85	oc05a095	sector	65	91	0.72	6.69	0.12	0.0703	0.0026	0.900	896.1	15.6	897	16	936	75	96
SW54-90	oc05a100	sector	65	100	0.65	6.65	0.10	0.0703	0.0027	0.901	902.5	13.9	904	14	936	79	97
SW54-49	oc05a070	oscillatory	65	94	0.69	6.13	0.10	0.0702	0.0024	0.907	975.6	16.1	974	16	935	70	104
SW54-30	oc05a050	chaotic	55	83	0.67	6.54	0.11	0.0702	0.0029	0.902	916.8	14.7	917	15	934	85	98
SW54-22	oc05a039	sector	69	119	0.58	6.66	0.14	0.0702	0.0027	0.901	900.6	18.0	902	18	933	80	97
SW54-66	oc05a085	chaotic	105	186	0.57	6.32	0.09	0.0701	0.0018	0.904	947.8	12.9	947	13	932	52	102
SW54-47A	oc05a066	sector	52	272	0.19	6.49	0.09	0.0701	0.0016	0.902	923.2	12.5	923	13	931	46	99
SW54-106	oc05a108	sector	69	86	0.80	6.67	0.13	0.0701	0.0027	0.900	898.9	16.9	900	17	930	79	97
SW54-51A	oc05a076	sector	62	88	0.71	6.19	0.11	0.0699	0.0027	0.906	966.3	17.2	965	18	927	80	104
SW54-25B	oc05a045	homogenous	181	378	0.48	6.49	0.08	0.0699	0.0014	0.902	923.7	11.3	924	12	925	40	100
SW54-40A	oc05a059	sector	42	227	0.18	6.35	0.10	0.0699	0.0023	0.904	943.5	14.6	943	15	925	68	102
SW54-24A	oc05a042	sector	128	236	0.54	6.47	0.10	0.0699	0.0015	0.903	926.1	13.9	926	14	925	44	100
SW54-3	oc05a018	sector	85	141	0.60	6.52	0.13	0.0698	0.0024	0.902	920.1	17.3	920	18	924	71	100
SW54-14	oc05a028	sector	70	99	0.71	6.52	0.10	0.0698	0.0025	0.902	920.4	13.5	921	14	923	74	100
SW54-51B	oc05a077	homogenous	174	1108	0.16	6.46	0.08	0.0693	0.0009	0.903	928.3	11.0	928	11	907	27	102
SW54-58	oc05a081	sector	80	98	0.81	6.54	0.13	0.0693	0.0029	0.902	917.0	17.9	917	18	907	87	101
SW54-89C	oc05a099	homogenous	138	1855	0.07	6.43	0.07	0.0693	0.0007	0.903	932.2	10.2	931	11	907	21	103
SW54-100C	oc05a107	homogenous	89	146	0.61	6.51	0.09	0.0692	0.0021	0.902	921.9	12.8	921	13	904	63	102
SW54-99B	oc05a104	homogenous	169	591	0.29	6.56	0.09	0.0692	0.0011	0.902	914.4	12.6	914	13	904	34	101
SW54-115B **ddd**	oc05a115	homogenous	170	760	0.22	6.57	0.09	0.0688	0.0010	0.902	913.7	12.2	913	13	893	31	102
SW54-52A	oc05a078	homogenous	72	115	0.63	6.55	0.11	0.0684	0.0023	0.902	917.3	15.2	916	15	881	69	104
SW54-82A	oc05a089	chaotic	73	114	0.64	6.46	0.11	0.0682	0.0022	0.903	929.5	14.8	928	15	875	66	106
SW54-40B	oc05a060	sector	71	90	0.79	6.51	0.10	0.0678	0.0023	0.902	923.2	14.0	921	14	863	71	107
SW54-62	oc05a083	patchy	63	118	0.54	6.93	0.12	0.0674	0.0022	0.898	870.1	14.8	869	15	850	68	102
SW54-32	oc05a055	sector	86	204	0.42	6.78	0.09	0.0670	0.0019	0.899	888.2	11.8	887	12	837	59	106
SW54-10	oc05a025	sector	63	87	0.73	6.61	0.12	0.0664	0.0024	0.901	911.6	16.2	909	16	820	75	111

	Appendix A: Table 5: FS0223					Ratios for concordia											
Sample	Analysis no.	CL zoning	Th	U	Th/U	238U/206Pb	+/-1 std err	207Pb/206Pl	+/-1 std err	Common Pb 207Pb/206Pb	206Pb/238U 207 corr	1s	206/238 age	+/-1s	207/206 age	+/-1s	conc.
FS0223-19 a	OC27b144	sector	8	576	0.01	4.11	0.13	0.0915	0.0040	0.944	1400.6	43.9	1405	45	1457	82	96
FS0223-40 c	OC27b160	chaotic	24	149	0.16	6.41	0.13	0.0792	0.0034	0.903	925.4	18.8	935	19	1178	84	79
FS0223-59A	OC27b172	patchy	8	551	0.02	5.64	0.15	0.0786	0.0033	0.913	1046.9	28.0	1052	29	1161	84	91
FS0223-36	OC27b153	chaotic	14	193	0.07	6.11	0.13	0.0783	0.0032	0.907	969.7	19.7	977	20	1155	82	85
FS0223-81	OC27b190	chaotic	12	171	0.07	6.11	0.16	0.0770	0.0029	0.907	971.5	24.7	977	25	1120	76	87
FS0223-53	OC27b167	patchy	6	214	0.03	6.39	0.14	0.0758	0.0031	0.904	931.5	20.1	937	21	1090	81	86
FS0223-17	OC27b143	sector	6	193	0.03	6.20	0.13	0.0754	0.0027	0.906	959.3	19.7	964	20	1078	71	89
FS0223-93	OC27b206	chaotic	50	121	0.41	6.14	0.21	0.0751	0.0040	0.906	968.8	32.6	973	34	1072	108	91
FS0223-94	OC27b207	chaotic	25	171	0.14	6.48	0.19	0.0747	0.0030	0.903	920.1	25.8	925	27	1060	80	87
FS0223-77	OC27b187	sector	12	441	0.03	6.31	0.17	0.0741	0.0020	0.904	944.2	25.2	948	26	1044	54	91
FS0223-58	OC27b171	sector	24	239	0.10	6.15	0.13	0.0739	0.0025	0.906	968.7	20.3	971	21	1040	69	93
FS0223-86	OC27b199	sector	47	192	0.25	6.32	0.16	0.0739	0.0026	0.904	943.1	23.2	947	24	1038	71	91
FS0223-4	OC27b129	sector	8	181	0.04	6.40	0.13	0.0737	0.0031	0.903	932.2	19.0	936	19	1033	86	91
FS0223-67	OC27b181	patchy	14	321	0.04	5.31	0.19	0.0736	0.0038	0.918	1116.4	37.9	1112	39	1029	106	108
FS0223-88	OC27b201	sector	7	186	0.04	6.05	0.20	0.0735	0.0042	0.908	984.1	31.6	986	32	1029	117	96
FS0223-52	OC27b166	chaotic	20	261	0.08	6.25	0.14	0.0733	0.0023	0.905	954.1	20.9	957	22	1023	65	94
FS0223-8	OC27b134	chaotic	7	200	0.04	6.55	0.14	0.0732	0.0030	0.902	912.7	19.7	916	20	1019	82	90
FS0223-30	OC27b149	homogenous	12	162	0.07	6.25	0.12	0.0731	0.0029	0.905	953.8	17.9	956	18	1016	81	94
FS0223-38	OC27b154	patchy	13	283	0.05	6.44	0.12	0.0727	0.0024	0.903	928.2	16.9	931	17	1005	66	93
FS0223-89	OC27b202	patchy	16	169	0.09	6.22	0.16	0.0726	0.0030	0.905	959.5	24.3	961	25	1003	84	96
FS0223-69	OC27b182	sector	27	252	0.11	6.31	0.16	0.0724	0.0024	0.904	946.3	23.3	948	24	998	68	95
FS0223-31	OC27b150	chaotic	20	187	0.11	6.32	0.13	0.0723	0.0029	0.904	945.1	19.6	947	20	995	82	95
FS0223-85	OC27b194	homogenous	35	170	0.21	6.37	0.19	0.0723	0.0030	0.904	938.2	26.9	940	28	995	85	95
FS0223-49	OC27b163	homogenous	26	190	0.14	6.49	0.12	0.0723	0.0030	0.902	921.7	16.2	924	17	995	85	93
FS0223-28	OC27b148	chaotic	16	498	0.03	6.23	0.16	0.0722	0.0029	0.905	957.9	23.3	959	24	993	83	97
FS0223-82	OC27b191	sector	12	167	0.07	6.48	0.16	0.0722	0.0029	0.903	923.3	22.5	926	23	992	83	93
FS0223-41	OC27b161	sector	9	154	0.06	6.57	0.15	0.0722	0.0035	0.902	910.4	19.8	913	20	992	100	92
FS0223-76	OC27b186	sector	19	194	0.10	6.27	0.18	0.0718	0.0031	0.905	953.1	26.6	954	27	979	87	97
FS0223-20	OC27b145	sector	34	230	0.15	6.53	0.13	0.0716	0.0030	0.902	915.8	18.4	918	19	976	85	94
FS0223-11	OC27b140	chaotic	10	213	0.05	6.47	0.12	0.0716	0.0027	0.903	925.1	17.3	927	18	973	76	95
FS0223-10	OC27b139	homogenous	30	203	0.15	6.39	0.12	0.0714	0.0028	0.904	936.0	17.2	937	18	970	80	97
FS0223-1	OC27b127	sector	7	176	0.04	6.42	0.14	0.0714	0.0031	0.903	931.9	19.9	933	20	968	87	96
FS0223-56	OC27b169	sector	19	205	0.09	6.20	0.13	0.0712	0.0026	0.906	963.4	20.0	963	21	962	75	100
FS0223-6	OC27b132	chaotic	29	166	0.17	6.41	0.14	0.0709	0.0032	0.903	933.6	19.9	934	20	955	92	98
FS0223-92	OC27b205	chaotic	16	192	0.08	6.29	0.17	0.0708	0.0026	0.905	951.0	24.7	951	25	953	76	100
FS0223-47	OC27b162	chaotic	21	195	0.11	6.52	0.14	0.0708	0.0027	0.902	918.8	19.2	920	20	952	79	97
FS0223-90	OC27b203	chaotic	19	198	0.09	6.39	0.16	0.0708	0.0026	0.904	937.2	22.3	938	23	951	76	99
FS0223-5B	OC27b131	chaotic	35	180	0.20	6.34	0.12	0.0706	0.0030	0.904	944.1	18.1	944	18	945	86	100
FS0223-57	OC27b170	chaotic	23	221	0.10	6.42	0.13	0.0705	0.0024	0.903	932.8	17.8	933	18	943	71	99
FS0223-59B	OC27b173	sector	19	273	0.07	6.35	0.11	0.0703	0.0022	0.904	943.5	15.5	943	16	938	65	101

Sample	Appendix A: Table 5: FS0223					Ratios for concordia											
Sample	Analysis no.	CL zoning	Th	U	Th/U	238U/206Pb	+/-1 std err	207Pb/206P	+/-1 std err	Common Pb 207Pb/206Pb	206Pb/238U 207 corr	1s	206/238 age	+/-1s	207/206 age	+/-1s	conc.
FS0223-51	OC27b165	chaotic	31	113	0.28	6.50	0.18	0.0703	0.0042	0.902	922.0	25.5	923	26	938	123	98
FS0223-79	OC27b188	chaotic	6	226	0.03	6.23	0.19	0.0702	0.0024	0.905	960.7	28.0	960	29	933	71	103
FS0223-55	OC27b168	sector	6	261	0.02	6.39	0.12	0.0701	0.0022	0.904	937.8	16.8	938	17	931	63	101
FS0223-13	OC27b142	chaotic	24	229	0.10	6.29	0.12	0.0698	0.0025	0.905	952.7	17.9	952	18	921	73	103
FS0223-87	OC27b200	sector	7	331	0.02	6.35	0.16	0.0697	0.0020	0.904	944.2	23.1	943	24	920	60	102
FS0223-35	OC27b152	homogenous	57	394	0.14	6.65	0.10	0.0695	0.0021	0.901	902.9	13.7	903	14	915	61	99
FS0223-65	OC27b180	chaotic	8	192	0.04	6.41	0.16	0.0695	0.0029	0.903	935.9	23.0	935	24	913	84	102
FS0223-39	OC27b159	homogenous	24	133	0.18	6.45	0.13	0.0693	0.0033	0.903	930.4	18.7	930	19	907	99	102
FS0223-75	OC27b185	chaotic	21	268	0.08	6.36	0.17	0.0693	0.0022	0.904	943.1	24.6	942	25	906	67	104
FS0223-23 dd	OC27b146	chaotic	20	163	0.12	6.39	0.14	0.0690	0.0029	0.904	939.3	19.7	938	20	898	87	104
FS0223-7	OC27b133	chaotic	18	218	0.08	6.56	0.13	0.0688	0.0026	0.902	916.0	17.3	915	18	894	77	102
FS0223-27	OC27b147	chaotic	19	340	0.06	6.47	0.12	0.0686	0.0020	0.903	927.2	16.1	926	17	886	59	104
FS0223-62	OC27b174	sector	20	216	0.09	6.16	0.13	0.0682	0.0027	0.906	974.1	20.8	970	21	874	81	111
FS0223-70	OC27b183	sector	8	275	0.03	6.48	0.15	0.0680	0.0023	0.902	926.7	21.4	925	22	868	71	107
FS0223-12	OC27b141	sector	7	204	0.03	6.37	0.14	0.0680	0.0026	0.904	942.0	19.8	939	20	868	81	108
FS0223-2	OC27b128	sector	46	184	0.25	6.64	0.14	0.0679	0.0030	0.901	905.4	18.9	904	19	865	92	105
FS0223-83	OC27b192	sector	22	203	0.11	6.78	0.16	0.0676	0.0027	0.899	887.3	20.5	886	21	857	84	103
FS0223-84	OC27b193	sector	10	172	0.06	6.21	0.17	0.0675	0.0031	0.906	966.2	25.6	962	26	852	95	113
FS0223-50	OC27b164	patchy	24	239	0.10	7.02	0.16	0.0674	0.0023	0.897	858.3	19.3	858	20	851	72	101
FS0223-72	OC27b184	sector	9	187	0.05	6.35	0.15	0.0670	0.0029	0.904	947.2	22.3	943	23	838	90	113
FS0223-91	OC27b204	homogenous	21	346	0.06	7.28	0.18	0.0669	0.0022	0.895	829.1	19.8	829	20	836	69	99
FS0223-80	OC27b189	chaotic	13	240	0.05	6.38	0.15	0.0666	0.0024	0.904	942.9	21.9	939	22	825	75	114
FS0223-64	OC27b179	chaotic	31	232	0.13	6.15	0.16	0.0664	0.0024	0.906	976.7	24.8	971	25	820	76	118
FS0223-34	OC27b151	sector	17	211	0.08	7.04	0.16	0.0662	0.0027	0.897	857.8	18.5	856	19	814	87	105

References

Andersen, T 2002, ‘Correction of common Pb in U-Pb analyses that do not report 204Pb’, *Chemical Geology*, vol. 192, pp.59-79.

Belousova, E, Griffin, W, O’Reilly, S & Fisher, N 2002, ‘Igneous zircon: trace element composition as an indicator of source rock type’, *Contributions to Mineral Petrology*, vol.143, pp.602-622.

Blichert-Toft, J, Chauvel, C & Albarède, F 1997 ‘The Lu-Hf geochemistry of chondrites and the evolution of the mantle-crust system’, *Earth and Planetary Science Letters*, vol.148, pp.243-258. Erratum: *Earth and Planetary Science Letters*, vol.154 (1998), p.349.

Dunkley, D, Clarke, G & White, R 2002, ‘Structural and metamorphic evolution of the mid-late Proterozoic Rayner Complex, Cape Bruce, East Antartica’, in J Gample, D Skinner & S Henrys (eds.), *Antarctica at the close of a millennium. The Royal Society of New Zealand Bulletin*, vol.35, The Royal Society of New Zealand, Wellington, pp.31-42.

Ellis, D 1983, ‘The Napier and Rayner Complexes of Enderby Land, Antarctica – Contrasting styles of metamorphism and tectonism’, in R Oliver, P James and J Jago (eds.), *Antarctic Earth Science,* Cambridge University Press, Cambridge, pp.20-24.

Gehrels, G, Valencia, V, Pullen, A & Baker, M 2006, ‘Detrital zircon U-Th-Pb geochronology by LA-MC-ICPMS at the Arizona LaserChron Center’, *Geological Society of America Abstracts with Programs*, vol.38, no.7, p.408.

Halpin, J, Gerakiteys, C, Clarke, G, Belousova, E & Griffin, W 2005, ‘In-situ U-Pb geochronology and Hf isotope analyses of the Rayner Complex, east Antarctica’, *Contributions to Mineral Petrology*, vol.148, pp.689-706.

Halpin, J, White, R, Clarke, G & Kelsey D 2007a, ‘The Proterozoic P-T-t evolution of the Kemp Land coast, east Antarctica; constrains from Si-saturated and Si-undersaturated Metapelites’, *Journal of Petrology*, vol.48, no.7, pp.1321-1349.

Halpin, J, Clarke, G, White, R & Kelsey, D 2007b, ‘Contrasting P-T-t paths for neoproterozoic metamorphism in MacRobertson and Kemp Lands, east Antarctica’, *Journal of Metamorphic Geology*, vol.25, pp.683-701.

Halpin, J, Clarke, G & White, R 2007c, ‘Evolution of the Stillwell Hills, Rayner Complex, east Antarctica; a reworked cratonic margin’, Halpin, J Thesis, University of Sydney, Sydney.

Harley, S & Kelly, N 2007, ‘Ancient Antarctica: the Archaean of the east Antarctic shield’, in *Earth’s oldest rocks*, Developments in Precambrian Geology, Vol.15

Howard, K, Hand, M, Barovich, K, Reid, A, Wade, B & Belousova, E 2009, ‘Detrital zircon ages: Improving interpretation va Nd and Hf isotopic data’, *Chemical Geology* , vol.262, pp.277-292.

Howard, K, Hand, M, Barovich, K, Payne, J & Belousova, E 2011, ‘U-Pb, Lu-Hf and Sm-Nd isotopic constraints on provenance and depositional timing of metasedimentary rocks in the western Gawler Craton: Implications for Proterozoic reconstruction models’, *Precambrian Research*, vol.184, pp.43-62.

Kelly, N & Harley, S 2004, 'Orthopyroxene-corundum in Mg-Al-rich granulites from the Oygarden Islands, east Antarctica'. *Journal of Petrology*, vol.45, pp.1481-1512.

Ludwig, K 2003, 'Isoplot 3.00: A Geochronological Toolkit for Microsoft Excel', *Berkeley Geochrological Centre Special Publication,* no.4.

MacKenzie, W & Adams, A 2009, '*A colour atlas of rocks and minerals in thin section'*, Manson Publishing Ltd, London.

Rignot, E, Bamber, J, van den Broeke, M, Davis, C, Li, Y, van de Berg, W & van Meijgaard, E 2008, 'Recent Antarctic ice mass loss from radar interferometry and regional climate modelling', *Nature Geoscience*, vol.1, pp.106–110.

Trail, D 1970, 'ANARE 1961 Geological Traverses on the Mac.Robertson Land and Kemp Land Coast', *Bureau of Mineral Resources Geology and Geophysics Report*, vol.135, pp.1-32.

Veevers, J (ed.), 2000, *Billion-year earth history of Australia & neighbours in Gondwanaland*, GEMOC Press, Sydney, pp. 1-400.

Veevers, J, Belousova, E, Saeed, A, Sircombe, K, Cooper, A & Read, S 2006, 'Pan-Gondwanaland detrital zircons from Australia analysed for Hf-isotopes and trace elements reflect an ice-covered Antarctic provenance of 700–500 Ma age, TDM of 2.0–1.0 Ga, and alkaline affinity', *Earth-Science Reviews,* vol.76, pp. 135–174.

Veevers, J & Saeed, A 2008, 'Gamburtsev Subglacial Mountains provenance of Permian–Triassic sandstones in the Prince Charles Mountains and offshore Prydz Bay: integrated U–Pb and TDM ages and host-rock affinity from detrital zircons', *Gondwana Research*, vol.14, pp.316–342.

Veevers, J & Saeed, A 2011, 'Age and composition of Antarctic bedrock reflected by detrital zircons, erratic and recycled microfossils in the Prydz Bay – Wilkes Land – Ross Sea – Marie Byrd Land sector (70° - 240°E)', *Gondwana Research*, Article in Press.

Wang, X, Griffin, W, Chen, J, Huang, P & Li, X 2011, 'U and Th contents and Th/U ratios of zircon in felsic and mafic magmatic rocks: improved zircon-melt distribution coefficients', *Acta Geologica Sinica*, English (ed.), vol. 85, no. 1, pp.164-174.

Xu, P, Wu, F, Xie, L & Yang, Y 2004, 'Hf isotopic compositions of the standard zircons for U-Pb dating, *Chinese Science Bulletin'*, vol.49, no.15, pp.1642-1648.

Young, D & Black, L 1991, 'U-Pb zircon dating of Proterozoic igneous charnockites from the Mawson Coast, East Antarctica'. *Antarctic Science*, vol.3, pp.205-216.

Zhao, J-X, Ellis, D, Kilpatrick, J & McCulloch, T 1997, 'Geochemical and Sr-Nd isotopic study of charnockites and related rocks in the northern Prince Charles Mountains, East Antarctica: implications for charnockite petrogenesis and proterozoic crustal evolution', *Precambrian Research*, vol.81, pp.37-66.